

# Sources of sediment depositing in the Pleasant River (Te Hakapupu) Catchment and Estuary

*Prepared for Otago Regional Council*

*June 2023*



Prepared by:  
Andrew Swales  
Greg Olsen  
Sean Handley  
Ron Ovenden  
Sanjay Wadhwa  
Andrew Marriner  
Julie Brown


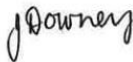

For any information regarding this report please contact:

Andrew Swales  
Programme Leader - Catchments to Estuaries  
Coastal and Estuarine Physical Processes Group  
+64 7 856 7026  
Andrew.Swales@niwa.co.nz

National Institute of Water & Atmospheric Research Ltd  
PO Box 11115  
Hamilton 3251

Phone +64 7 856 7026

NIWA CLIENT REPORT No: 2023175HN  
Report date: June 2023  
NIWA Project: ORC22202

Quality Assurance Statement		
	Reviewed by:	Dr Max Gibbs
	Formatting checked by:	Jo Downey
	Approved for release by:	Michael Bruce

---

© All rights reserved. This publication may not be reproduced or copied in any form without the permission of the copyright owner(s). Such permission is only to be given in accordance with the terms of the client's contract with NIWA. This copyright extends to all forms of copying and any storage of material in any kind of information retrieval system.

Whilst NIWA has used all reasonable endeavours to ensure that the information contained in this document is accurate, NIWA does not give any express or implied warranty as to the completeness of the information contained herein, or that it will be suitable for any purpose(s) other than those specifically contemplated during the Project or agreed by NIWA and the Client.

# Contents

- Executive summary ..... 7**
- 1 Introduction ..... 9**
  - 1.1 Background to study ..... 9
  - 1.2 Legislation considerations ..... 10
  - 1.3 Study Objective ..... 11
  - 1.4 Catchment and estuary characteristics ..... 12
- 2 Methods ..... 17**
  - 2.1 CSSI sediment source tracing - overview ..... 17
  - 2.2 Sediment source library ..... 20
  - 2.3 Soil and sediment sampling methods ..... 31
  - 2.4 Bulk carbon and fatty acid analyses ..... 34
  - 2.5 Multivariate ordination – source and tracer selection ..... 34
  - 2.6 Source isotopic polygons in CSSI analyses ..... 36
  - 2.7 Sediment source modelling ..... 44
- 3 Results ..... 46**
  - 3.1 Sources of river-sediment deposits ..... 46
  - 3.2 Sources of estuary-sediment deposits ..... 59
- 4 Discussion ..... 67**
  - 4.1 River sediment sources ..... 67
  - 4.2 Estuary sedimentation ..... 68
  - 4.3 Sediment management in the Pleasant River system ..... 70
- 5 Acknowledgements ..... 72**
- 6 References ..... 73**
- Appendix A Summary of CSSI Method ..... 80**
- Appendix B Soil sampling method ..... 86**
- Appendix C Soil source library for Pleasant River system ..... 88**
- Appendix D Mixing model descriptions and performance ..... 89**
- Appendix E Sampling information ..... 93**

## Tables

Table 1-1:	Pleasant River Estuary - summary of long-term annual average catchment sediment loads.	16
Table 2-1:	Summary of production forest harvesting operations during September 2019 to December 2021.	21
Table 2-2:	Summary statistics for Bulk C and FA biotracer %C and $\delta^{13}\text{C}$ values for catchment and estuary sediment sources used for modelling source proportions in river and estuary sediment deposits.	40
Table 3-1:	Proportional contribution (%) of upstream sediment sources to the river system at each confluence sampled in the Pleasant River Catchment.	48
Table 3-2:	Comparison of annual average suspended sediment loads at confluences for upstream sources (% , NZ River Maps) with Two Endmember Mixing Model estimates of confluence contributions to downstream mixture (%).	49
Table 3-3:	MixSIAR summary statistics for source contributions (% soil proportions) to river sediment deposits at catchment outlets.	52
Table 3-4:	Site PR5 Watkin Creek confluence. MixSIAR summary statistics for proportional contributions (Soil %) of sources to river sediment deposits.	54
Table 3-5:	Site PR6 Trotters Creek confluence. MixSIAR summary statistics for proportional contributions (Soil %) of sources to river sediment deposits.	55
Table 3-6:	Confluence PR7 - Pleasant River. MixSIAR summary statistics for proportional contributions (Soil %) of sources to river sediment deposits.	56
Table 3-7:	Confluence PR8 - Pleasant River. MixSIAR summary statistics for proportional contributions (Soil %) of sources to river sediment deposits.	57
Table 3-8:	Confluence PR9 - Pleasant River. MixSIAR summary statistics for proportional contributions (Soil %) of sources to river sediment deposits.	58
Table 3-9:	Estuary sedimentation - relative contributions of catchment sources.	61
Table 3-10:	Thorburn Road Creek. MixSIAR summary statistics for proportional contributions (Soil %) of sources to estuarine sediment deposits.	62
Table 3-11:	Intertidal flats -west of channel. MixSIAR summary statistics for proportional contributions (Soil %) of sources to estuarine sediment deposits.	63
Table 3-12:	Intertidal flats east of channel (NIWA Sites). MixSIAR summary statistics for proportional contributions (Soil %) of sources to estuarine sediment deposits.	64
Table 3-13:	Intertidal flats east of channel (Salt Ecology sites). MixSIAR summary statistics for proportional contributions (Soil %) of sources to estuarine sediment.	65
Table C-1:	Soil/sediment source library isotopic data from sampled sites – Pleasant River system.	88
Table D-1:	Summary of MixSIAR model convergence – River sediment deposits.	91
Table E-1:	Pleasant River Sampling Location Data.	93

## Figures

Figure 1-1:	Pleasant River Catchment and major tributaries.	10
-------------	---	----



Figure 1-2:	Pleasant River Catchment land use and soil and sediment sampling sites.	13
Figure 1-3:	Pleasant River Estuary and sand barrier (2014).	14
Figure 1-4:	Flood-tide delta sand body, lower estuary.	14
Figure 1-5:	Intertidal sand flats, lower and middle estuary.	14
Figure 1-6:	Intertidal mudflats flats with macroalgae in the Thorburn Road creek, lower estuary.	15
Figure 1-7:	Extensive areas of saltmarsh and Intertidal mudflats in the upper estuary.	15
Figure 2-1:	CSSI sediment source tracing.	18
Figure 2-2:	Summary of the CSSI sediment-source tracing method.	19
Figure 2-3:	Location of pine forest harvesting in the Pleasant River catchment, September 2019 - December 2021.	22
Figure 2-4:	Recently harvested pine forest, upper Pleasant River catchment, May 2022.	23
Figure 2-5:	Pastoral land use in the Pleasant River catchment (May 2022).	24
Figure 2-6:	Kale winter Cropping - Kensington Farm at end of Noones Run Rd, May 2022.	25
Figure 2-7:	Forest track established for harvesting, Venture Forest track accessed from Patterson Rd, May 2022.	26
Figure 2-8:	Area of subsoil erosion, sampled at Kensington Farm off Taieri Peak Rd (site Slip-Rep1), May 2022.	26
Figure 2-9:	Streambank erosion in Pleasant River at FAMILTON Farm off SH1 (site Slip-Rep3), May 2022.	27
Figure 2-10:	Sediment sampling at Site PR1A, outlet of small catchment discharging to the Thorburn Road tidal creek, May 2022.	28
Figure 2-11:	Sediment sampling site PR3, Watkin Creek outlet, above tidal reach, May 2022.	28
Figure 2-12:	Sediment sampling site Site PR4, Pleasant River outlet, above tidal reach, May 2022.	29
Figure 2-13:	Sediment sampling at Confluence PR5, upper reaches of Watkin Creek, May 2022.	29
Figure 2-14:	Sediment sampling at Confluence PR6, upper reaches of Trotters Creek, May 2022.	30
Figure 2-15:	Sediment sampling at Confluence PR7, middle reach of Pleasant River, May 2022.	30
Figure 2-16:	Sediment sampling at Confluence PR8, upper reach of Pleasant River, May 2022.	31
Figure 2-17:	Sediment Sampling at Confluence PR9, upper reach of Pleasant River, May 2022.	31
Figure 2-18:	Pleasant River Estuary - spatial distribution of major intertidal habitat types (2021) and location of estuarine sampling sites in the present study.	33
Figure 2-19:	Canonical Analysis of Principal Coordinates (CAP) plot – final model composed of four catchment sources and nine tracers.	36
Figure 2-20:	Marine sediment characteristics in the immediate vicinity of the Pleasant River estuary.	38
Figure 2-21:	Estuary site E12 output from MiXSIAR mixing model incorporating the Pelorus Marine source.	39
Figure 2-22:	Estuary site E12 output from MiXSIAR mixing model incorporating the Pleasant River Estuary Marine source.	40

Figure 2-23:	Isotopic biplots of average FA $\delta^{13}\text{C}$ values (a) C16:0 versus C26:0 and (b) C18:0 versus C24:0 Fatty Acids for potential catchment sediment sources (blue symbols), river (black) and estuarine sediment (mustard) deposits and marine plant samples (green).	42
Figure 2-24:	Isotopic biplots of average FA $\delta^{13}\text{C}$ values (c) Bulk $\delta^{13}\text{C}$ versus C16:0 and (d) C20:0 Fatty Acids for potential catchment sediment sources (blue symbols), river (black) and estuarine sediment (mustard) deposits and marine plant samples (green).	43
Figure 2-25:	Example of a probability distribution of % soil proportions.	45
Figure 3-1:	Map of Pleasant River Catchment and location of river confluence sampling sites and contributions (red text, %) of upstream main stem and tributary sources to the downstream sediment deposit (mixture).	47
Figure 3-2:	Pleasant River Catchment (northern branch). Average % soil source proportions for river sediment deposits at sampling sites (May 2023).	50
Figure 3-3:	Pleasant River Catchment (southern branch). Average % soil source proportions for river sediment deposits at sampling sites (May 2023).	51
Figure 3-4:	Sites PR1 - PR3, source proportion distribution (%) summaries for MixSIAR model runs.	52
Figure 3-5:	Site PR4, source proportion distribution (%) summaries for MixSIAR model runs.	53
Figure 3-6:	River Confluence PR5 (Watkin Creek), source proportion distribution (%) summaries for MixSIAR model runs.	54
Figure 3-7:	River Confluence PR6, source proportion distribution (%) summaries for MixSIAR model runs.	55
Figure 3-8:	River Confluence PR7, source proportion distribution (%) summaries for MixSIAR model runs.	56
Figure 3-9:	River Confluence PR8, source proportion distribution (%) summaries for MixSIAR model runs.	57
Figure 3-10:	River Confluence PR9 (upper Pleasant River catchment), source proportion distribution (%) summaries for MixSIAR model runs.	58
Figure 3-11:	Pleasant River Estuary - contributions of sediment sources to recent deposition at sampling sites, May 2023.	60
Figure 3-12:	Thorburn Road Creek – estuary sites E7 to E9, source proportion distribution (%) summaries for MixSIAR model runs.	62
Figure 3-13:	Intertidal flats – west of channel – estuary sites E12, G4 and G6, source proportion distribution (%) summaries for MixSIAR model runs.	63
Figure 3-14:	Intertidal flats east of channel – estuary sites E10, E11 and E14, source proportion distribution (%) summaries for MixSIAR model runs.	65
Figure 3-15:	Intertidal flats east of channel – estuary sites E15 and E16, source proportion distribution (%) summaries for MixSIAR model runs.	66
Figure 3-16:	Intertidal flats east of channel – estuary sites G1, G3 and G8a, source proportion distribution (%) summaries for MixSIAR model runs.	66
Figure B-1:	Hand corer for soil sampling.	86

## Executive summary

Otago Regional Council is working with Kāti Huirapa Rūnaka ki Puketeraki, East Otago Catchment Group and the local community to improve the environmental condition of the Pleasant River Catchment and Estuary. The ecological health of the estuary has been adversely impacted by sedimentation and nutrient runoff, with dense algal mats, anoxic water conditions and mud accumulation in the estuary. The Pleasant River Catchment Project aims to reduce diffuse-source sediment and nutrient run off into the river, estuary and coastal receiving environments. ORC commissioned the National Institute of Water and Atmospheric Research (NIWA) to undertake a study of the Pleasant River Catchment and Estuary (Te Hākapupu) to determine:

- Contemporary sources of river sediment deposits (by sub-catchment and land use) for selected confluences and at sub-catchment outlets to the Pleasant River Estuary.
- Contemporary sources of sediment depositing in the Pleasant River Estuary, by sub-catchment and land use.

NIWA's compound specific stable isotope (CSSI) sediment-tracing technique was used to determine sources of contemporary sediment deposits accumulating in the Pleasant River Catchment and Estuary. The CSSI method employs the isotopic signatures (i.e.,  $\delta^{13}\text{C}$ ) of fatty-acid (FA) biomarkers secreted by plant roots. These FAs are naturally bound to soil particles thereby labelling that soil as coming from a specific land use, defined by that plant community.

Samples of soils and sediment from potential sources and sediment deposits from the river network and the Pleasant River Estuary (PRE) were collected in May 2022 for isotopic analysis. Sampling included topsoil (i.e., land uses, 26 sites), subsoil (4 sites), streambank sediment (4 sites), river-sediment deposits (37 sites) and in the estuary (20 sites). Tissue samples from estuarine/marine plants (i.e., kelp, algae, saltmarsh) were also analysed. The  $\delta^{13}\text{C}$  FA data for these samples were used to: (1) create a soil/sediment source library; and (2) apportion the contribution of the potential sources to the sediment mixtures (i.e., deposits) from the river and estuarine receiving environments. Mixing models were used to determine the contribution of sub-catchments and land use activities to river sedimentation downstream of major confluences as well as the contribution of land use to present-day estuary sedimentation. A two-endmember mixing model (2-EMM) was used to determine sub-catchment contributions and the MiXSIAR model was used to apportion sources (i.e., % soil) by land use, subsoil and streambank erosion.

Pasture and fodder crop land uses were not isotopically distinct from each other and were subsequently merged into a single source. Estuarine sediment deposits were substantially isotopically enriched (i.e., up to 10 per mil (‰)) in comparison to catchment soils and river sediment deposits. This indicated a missing source for the contemporary estuarine sediment deposits. Previous CSSI sediment studies identified a marine sediment endmember as the likely missing source. This marine endmember will typically include a substantial fraction of legacy terrigenous sediment discharged to the marine environment that is isotopically altered over time. In the present study, samples from the flood-tide delta of the estuary were ultimately used as a marine source proxy (Section 2.6).

This study has identified the major contemporary sources of sediment in the Pleasant River–Estuary system. The main conclusions and recommendations of this study are:

- Trotters Creek contributes a large fraction of the long-term suspended sediment load discharged (i.e., ~77%) from the Pleasant River Catchment. The results of the 2-EMM analysis (Table 3-2) yield sub-catchment proportional contributions in general agreement with NZ River Maps long-term suspended sediment loads.
- A substantial fraction of present land use in the Trotters Creek sub-catchment is dry stock pasture, with production forest progressively being established. Land use intensification and/or disturbance of vegetation cover on steeplands will likely exacerbate soil erosion in this sub-catchment. Given the underlying susceptibility of Trotters Creek to soil erosion, it would be prudent to manage land use in a way that is consistent with long-term restoration plans for the Pleasant River Catchment.
- Streambank and subsoil erosion are the primary sources of sediment depositing in the river system (Figure 3-2 and Figure 3-3). Streambank and subsoil erosion, combined, account for more than 80% of sediment deposited at most sampling sites. At catchment outlets (i.e., PR1–PR4), streambank erosion accounted for as much as 98% of deposited sediment. Streambank and hillslope slip mapping would inform soil conservation activities in line with restoration outcomes sought by the community.
- Production forestry is a major land use in the Pleasant River catchment. The land use sources of recent sedimentation in the estuary suggests that pine harvest areas have specific proportional yields of topsoil (% soil km<sup>-2</sup>) that are ~69-fold higher than from pasture-fodder crops. This yield estimate is based on the area of pine harvest during the period September 2019 – December 2021 (i.e., 1.07 km<sup>2</sup>), prior to sediment sampling (May 2022). Production forestry practices result in ongoing vegetation removal and expose steepland soils to erosion. Large areas of first rotation pine forest have yet to be harvested. Careful management of future pine forest harvesting will be required to mitigate excessive soil erosion.
- The majority of recent sediment depositing in the Pleasant River Estuary is derived from the isotopically-enriched marine source (i.e., mean 87–97%, Figure 3-11). This legacy marine sediment will ultimately be derived from catchment soil erosion. This legacy sediment is likely remobilised from a nearshore mud deposition zone (Figure 2-20). The dominance of the marine source in the estuarine sediment (i.e., 87–97%) indicates that coastal processes regularly transport fine sediment into the estuary. Most of this sediment is accumulating in the sheltered side arms/creeks and saltmarsh habitat. The marine mud sink will be replenished from time to time by catchment floods. Managing the major catchment sources of sediment would reduce the supply of legacy marine sediment over the long-term, assuming that most of the marine sediment originates from the Pleasant River.
- Sediment management in the Pleasant River catchment is required to mitigate chronic effects of episodic fine-sediment inputs during flood events. Potential effects include reduced optical water quality (i.e., visual clarity, light penetration), smothering of benthic communities and changes sediment quality. For example, the loss of subtidal seagrass habitat in NZ estuaries (Tan et al. 2020) has been exacerbated by poor optical water quality and increased substate mud content associated with fine-sediment inputs (Mangan et al., 2020; Zabarte-Maeztu et al., 2021). Seagrass is absent from the Pleasant River Estuary (Roberts et al., 2022), despite extensive areas of intertidal flat.

# 1 Introduction

## 1.1 Background to study

The Pleasant River (Te Hākapupu) catchment is located on the Otago Coast some 40 km north of Dunedin City (Figure 1-1). The Otago Regional Council (ORC) are presently working in partnership with Kāti Huirapa Rūnaka ki Puketeraki to restore and enhance the mauri and health of this catchment-estuarine system. The ecological health of the system has been impacted by sedimentation and nutrient runoff from the catchment, with dense algal mats, anoxic water conditions and mud accumulation in the estuary. Restoration of the Pleasant River catchment (2021–2025) is presently being undertaken with central government funding (Otago Daily Times, 21 December 2021).

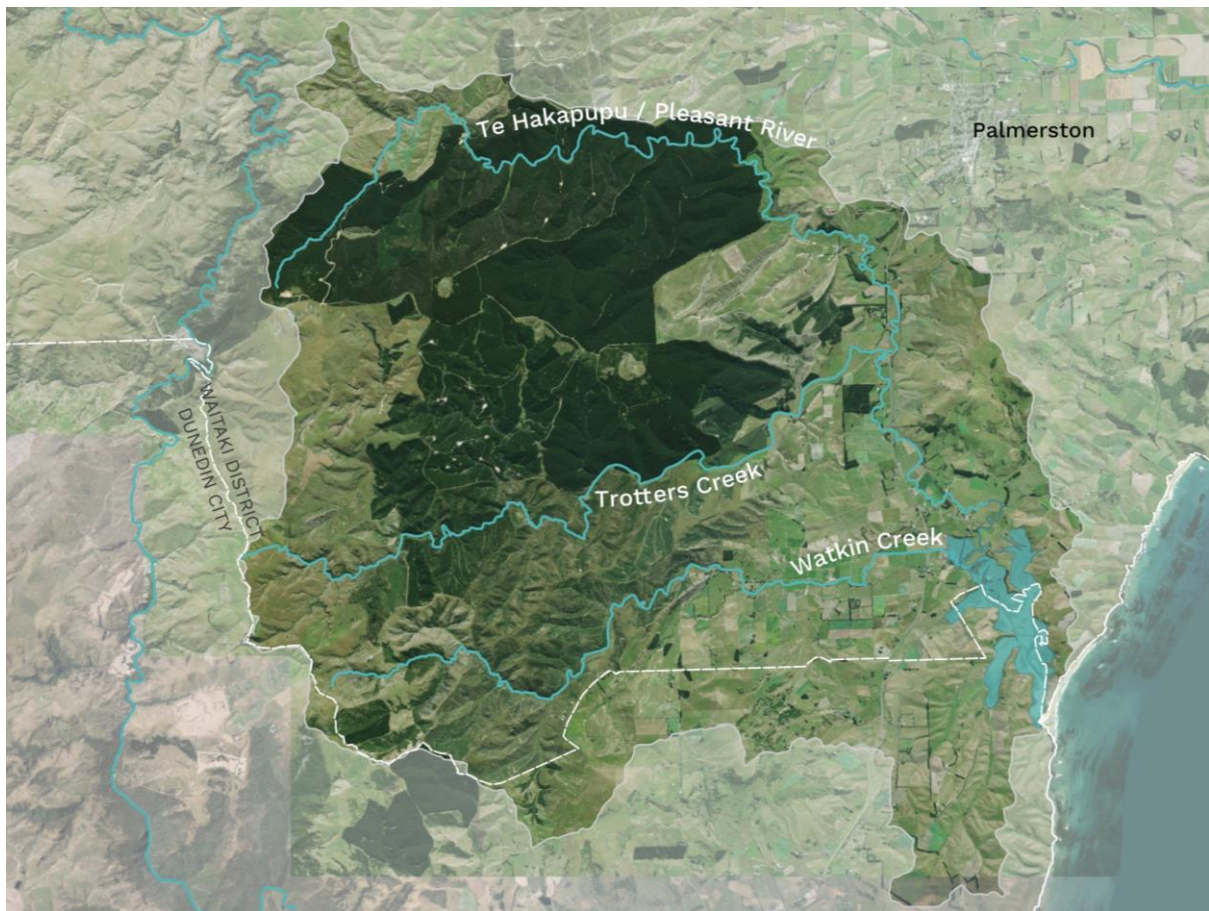
Otago Regional Council is working with the Pleasant River community to improve the environmental condition of the river and estuary. The Pleasant River Catchment Project aims to reduce sediment and nutrient run off into rivers and streams within the catchment, Pleasant River Estuary, and the receiving coastal environment. The Pleasant River Estuary has experienced increased sedimentation over the past few years (Sam Thomas, ORC Coastal Scientist). Areas with gross eutrophic conditions (i.e., muddy anoxic sediment with high biomass nuisance algal beds) have also developed in the estuary and anecdotal accounts indicate that mud deposition is progressively spreading from the upper reaches of the estuary to the intertidal sand flats of the mid-estuary (pers comm: Mr Hamish McFarlane, East Otago Catchment Group [EOCG], February 2022). Kelp forest on the adjacent open coast is also under threat from warming seas, with sedimentation reducing the resilience of the kelp to adapt to higher sea temperatures. Reductions in sediment load to the coastal environment will also reduce stress on these kelp forests.

To effectively reduce sediment and nutrient run off through catchment interventions, an understanding of the critical sources of these key stressors is required, so that effective mitigation options can be targeted optimally. This will be achieved by working with the community, iwi and other key stakeholders, utilising information that identifies the sources of fine sediment and nutrients. This information will inform a collaborative approach to develop solutions that will reduce contaminant loads, thereby improving freshwater and estuarine health over the long term.

The objective of the Toitū Te Hākapupu - Pleasant River Catchment Restoration Project (PRCRP) is to develop a management plan to enhance water quality and ecosystem values. The aim of which is to restore the estuary as a source of kai, that in the past included tuna (eels), pātiki (flounders) and īnaka (whitebait). The PRCRP work programme includes:

- Identifying sites where the most sediment and/or nutrients are getting into the river and working with landowners to find ways to reduce the effects on water quality.
- Working with landowners to develop sediment management plans to help reduce sediment and nutrient input into the water.

The draft catchment management plan will be released in March 2024 for consultation.



**Figure 1-1: Pleasant River Catchment and major tributaries.** Source: <https://yoursay.orc.govt.nz/te-hakapupu>

## 1.2 Legislation considerations

The Pleasant River restoration project is in line with recent policy - *Essential Freshwater: Action for healthy waterways – decisions on the national direction and regulations for freshwater management*” (Ministry for the Environment, 2020). This NPS-FM refresh signals a new direction for freshwater management with the key objectives of:

- stopping further degradation of New Zealand’s freshwater resources and make immediate improvements so that water quality is materially improving within five years, and
- reversing past damage to bring New Zealand’s freshwater resources, waterways, and ecosystems to a healthy state within a generation.

The NPS-FM (2020) recognises that land use intensification has contributed to major degradation of estuaries and that sediment is one of the most prominent environmental stressors in New Zealand freshwater and estuarine environments. Councils are required to develop plans that address degradation of freshwater and estuaries (enact by 2026) and to shift the emphasis from effects- to limits-based management. The framework for limit-setting will change with the introduction of the Natural & Built Environment Act (NBA). The purposes of setting environmental limits under the NBA will be prevent further degradation the ecological integrity of the natural environment and to protect human health. Environmental limits will be mandatory for coastal water, estuaries, freshwater and



soil among other considerations and be expressed in relation to the ecological integrity of the natural environment or to human health. Environmental limits must also be set to reflect the state existing in a management unit or the amount of harm or stress occurring to the natural environment (i.e., when the NBA becomes law). Under the NBA, environmental limits *may be qualitative or quantitative, set at different levels for different management units, and in a way that integrates more than one aspect of the natural environment.*

Nearshore coastal waters, especially estuaries, have been increasingly degraded by excessive land-derived contaminants, in particular sediment, nutrients and urban-derived stormwater contaminants. This degradation has been exacerbated by land-use intensification, urban expansion, and coastal development (Schiel and Howard-Williams, 2016). Sediment has been ranked in the top three threats to New Zealand's marine habitats, along with ocean acidification and global warming (MacDiarmid et al. 2012). Although soil erosion and deposition in New Zealand estuarine and coastal marine receiving environments is a natural process, the rate at which sedimentation is now occurring is ten-fold higher than before human activities disturbed the natural land cover (e.g., Swales et al. 2002, Thrush et al. 2004, Hunt, 2019). In New Zealand, increases in sediment loads to estuaries and coastal ecosystems coincided with large-scale deforestation, which followed the arrival of people about 700 years ago (Wilmshurst et al. 2008).

Soil erosion rates in New Zealand are naturally high by global standards due to steep terrain, weathered and erodible rocks, generally high rainfall, and frequency of high-intensity rainstorms (Basher, 2013). Historical catchment deforestation, large-scale conversion to pastoral agriculture and land-use intensification and catchment disturbance have increased erosion rates. Important erosion processes include rainfall-triggered shallow landslides, earthflows and slumps, gully and surface erosion (i.e., sheet, rill) and streambank erosion. Landslide occurrence is reduced by 70 to 90% by closed-canopy woody vegetation and maintenance of groundcover on hillslopes is an important factor reducing surface erosion (Basher, 2013).

### 1.3 Study Objective

The present study by the National Institute of Water and Atmospheric Research (NIWA) of contemporary sources of sediment depositing in the river system and estuary has been commissioned by ORC. The specific objective of the work is to determine the proportional contributions of major land use activities and sub-catchments to recent sedimentation (ORC - weblinks, References). The sources of fine sediment depositing in the river and estuary were determined using NIWA's Compound Specific Stable Isotope (CSSI) sediment tracing method. Sediment sources were identified by land use (i.e., topsoil), subsoil and streambank sediment erosion.

The specific objectives of the proposed study were to determine:

- Contemporary sources of river sediment deposits (by sub-catchment and land use) for selected confluences and at sub-catchment outlets to the Pleasant River Estuary.
- Contemporary sources of sediment depositing in the Pleasant River Estuary (by sub-catchment and land use).

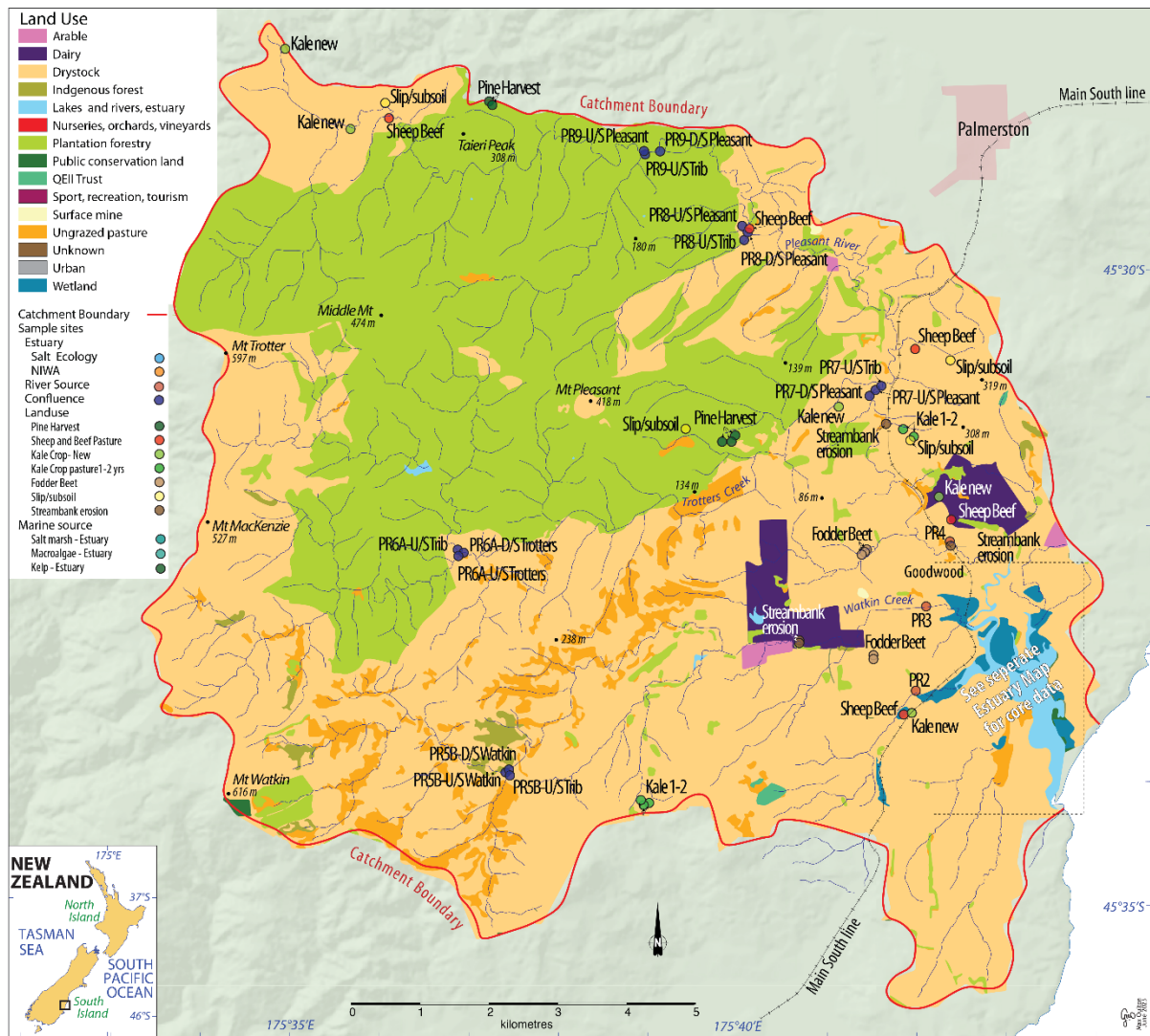
## 1.4 Catchment and estuary characteristics

Land use in the 128 km<sup>2</sup> Pleasant River catchment is primarily pastoral agriculture (largely sheep and/or beef, 58%), plantation forestry (26%) and deer and mixed livestock (5%) (Figure 1-2). The catchment discharges to the Pleasant River Estuary. Although there are no rainfall or flow data for the catchment, measurements are available for the Waikouaiti River Catchment that is located immediately to the south (Otago Regional Council, 2008). Both catchments have a similar physiographic setting on the North Otago coast. Freshwater discharge from Waikouaiti River is limited under normal conditions because of low and sporadic rainfall across the catchment. Annual rainfall averages 600–800 mm within several kilometres of the coast (ORC, 2008, Fig 3.1). Specific discharges are  $\leq 0.01 \text{ m}^3 \text{ s}^{-1} \text{ km}^{-2}$  (mean flow) and  $< 0.64 \text{ m}^3 \text{ s}^{-1} \text{ km}^{-2}$  (mean annual flood).

The estuary is relatively small in comparison to its land catchment, with a high-tide area of 0.97 km<sup>2</sup> and infilled with sediment, being 76% intertidal and a spring-tidal prism of some 972,000 m<sup>3</sup>. Estimated spring- and neap-tidal ranges are 1.6 and 1.24 m respectively (NZ Estuary Classification database, Hume et al., 2007). The estuary is permanently open to the sea, unlike some Otago estuaries (Figure 1-3). The estuary has several ecological and physical characteristics that are relatively rare in the Otago Region, as well as significant natural values (key species: Glasswort, *Puccinellia*, Rekoreko, Sea primrose and Jointed rush). The estuary is also a habitat for coastal bird species (Bar-tailed Godwit, Banded Dotterel, Pied Stilt, Southland Pied Oyster Catcher). The estuary is listed in the Waitaki District Plan Schedule of Area of Significant Nature Conservation Value and Geopreservation Sites.

Major estuarine habitats in the Pleasant River Estuary include mudflats, sandflats, saltmarsh (84 ha) and a flood-tide delta composed of mobile sand near the mouth of the estuary. Mud deposits (i.e., > 50% mud) comprise ~17% of the intertidal flats and primarily occur in the low-energy side arms/creeks and saltmarsh habitat (Figure 1-4 to Figure 1-7). Eutrophic conditions occur in sediment deposits in the side arms/creeks and parts of the mid estuary. Saltmarsh (mainly herbfield) is a major habitat type, covering 37% (48 ha) of the intertidal area (Roberts et al., 2022). The present condition of the estuary indicates that the Pleasant River estuary's capacity to assimilate nutrient and sediment inputs is currently being exceeded (Roberts et al., 2022).





**Figure 1-2: Pleasant River Catchment land use and soil and sediment sampling sites.** Land use data: Otago Regional Council (October 2021). Refer to Figure 2-18 map of estuary sediment sampling site locations.



**Figure 1-3: Pleasant River Estuary and sand barrier (2014).** Source: Foote (2016).



**Figure 1-4: Flood-tide delta sand body, lower estuary.** Mobile sand transported into the estuary by flood-tide currents. Estuary sediment sampling sites E1 and E2 located in this area. Photo: A. Swales (NIWA), 20 February 2022.



**Figure 1-5: Intertidal sand flats, lower and middle estuary.** Estuary sediment sampling sites E3–E4, E6, E7 and G7 for CSSI analysis located in this area. Photo: A. Swales (NIWA), 20 February 2022.





**Figure 1-6: Intertidal mudflats flats with macroalgae in the Thorburn Road creek, lower estuary.** Estuary sediment sampling sites E8–E10 and G1 located in the lower reaches of this creek. Samples of macroalgae collected in the upper reaches of creek, shown here. Photo: A. Swales (NIWA), 20 February 2022.



**Figure 1-7: Extensive areas of saltmarsh and Intertidal mudflats in the upper estuary.** Estuary sediment sampling sites E16 and G8A located in this area. Photo: A. Swales (NIWA), 19 February 2022.

#### 1.4.1 Catchment sediment loads

Estimates of long-term annual average suspended sediment loads for sub-catchments draining to the Pleasant River estuary are provided by NIWA's NZ River Maps (NZRM, Booker and Whitehead, 2017). The NZRM tool is a national-scale multi-variate statistical model based on data provided by the River Environment Classification (REC-1). Sediment yield data incorporated in NZRM is derived from measured suspended sediment yields from 233 New Zealand catchments (Hicks et al. 2011). Estimates of annual average suspended sediment loads are summarised in Table 1-1. Annual average suspended sediment load estimates for the Pleasant River catchment at various locations are presented in Table 1-1. The total annual average suspended sediment load to the Pleasant River estuary is 12,860 t yr<sup>-1</sup> of which 77% is derived from the Trotters Creek sub-catchment.

**Table 1-1: Pleasant River Estuary - summary of long-term annual average catchment sediment loads.**  
 Sub-catchment suspended sediment loads and mean annual flow (Source NZ River Maps, <https://shiny.niwa.co.nz/nzrivermaps/> Booker and Whitehead, 2017).

Sub-catchment	Area (km <sup>2</sup> )	Mean flow (m <sup>3</sup> s <sup>-1</sup> )	SS Load (t yr <sup>-1</sup> )	Specific SS Load (t km <sup>-2</sup> yr <sup>-1</sup> )
<b>Estuary Catchment</b>	<b>130.1</b>		<b>12 860</b>	<b>98.8</b>
<u>Pleasant River at outlet</u>	118.1	0.89	<b>12 360</b>	104.7
Trotters Creek at PR confluence	38.6	0.27	9 922 (77%)	257.0
Watkin Creek at PR confluence	85.7	0.21	847 (7%)	9.9
Pleasant River upstream of Trotters Creek confluence	36.7	0.22	2 529	68.9
Pleasant River at Stenhouse Road crossing	32.9	0.20	2 444	74.3
Pleasant River at Noones Road crossing	8.9	0.05	577	64.8
<u>Bendigo-Thorburn Rd catchment</u> – eastern shore of estuary	7.0	0.05	<b>354</b> (3%)	50.6
<u>Thorburn Rd catchment</u> – eastern shore of estuary	5.0	0.04	<b>146</b> (1%)	29.2

## 2 Methods

### 2.1 CSSI sediment source tracing - overview

Sediment source tracing (aka sediment fingerprinting) is a widely used technique for determining the proportional contributions of catchment soil sources to sediment mixtures transported and deposited in rivers, estuaries and marine environments (e.g., Blake et al. 2012, Wildhaber et al. 2012, Hancock and Revill, 2013, Smith et al. 2018, Gibbs, 2008, 2014a, 2020). Sediment tracing techniques calculate source proportions from a whole (e.g., %) rather than absolute quantities. However, by combining source proportion information with sediment yield ( $\text{t km}^{-2}$ ) or sedimentation rate ( $\text{t m}^{-2} \text{yr}^{-1}$ ) data the contribution of various sources can be quantified. The technique has developed rapidly over the last several decades to address research questions and inform catchment management (Owens et al. 2016, Smith et al. 2018). Sediment tracing studies have employed a range of tracers, including sediment properties (i.e., size, shape, colour), fallout radionuclides ( $^7\text{Be}$ ,  $^{137}\text{Cs}$ ,  $^{210}\text{Pb}$ ), geochemistry (e.g., trace metal concentrations), pollen, microbes, magnetic susceptibility, and organic compounds. Source tracing used together with information on sediment transport can provide insights into landform processes and evolution (Owens et al. 2016).

In the present study, a sediment tracing method developed by NIWA employing compound specific stable isotopes (CSSI) is used to apportion sediment sources. The CSSI sediment tracing technique is based on the natural abundance isotopic signatures of specific organic compounds, primarily fatty acids (FA) (i.e., delta carbon-13,  $\delta^{13}\text{C}$ , referred to as FA isotopic value, units: per mil, ‰) in soils and sediment. In the present study, FA biomarkers were used to determine sources of riverine and estuarine sediment deposits in the Pleasant River system. A unique attribute of the CSSI tracing technique that makes it particularly useful for land management is that sediment sources are identified by stable isotope signatures of the FA biotracers produced by plant communities (i.e., land use) (Figure 2-1).

The CSSI sediment tracing technique is based on the following key concepts:

- Plants label the soils they grow in with organic compounds, including FAs, that are primarily exuded by their roots (Gibbs 2008). The molecular weight and size of the FA hydrocarbon chain also imparts hydrophobicity to the molecule. This means that larger FA molecules (i.e.,  $>\text{C}_{20}$  atoms) will also be bound to soil through non-polar interactions such as van der Waals forces.
- Plant FAs are slightly water soluble but highly polar, so that they spread through the soil in the root zone and ionically bind to the soil particles.
- The suite of FA  $\delta^{13}\text{C}$  values from carbon chain lengths of 12 (C12:0) to 32 (C32:0) provides a unique ‘fingerprint’ for different plant communities (i.e., land uses).
- Although the quantity or concentration of FAs in sediment may reduce over time due to microbial decay, the isotopic value does not change (i.e., FA isotopic values are conservative) (e.g., Glaser, 2005, Kohn, 2010).
- Plant FAs label soils irrespective of particle size so that adoption of isotopic values (as opposed to concentration) avoids issues with using concentration due to particle-size dependency (Owens et al. 2016, Smith et al. 2018).

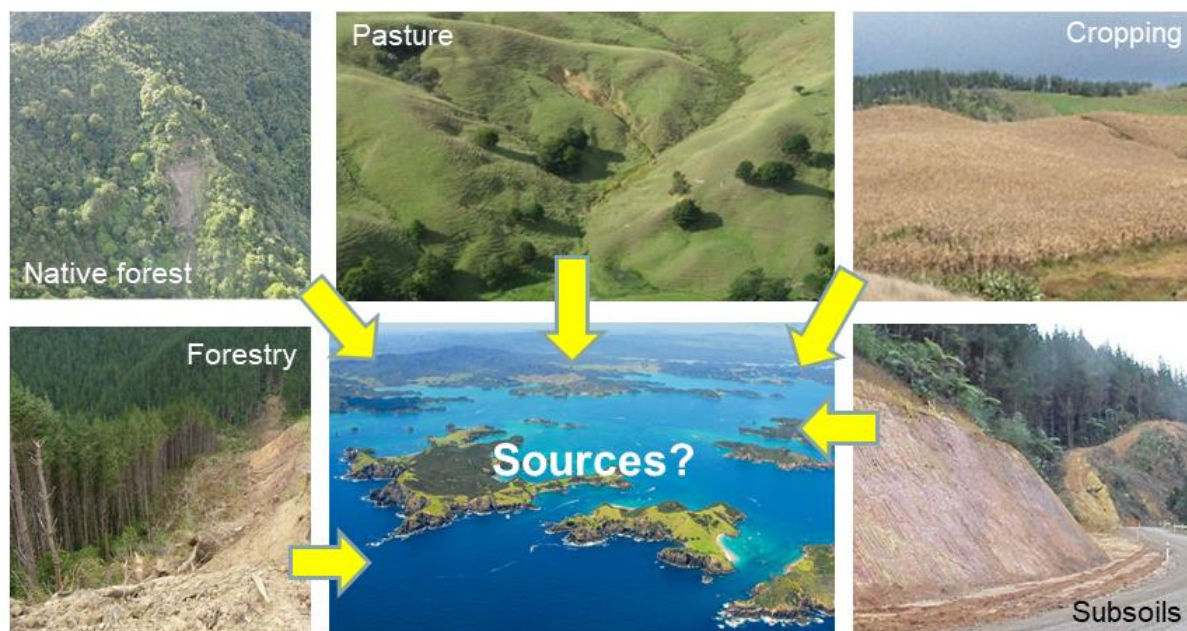
- Changes in the isotopic signatures of FAs in soils occur in response to changes in plant communities over time (e.g., native forest > radiata pine > pasture grass). These changes occur over time scales of months to years (Swales and Gibbs, 2020).

FAs persist in sediment over long time scales (i.e., decades–centuries) (e.g., Gibbs, 2008). By linking these CSSI fingerprints of land use to sediment in depositional environments, this approach has been shown to be useful for determining sources of catchment sediment (e.g., Blake et al. 2012, Wildhaber et al. 2012, Hancock and Revill 2013, Alewell et al. 2016, Upadhayay et al. 2018, Gibbs et al. 2020). The CSSI sediment-source tracing method is summarised in Figure 2-2 and details of the key concepts underpinning the method are described in more detail in Appendix A.

In the present study, CSSI sediment tracing can be applied in a catchment-to-sea sediment accounting approach. The CSSI sediment-tracing approach can be used to:

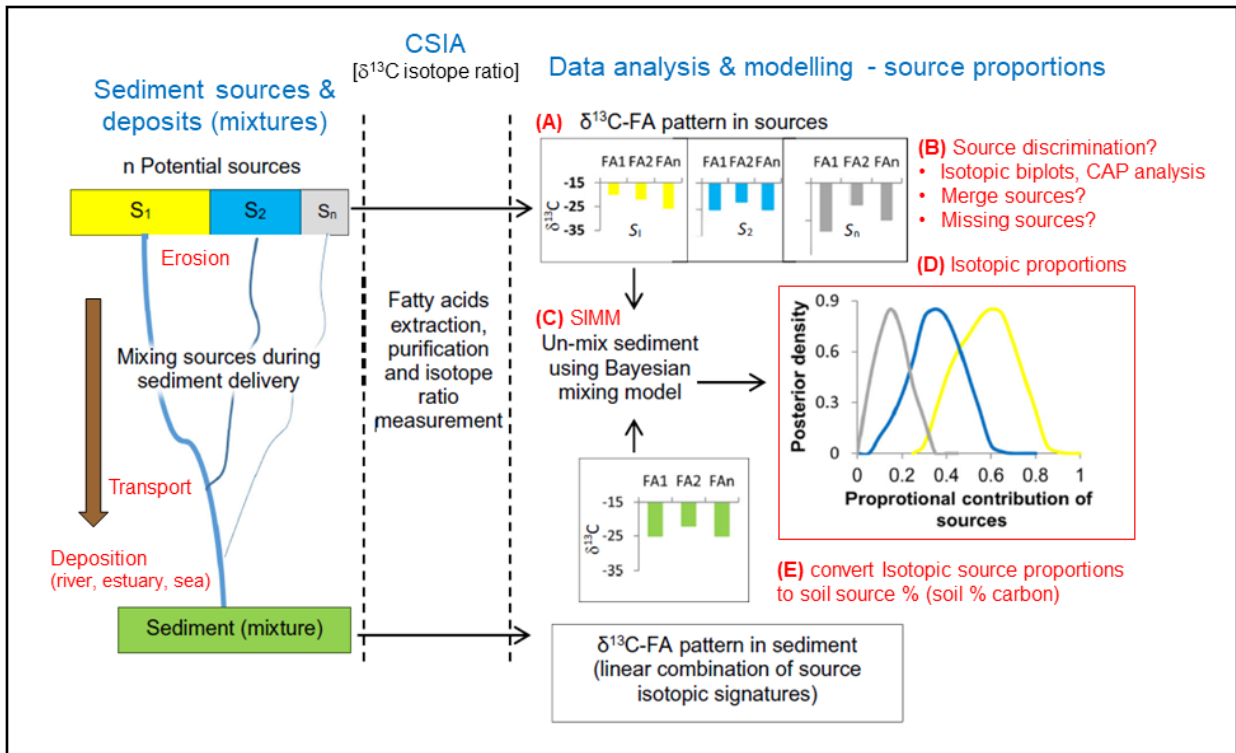
- Differentiate sediment sources by land use (i.e., plant community) type.
- Differentiate sediment derived from streambank and subsoil sources from land use sources.
- Determine the contribution of sediment by subcatchment.

Estimate source-specific sediment yields (e.g., tonnes km<sup>-2</sup>) when percentage source proportions are coupled with sediment yield data, by subcatchment and/or for a specific land use.



**Figure 2-1: CSSI sediment source tracing.** A sediment-tracing method based on the concept of compound specific stable isotope (CSSI) signatures of fatty-acid (FA) soil biomarkers that are produced by plants. The isotopic signatures of these biomarkers can be used to identify different plant communities (i.e., land use).





**Figure 2-2: Summary of the CSSI sediment-source tracing method.** Definitions: (1) Compound Specific Stable Isotope Analysis (CSIA), (2) Stable Isotope Mixing Model (SIMM) Figure adapted from: Upadhyay et al. (2017).

Two fundamental decisions are required in any sediment source tracing study:

- **Which potential sources to include?** Potential sources can be selected based on a number of criteria. Land use and topographic maps and land use classifications incorporating information on erosion susceptibility (e.g., slope, soil type, vegetation cover) can be used to identify potential contemporary sources. General understanding of catchment geomorphology can also be applied. For example, streambanks can be important sources of fine sediment in many New Zealand catchments (Basher, 2016, Smith et al. 2019). In production forests, soil erosion risk on hill slopes is substantially higher after harvesting and persists for several years after harvested areas are replanted (Phillips et al. 2012). Council land management officers and scientists can provide catchment-specific information to guide selection of potential sediment sources. Development of a reliable land-use history is also important if the assessment of sediment sources includes reconstruction of historical changes using tracers preserved in sediment cores. The possibility of a missing source(s) can also be identified by plotting source and mixture tracer data. Reviewing knowledge of the system and/or literature can be helpful to identify a potential missing source. Potential sources may also need to be combined if sample variability is such that individual sources cannot be distinguished based on statistical measures (Phillips et al. 2014).
- **Which tracers to use?** Identify the most suitable **suite of tracers** to determine sediment source contributions to a sediment mixture. The standard approach to tracer selection in studies employing a large number of geochemical and radioisotope tracers

(e.g., dozens) employs a number of steps. These steps typically include exploratory data analysis (e.g., plotting data to identify outliers, separation of sources by tracer), statistical analysis of tracer discrimination, identification and exclusion of tracers exhibiting non-conservative behaviour and/or sediment-property specific behaviour (e.g., concentration dependency on particle size), and inform tracer selection based on knowledge of hydrological and geochemical processes that control tracer behaviour. The overall objective is to minimise the number of tracers employed in a mixing model employing least-squares optimisation in combination with Monte-Carlo (i.e., random) sampling (Owens et al. 2016; Smith et al. 2018).

In the present study, the Bayesian mixing model, MixSIAR, employing a Markov Chain Monte Carlo (MCMC) sampling approach was used to construct the probability distributions of sources (Stock et al. 2018). A key advantage of MixSIAR is that it can incorporate and account for uncertainty in the isotopic signatures of each source and resulting estimates of source contributions to a sediment mixture. Using this approach, Smith et al. (2018) evaluated tracer selection using synthetic sediment mixtures and found that: (1) the most accurate source apportionment results were achieved by retaining tracers that exhibited conservative behaviour, and (2) selection based on minimising the number of tracers and maximising source discrimination did not produce more accurate results.

A key selection criterion for tracers and sources is that they must conform to the isotopic biplot polygon principle, which is the fundamental basis of isotopic mixing models. Specifically, the  $\delta^{13}\text{C}$  values of the mixture samples (i.e., sediment from aquatic receiving environments) must be enclosed with a polygon (two tracers) defined by the  $\delta^{13}\text{C}$  values of potential sources (Phillips et al. 2014). Typically, multiple tracers are employed in modelling of sources to improve the discrimination of sources and confidence in the results.

## 2.2 Sediment source library

The contribution of catchment soils to sedimentation in the river and estuary was evaluated by developing a catchment-specific FA source soil library. This library is composed of samples of topsoil from major land uses, streambank sediment and subsoil from a total of 33 catchment sites, as well as a marine sediment source as described below. Soil samples of each catchment source type as well as sediment from river deposits were collected during 16–18 May 2022). A table listing all sampling locations and GPS coordinates are provided in Appendix E. Soils were sampled at sites that were easily accessible by vehicle and/or foot. The soil samples were used to assemble a FA soil source library for contemporary sediment sources. These data were used to:

- Determine the relative contribution of fine soil sources to river sediment deposits by sampling at major confluences.
- Identify the sources of fine sediment depositing in the Pleasant River Estuary.

Modelling of land use at confluences requires two or more sources in the upstream catchment.

Exploratory data analysis and modelling of FA isotope data for the estuarine sediment samples unambiguously indicated a missing end-member sediment source with a highly enriched isotopic signature (i.e., less negative  $\delta^{13}\text{C}$  values) in comparison with the catchment sources. Based on



previous work (e.g., Swales et al., 2016a; 2021a, b), this missing end-member source was most likely derived from an isotopically enriched marine sediment transported into the estuary by flood tides. Various options were considered to address this data gap, including sampling muddy sand deposits in the nearshore and immediately south of the estuary mouth, as well as using marine sediment FA data from a recent CSSI study of Pelorus Sound (i.e., Swales et al., 2021a). The approach ultimately used to determine  $\delta^{13}\text{C}$  FA values to represent a marine sediment source in the isotopic mixing model are described below.

### 2.2.1 Land use sources

Topsoil, subsoil, and streambank samples were collected from locations across the entire catchment representative of the range of land uses. The potential sources sampled included pasture, fodder beet, kale and maize crops, slips and streambank erosion sites and from plantation forests where pine trees had recently been harvested. A total of sixty land use samples were collected from 27 separate locations within the catchment. Soil erosion sources considered in this study include land use (harvested pine forest; beef and sheep pasture; fodder crops), subsoils and streambanks and river sub-catchments.

**Harvested pine forest** is defined as land predominantly with bare ground post-harvest and prior to replanting (LCDB-5 definition). This source was included as a potential sediment source rather than mature pine forest because the harvesting phase of a production forest rotation coincides with the so-called 'window of vulnerability' (O'Loughlin and Watson, 1979) during the 1–6-year period following tree removal (Phillips et al. 2012) for substantially increased soil loss. Forested landscapes (including exotic forests) generally generate less sediment than pasture landscapes (e.g., Eyles and Fahey, 2006, Phillips et al. 2012). However, when plantation forests are harvested there is the potential for increased erosion due to soil disturbance, removal of protective ground cover exposing soils to direct rainfall impact and loss of root strength (reinforcement) (e.g., Phillips et al. 2012). This increased vulnerability to soil loss occurs after harvesting, between the decay of harvested tree root systems and the establishment of the next forest rotation. This period of elevated susceptibility to soil erosion varies "depending on site conditions, tree density and other factors" (Phillips et al. 2012).

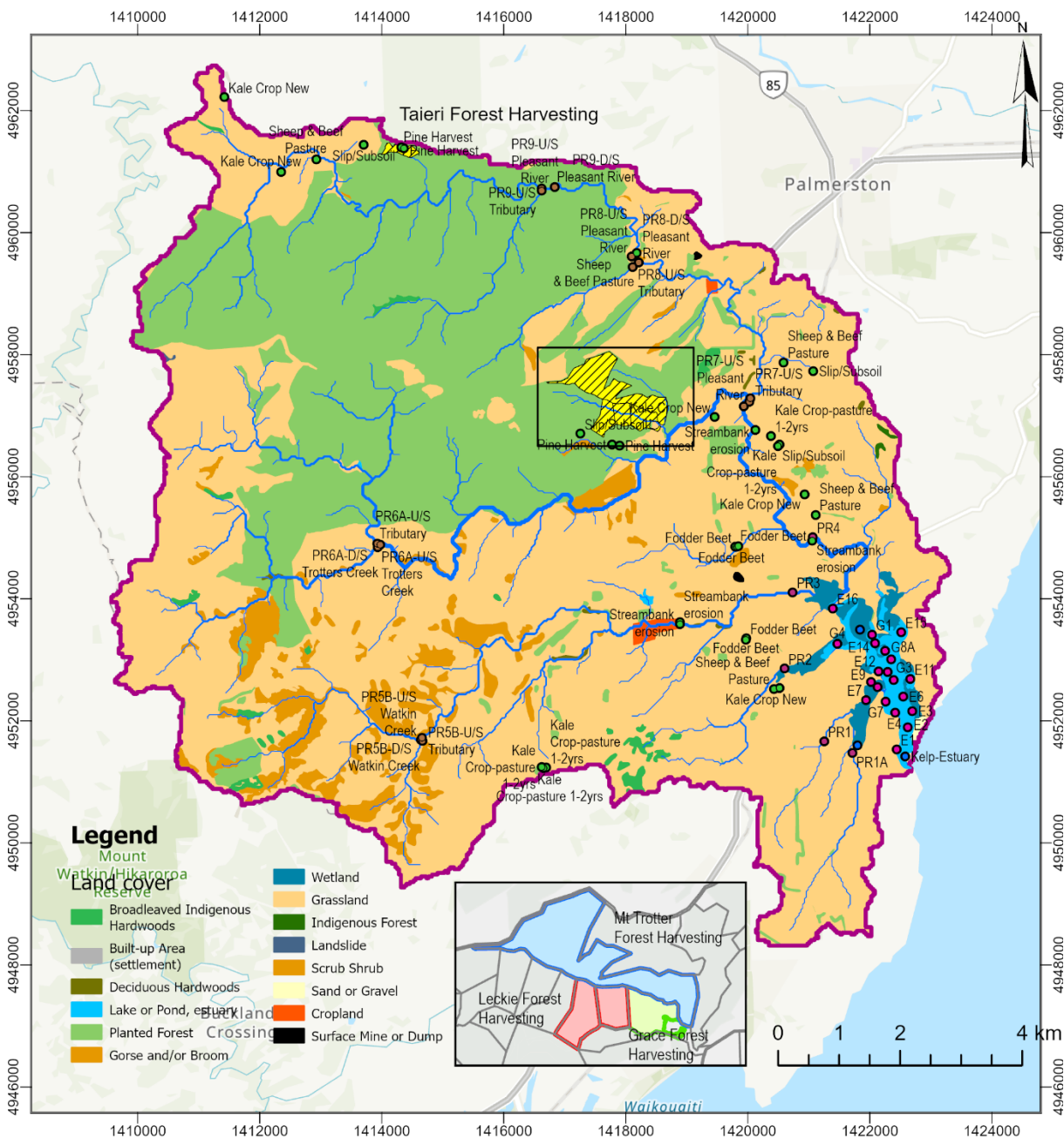
Production pine forestry was established in the 1980s, with Ngai Tahu acquiring several farms in the upper Pleasant River catchment for conversion to forestry. Today, pine forest accounts for 26% of land use in the Pleasant River catchment (Figure 1-2). The establishment of new pine forest in the upper reaches of the Watkin Creek catchment in ~2018-2019 utilized fire to clear gorse and scrub (source: Mr Hamish McFarlane, EOCG, February 2022). Details of pine harvesting operations during the 2019–December 2021 period (Source: ORC), prior to soil and sediment sampling are summarised in Table 2-1 and Figure 2-3.

**Table 2-1: Summary of production forest harvesting operations during September 2019 to December 2021.** Source: Otago Regional Council.

Site name	Area (ha)	Harvesting Period	NZTM (Easting)	NZTM (Northing)	Comments
Taieri Peak Forest	7.61	26/01/21 – 19/04/21	1413953	4961280	Noone Run Rd
Mount Trotter	63.75	04/09/19 – 31/03/20			Mt Trotter Rd
Leckie – 2 parcels	13.34, 9.64	19/05/21 – 19/08/21	1416482	4957497	Mt Trotter Rd

Site name	Area (ha)	Harvesting Period	NZTM (Easting)	NZTM (Northing)	Comments
Grace	13.17	16/10/21 – 24/12/21	1420528	4957101	Mt Trotter Rd

The main focus of forest harvesting operations during the 2019–2021 period was in the Trotters sub-catchment (i.e., Mount Trotter, Leckie and Grace sites), with a total of 99.89 ha (~1km<sup>2</sup>) harvested. These sites are located upstream of the Pleasant River-Trotters Creek confluence (i.e., PR7). The Taieri Peak Forest (7.6 ha) is located upstream of the PR9 confluence (Figure 1-2).



**Figure 2-3: Location of pine forest harvesting in the Pleasant River catchment, September 2019 - December 2021.** Source: Otago Regional Council.

Topsoil from recently harvested pine forest were sampled from 5 sites located in the Pleasant River Catchment (i.e., Trotters, Taieri Peak Forest).



**Figure 2-4: Recently harvested pine forest, upper Pleasant River catchment, May 2022.** Venture Forest sampling site at the end of Patterson Road. Harvested Pine-Rep3, Photo: 20220516\_162543.JPG, Greg Olsen (NIWA).

**Beef and sheep pasture** accounts for 43% of catchment land use and largely occurs in the lower and middle reaches of the catchment. This land use activity occupies a large proportion of the catchment not utilised for production forestry, with the largest areas in the Trotters and Watkin Creek catchments (Figure 1-2).





**Figure 2-5: Pastoral land use in the Pleasant River catchment (May 2022).** Eason’s Farm off Quarry Road. Photo: 20220518\_091058.JPG, Greg Olsen (NIWA).

**Fodder crops** grown in spring and summer are utilised with livestock farming throughout the catchment to provide bulk and quality feed during summer and winter months. Crops include Kale, swedes, turnips, rape, and fodder beet that alternate over several years with rye grass-based pastures. Cropped areas at any given time are not large in comparison to the area of pasture. In the case of winter grazing of Dairy cows, the proportion of crop areas will be larger than for drystock. Although, dairy grazing is less common in the Pleasant River Catchment than ten years or so ago. Pasture is prepared for crops by application of glyphates and other agents to suppress clovers and thistles during crop establishment (i.e., August–October).

For winter crops, sites are usually drilled in November–December or January – February depending on soil moisture levels. On some farms, pasture is sprayed once and when grass has died off, the soil is disced in a more traditional manner. The discing is effective at breaking up matted organic material at the base of the old pasture. Direct drilling has become the most common practice and usually would involve a second herbicide spray, prior to drilling to remove any pasture regrowth or weeds. Fertilisers and lime are also applied prior to drilling, usually at the spray out/drill stage and additional fertiliser is applied via the drill (i.e., DAP). Brassicas are usually planted only for two successive years because disease can affect them beyond that period. Pasture is then re-established and maintained over several years, with the actual time span depending on declines in pasture yields due to the climatic stress and ground grubs. Fodder beet cropping follows a similar rotation, although the rotation length is determined largely by pasture renewal management rather than crop disease.

Summer crops, mainly Rape, is drilled during October – November and is typically used for lamb fattening. These crops are grazed several times over summer and are re-sown in late summer–autumn, either into permanent or short-term pasture. The frequency of pasture renewal depends the land management practices on individual farms and the seasonal effects of climatic and insect stressors on pasture and crop production.



**Figure 2-6: Kale winter Cropping - Kensington Farm at end of Noones Run Rd, May 2022.** Photo: 20220516\_120156.jpg, Greg Olsen (NIWA).

**Subsoils and streambanks:** Subsoils consist of weathered regolith that underlie the topsoil (i.e., A Horizon) and are exposed at the surface by erosion processes. Unlike most topsoil's, subsoils contain relatively small amounts organic matter, including small quantities of FAs exuded from the overlying vegetation. Typically, concentrations of FAs in subsoils are ~10-fold lower than in topsoil. Subsoils gradually accumulate small quantities of FAs that percolate down through the soil profile, associated with past plant communities (i.e., over decades–centuries) as well as integrating contributions from contemporary plant communities. Consequently, the FA isotopic signatures of subsoils can be substantially different from those of the overlying topsoil. Subsoil erosion processes include hillslope failure and gullyng and can be associated with a range of land uses.

Streambanks can also be important sources of fine sediment in many New Zealand catchments (Basher, 2016, Smith et al. 2019). Streambank deposits on floodplains are composed of mixtures of sediment eroded from upstream sources that may include both topsoil associated with various land uses (i.e., plant communities), subsoils, regolith and streambanks. Streambank samples from active erosion sites were collected at four locations in the Pleasant River catchment.





**Figure 2-7: Forest track established for harvesting, Venture Forest track accessed from Patterson Rd, May 2022.** Photo: 20220516\_154439.jpg, Greg Olsen (NIWA).



**Figure 2-8: Area of subsoil erosion, sampled at Kensington Farm off Taieri Peak Rd (site Slip-Rep1), May 2022.** Photo: 20220516\_130633.JPG, Greg Olsen (NIWA).



**Figure 2-9: Streambank erosion in Pleasant River at FAMILTON FARM off SH1 (site Slip-Rep3), May 2022.**  
Photo: IMG\_3768.jpg, Elliot Bowie (NIWA).

**River sub-catchments:** Sediment deposits were collected at five confluences of major tributaries of the Pleasant River and the Trotters and Watkin Creeks sub-catchments. Sediment deposits were also collected above the tidal reach at outlets to three first-order catchments discharging to the western shore of the estuary. Sets of three samples were collected at each confluence – one in the main river channel (i.e., first end member), one in the tributary channel upstream of the confluence (i.e., second end member), and a third downstream of the confluence (i.e., mixture) at sufficient distance to ensure sufficient mixing of suspended sediment upstream of the sediment deposit sampling site. This maybe tens or hundreds of metres depending on the system scale or two or more meanders downstream of the confluence. Ideally, sampling of river deposits is undertaken within several weeks to months of a storm event that generates soil erosion, sediment transport and deposition through the river system. In the present study, the most recent notable storm occurred in January 2021 (pers. comm: Mr Hamish McFarlane, EOCG, February 2022). Figure 2-13 to Figure 2-17 show the river sediment sampling sites at major confluences and Figure 2-10 to Figure 2-12 show catchment outlets to the estuary.





**Figure 2-10: Sediment sampling at Site PR1A, outlet of small catchment discharging to the Thorburn Road tidal creek, May 2022.** Photo: Greg Olsen (NIWA).



**Figure 2-11: Sediment sampling site PR3, Watkin Creek outlet, above tidal reach, May 2022.** Photo: Elliot Bowie (NIWA).





**Figure 2-12: Sediment sampling site Site PR4, Pleasant River outlet, above tidal reach, May 2022.** Photo: Elliot Bowie (NIWA).



PR5 Upstream

PR5 Tributary

PR5 Downstream

**Figure 2-13: Sediment sampling at Confluence PR5, upper reaches of Watkin Creek, May 2022.** Photos: Greg Olsen (NIWA).



PR6 Upstream



PR6 Tributary



PR6 Downstream

**Figure 2-14: Sediment sampling at Confluence PR6, upper reaches of Trotters Creek, May 2022.** Photos: Greg Olsen (NIWA).



PR7 Upstream



PR7 Tributary



PR7 Downstream

**Figure 2-15: Sediment sampling at Confluence PR7, middle reach of Pleasant River, May 2022.** Photos: Martin Bylsma (NIWA).





PR8 Upstream

PR8 Tributary

PR8 Downstream

**Figure 2-16: Sediment sampling at Confluence PR8, upper reach of Pleasant River, May 2022.** Photos: Elliot Bowie (NIWA).



PR9 Upstream

PR9 Tributary

PR9 Downstream

**Figure 2-17: Sediment Sampling at Confluence PR9, upper reach of Pleasant River, May 2022.** Photos: Greg Olsen (NIWA).

## 2.3 Soil and sediment sampling methods

Catchment soil and sediment sampling sites are shown in Figure 1-2 and estuarine sediment sampling sites are shown in Figure 2-18.

### 2.3.1 Topsoil and subsoil

Topsoil and subsoil samples were collected at the sampling sites as composites composed of 7–10 randomly located 100 mm diameter by 20 mm thick cores collected within a ~100 m<sup>2</sup> area (i.e., quadrat). Each core was shaken to remove overlying plant material and roots. The soil released from each core was then combined and mixed to generate a composite sample. Approximately 300–400g of the composite soil was retained for analysis and remaining unused soil returned to the land. Up to five replicate composite samples were collected from each land use. Compositing of

subsamples provides an average FA isotopic signature for the land use. This method also avoids the possibility of a single sample not being representative of a sampling quadrat. Each subsample was collected using a purpose-built hand corer with the top-most 20 mm retained. This ensured that soil subsample volumes were similar and prevented bias in the composite sample. Details of the sampling protocol are described in Appendix B.

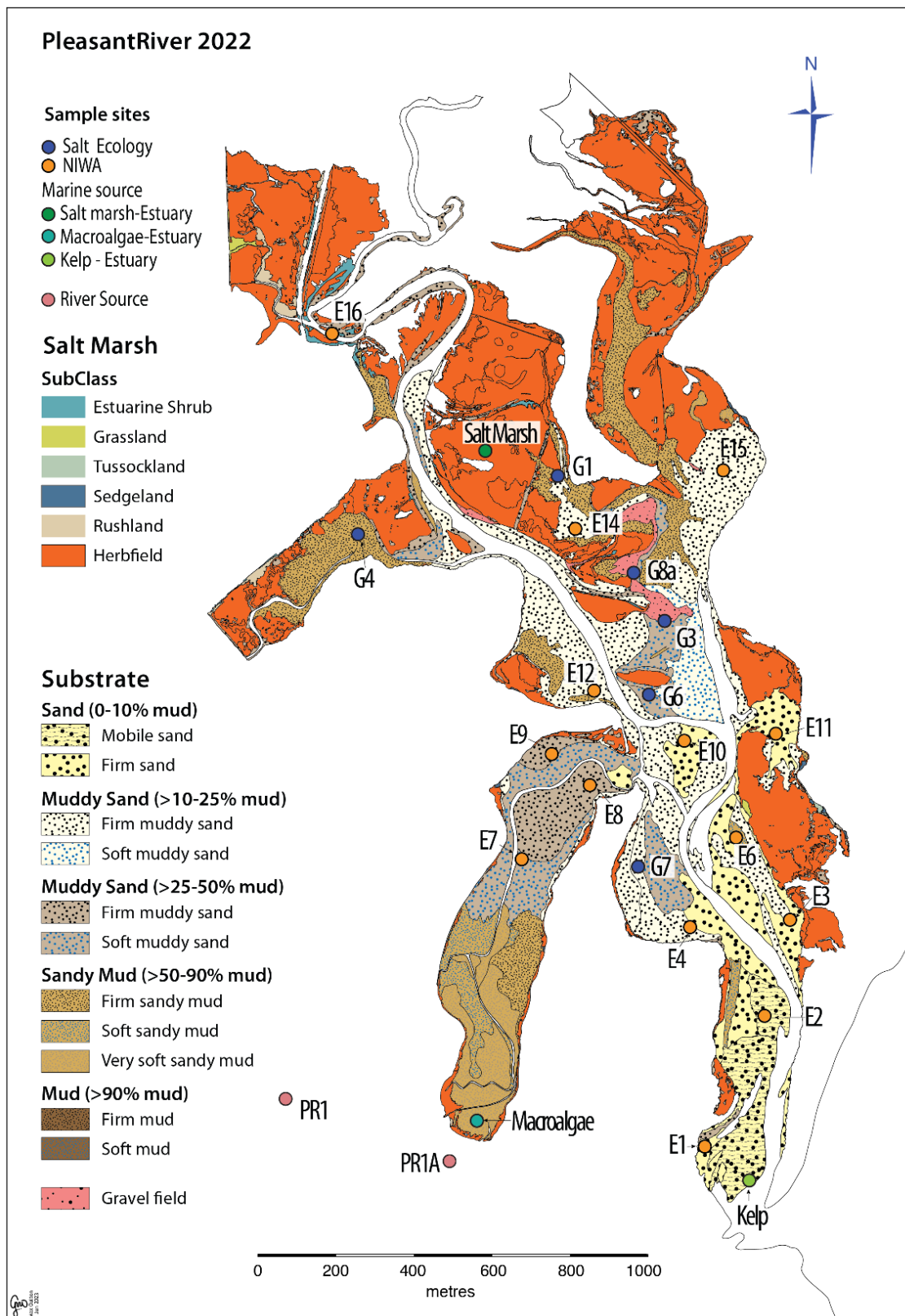
### 2.3.2 Riverine and estuarine sediment

Fine sediment deposits were collected from riverbeds, estuaries and riverbanks by taking several scrapes of the deposited layer (i.e., typically less than 20 mm) using a stainless-steel hand trowel (approximately 300-400g) and combining these into a single composite sample. This method recognises that suspended sediment associated with a flood event may be deposited as a layer of variable thickness in river networks. This is acceptable as the sediment is homogenised during transport (IAEA, 2019). Recent flood deposits can be discriminated by eye based on sediment colour and deposit morphology. The fine sediment deposits sampled from riverbeds and banks represent a mixture of all of the upstream sources that contributed to the deposit.

In estuaries we avoid sampling surficial sediment with algal growth (e.g., *Ulva* or green-pigmented sediment deposits ([microphytobenthos])).

The last notable flood event occurred in the catchment in January 2021, some 16 months prior to the sediment sampling for the present study (pers. comm: Mr Hamish McFarlane, EOCG).





**Figure 2-18: Pleasant River Estuary - spatial distribution of major intertidal habitat types (2021) and location of estuarine sampling sites in the present study.** Source: habitat mapping - Salt Ecology.

## 2.4 Bulk carbon and fatty acid analyses

The CSSI sediment-tracing technique employs two different sets of stable isotope signatures:

- Bulk  $\delta^{13}\text{C}$  values and percentage carbon (%C) of the whole soil or sediment. These were analysed on a continuous flow, isotope ratio mass spectrometer (IRMS) after acidification to remove inorganic carbonates.
- Compound specific stable isotopes (CSSI) using the  $\delta^{13}\text{C}$  values of the carbon atoms in of individual FAs biomarkers bound to soil and sediment particles.

The FA biomarkers were extracted from a known mass of unacidified freeze dried soil/sediment with dichloromethane (DCM) at 100 °C at 1500 psi in a DIONEX ASE350 accelerated solvent extraction system. The extracts were concentrated, dried and derivatised to generate fatty acid methyl esters (FAMES). Full details of the analytical method and the CSSI technique are included in Appendix A. The CSSI source library data for the Pleasant River system are presented in Appendix C

## 2.5 Multivariate ordination – source and tracer selection

The  $\delta^{13}\text{C}$  data was evaluated to identify which FA biomarkers that would be incorporated into isotopic mixing models to determine source contributions to riverine and estuarine sediment mixtures. In particular, potential sediment sources were assessed to determine to what extent they were discriminated from each other and inform decisions about merging sources where discrimination was not sufficient. The pre-modelling analysis also identified the most appropriate suite of FA biotracers to model the sediment mixtures. This data analysis is described in more detail below and in IAEA (2019).

### 2.5.1 Isotopic bi-plots of sources and mixtures

The isotopic bi-plot analysis indicated that Bulk  $\delta^{13}\text{C}$  and a sub-set of the available FA tracers (i.e., C14:0, C16:0, C18:0, C20:0, C22:0, C24:0, C26:0) best satisfied the fundamental isotopic polygon condition (i.e., sediment mixtures constrained within source polygons). The longest-chain length FAs (C28:0, C30:0, C32:0) could not be employed in the mixing model as these FAs were not detected in Pleasant River streambank sediment or subsoil.

The isotopic bi-plot analysis also indicated that the beef and sheep pasture and fodder crop soils (i.e., New Kale, Kale Crop 1–2 yr, Fodder Beet) were poorly discriminated from each other, so that incorporating these as individual sources would substantially degrade mixing-model performance. Consequently, these four sources were merged into a single source (i.e., Pasture and Fodder Crop).

### 2.5.2 Multivariate ordination analysis

Independent verification of the sources and tracer selection was undertaken using Canonical Axis of Principal Coordinates (CAP) analysis. This multivariate statistical procedure identified the most appropriate combinations of sediment sources and tracers to model the contributions of sources to sediment deposition in the river and estuary.

Multivariate ordination methods (including Principal Components Analysis, PCA) can be used to reduce dimensionality and to visualize patterns in multivariate data. Ordination<sup>1</sup> procedures can be

---

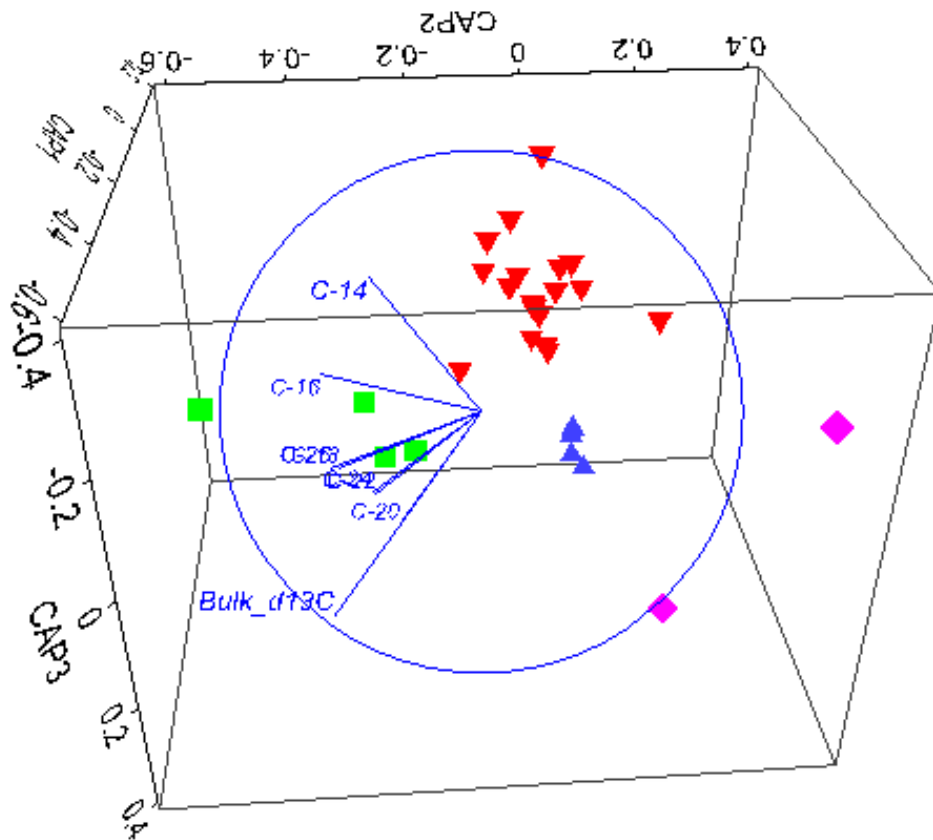
<sup>1</sup> An ordination is a map of the samples, usually in two or three dimensions, in which placement of the samples, is achieved by ordering samples so that similar objects are near each other and dissimilar objects are farther apart (Clarke, K.R., Gorley, R., Somerfield, P.J., Warwick, R. (2014) Change in marine communities: an approach to statistical analysis and interpretation. ).

classified as either constrained or unconstrained in relation to a-priori hypotheses. An unconstrained ordination procedure does not use a priori hypotheses in any way but reduces dimensions on the basis of some general criterion, such as minimizing residual variance (e.g., PCA). Unconstrained methods include PCA and are useful for visualising broad patterns in data sets (Anderson and Willis 2003). PCA is used to find axes that maximise the total variance (or equivalently, that minimises the total residual variation).

Constrained ordinations, on the other hand, use an a-priori hypothesis in some manner to produce the plot, for example concerning differences among groups. **Canonical Analysis of Principal Coordinates (CAP)**, is a flexible and particularly useful constrained ordination procedure developed for ecology (Anderson and Willis, 2003). It has the advantage of allowing any distance or dissimilarity measure to be used, and also considers the correlation structure among variables in the response data cloud. Thus, like the traditional canonical methods, it can uncover important patterns in the multivariate data by reference to relevant hypotheses (e.g., null hypothesis: source soils cannot be separated based on the tracers used). Both PCA and CAP analyses were undertaken using the PRIMER ver. 7 software package (Plymouth Routines in Multivariate Ecological Research) (Clarke and Gorley, 2015).

The CAP input data were processed as follows: isotope values were first transformed by multiplying by -1 (CAP cannot be performed on negative values). The data were then examined using Draftsman's plots, which indicated skewed distributions. A "log (x+1)" transform was applied to the data to minimise skewness, following recommended best practice in PRIMER. Data were then normalised, and a Euclidean distance matrix created to perform CAP analyses. Samples with missing data were excluded from the analysis. In particular, two of the composite streambank samples (OA230/87 & 88) were excluded from the CAP analysis due to missing  $\delta^{13}\text{C}$  FA data (i.e., C16:0, C26:0). Initially, all remaining fatty acid tracers and sources were analysed to determine the variation explained. Subsequently, in an iterative approach, FA tracers were discarded, and sources merged, with the objective being to increase the allocation success of the CAP analyses.

CAP analysis was initially conducted using all 7 potential sources and 7 fatty-acid tracers under the *a-priori hypothesis that the sources are distinct and dissimilar*. The sources included the various fodder crops (i.e., new Kale, 1-2 yr Kale, Beets) and Beef and Sheep pasture as distinct sources. The CAP model for these seven sources produced a total allocation success of 61% (i.e., mis-classification error: 39%). In the next iteration, CAP analysis was performed for the same sources with the addition of the bulk  $\delta^{13}\text{C}$  data and this marginally increased the allocation success (i.e., 69%). Further improvement of the CAP model required the individual pasture and fodder crop sources to be merged into a single new source (i.e., Pasture and Fodder Crops) due to the poor discrimination between them. Accordingly, the reduced set of four catchment sources and eight tracers (i.e., bulk  $\delta^{13}\text{C}$ , C14–C26 FAs) substantially improved the allocation success to 96% (Figure 2-19) and informed subsequent source modelling.



**Figure 2-19: Canonical Analysis of Principal Coordinates (CAP) plot – final model composed of four catchment sources and nine tracers.** The length of the vectors (blue lines) is proportional to the strength of the influence of each tracer on the CAP components. This final CAP model for 4 sources and 8 tracers has a 96% allocation success. **Key:** Pine harvest topsoil (blue), merged sources - Pasture and Fodder Crop topsoil (red), subsoil (green), Stream bank sediment (pink).

The results of the CAP analyses were broadly consistent with the isotopic polygon analysis (next section) and supports the selection of sources and tracers. It should be borne in mind that PCA/CAP analysis does not address a key selection criterion, that is tracers and sources must conform to the isotopic-biplot polygon principle.

## 2.6 Source isotopic polygons in CSSI analyses

The application of the CSSI technique to identify the land use sources of sediments deposited in rivers and estuaries is a multi-step process. Development of source isotopic polygons enclosing sediment mixtures underpins the application of mixing models (Phillips et al. 2014). These “unmixing” models, are used to calculate the proportional contributions of each potential source to a sediment mixture.

The selection of FA tracers for modelling source soil contributions to river and estuarine sediment mixtures (i.e., deposits) was informed by isotopic biplots. The isotopic polygons underpin and inform the application of isotopic mixing models to determine the proportional contributions of sources to a mixture (Phillips et al. 2014). The fundamental requirement is that the isotopic values of the tracers in a sediment mixture must be enclosed within a polygon (two tracers) or multi-dimensional volume (i.e., three or more tracers) defined by the isotopic values of the potential sources, within their range of uncertainty (e.g., standard deviation).



## Modelling sources of river and estuary sediment deposits

Comparison of the source library with the deposited river and estuary sediment (i.e., sediment mixtures) was conducted for every combination of the Bulk  $\delta^{13}\text{C}$  and FA biotracers. Figure 2-23 and Figure 2-24 present examples of isotopic biplots for four combinations of the Bulk  $\delta^{13}\text{C}$  and several FA biotracers. The CAP analysis indicated that an isotopic tracing system based on the bulk carbon isotope ( $\delta^{13}\text{C}$ ) in combination with the even-numbered mid-chain length FAs C14:0, C16:0, C18:0, C20:0, C22:0, C24:0, C26:0 provided the most discrimination between the catchment land use and streambank sources.

The isotopic biplots show the distribution of the four catchment sources, river and estuarine sediment deposits and indicative data (i.e., single replicate samples) for three estuarine/marine plants (i.e., kelp, saltmarsh and macroalgae) that were sampled. The isotopic bi-plots showed that the river deposits are within the ranges of the potential catchment sediment sources, whereas the estuarine sediment deposits are substantially isotopically enriched (i.e., up to 10 ‰ [less -ve values]) relative to the catchment soils and river sediment deposits. In many of the Bulk  $\delta^{13}\text{C}$  and FA isoplot combinations the isotopic values for the single kelp sample were substantially isotopically enriched relative to the catchment soil and river sediment deposits. These data indicated a missing source for the estuary sediment deposits.

Previous CSSI sediment source studies (e.g., Swales et al. 2016a; 2021a) have observed similar patterns, with the missing source identified as a marine sediment endmember. Marine sediment will include a substantial fraction of catchment sediment discharged to the marine receiving environment. Over time this terrigenous sediment is isotopically altered, directly or indirectly. Potential mechanisms for isotopic enrichment of catchment sediment after deposition in marine environments include: (1) in situ primary production by plants (e.g., microphytobenthos, seagrass) (Dalsgaard et al. 2003, Alfaro et al. 2006, Yi et al. 2017), (2) primary production by plants living in/on bed sediment (as above) that is eroded, transported and redeposited elsewhere in the system, and (3) deposition and incorporation of the organic component of marine seston (i.e., dead phytoplankton) into the terrigenous sediment deposits.

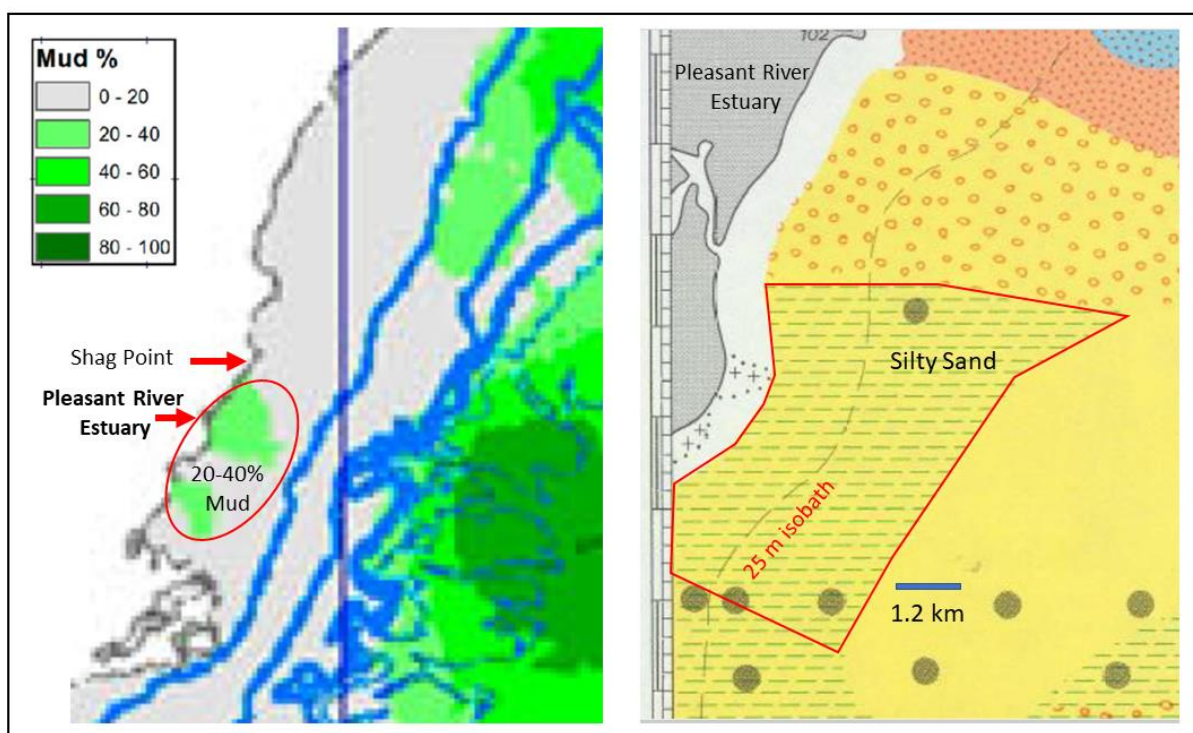
Fatty acids typically account for 15–25% (C14:0 to C22:6) of the dry biomass of diatoms (single cell algae). The most common FA types found in diatoms include the C14:0 and C16:0 FAs (Yi et al. 2017) employed in CSSI sediment tracing studies. Microphytobenthos living in bed sediments typically dominate primary production in shallow estuaries and coastal habitats. Their spatial distribution in estuaries is influenced by light availability at the seabed for photosynthesis. This is primarily influenced by water depth and suspended sediment concentrations (e.g., Thrush et al. 2014, Jones et al. 2017, Pivato et al. 2018).

In the present study, sampling of marine sediment in the nearshore zone was outside the scope of work so that two alternative suites of bulk  $\delta^{13}\text{C}$  and FA isotopic signatures were evaluated as potential representative marine sediment sources:

- **Pelorus Sound Marine source** (Swales et al., 2021a) based on sediment samples (n =7) collected from the waters around the Chetwode Islands, located several kilometres seaward of the entrance to Pelorus Sound. These sediments were substantially isotopically enriched in comparison to the sediment deposits of the inner Pelorus Sound. Inter-batch corrections were applied to the Pelorus data, using the NIWA FA standard (included with all batches and every CSSI project) to enable direct comparison with the Pleasant River data.

- Pleasant River **Estuary Marine source**, based on the isotopic characteristics of samples from the flood-tide delta and sandflats of the lower Pleasant River estuary (n = 6, E1–E4, E6 and G7). Exploratory data analysis showed that these lower-estuary samples had bulk  $\delta^{13}\text{C}$  isotopic values (mean  $-15.86\text{‰}$ , sd = 5.4) that were isotopically enriched in comparison to estuarine sediment sampled in the middle (mean  $-20.58\text{‰}$ , sd = 1.14) and upper reaches (mean  $-21.22\text{‰}$ , sd = 1.8) of the estuary. The large variation in the lower estuary was accounted for by a single sample.

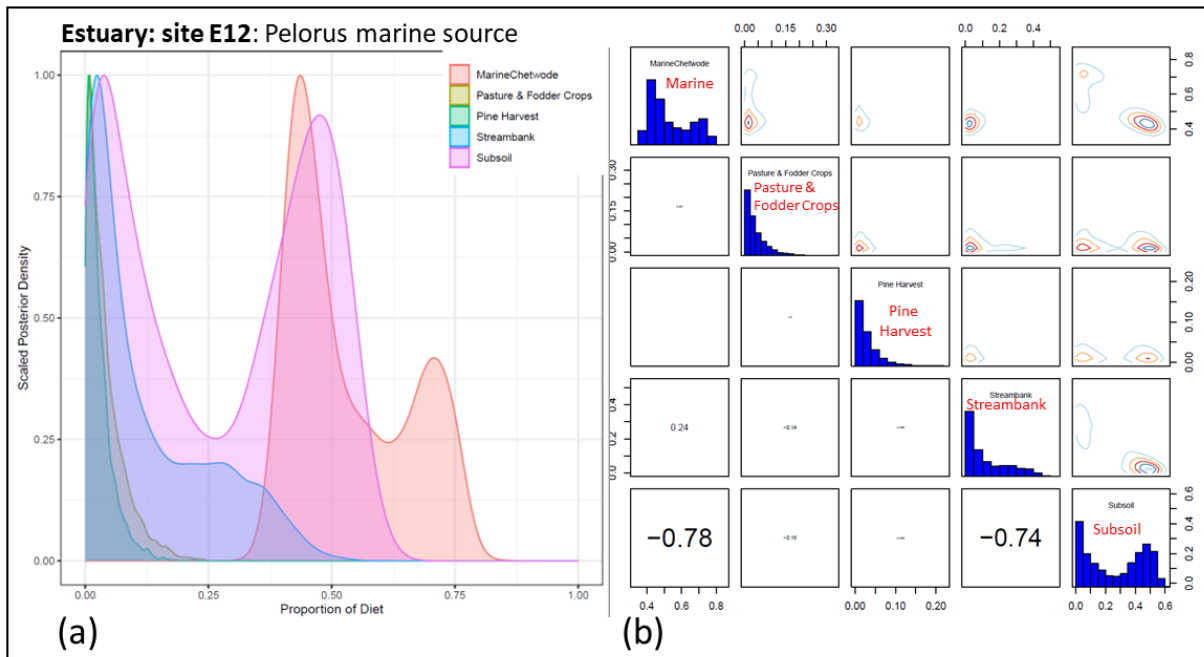
In addition to these isotopic data, geomorphic and sedimentological aspects of the system also suggested that these flood-tide delta deposits would largely reflect a marine, rather than a catchment source. These include: (1) the sand-rich nature of the sediment; (2) dominant and regular flood-tide transport of sand into the estuary indicated by the delta morphology; and (3) presence of a mud-rich sediment deposition zone in the nearshore–inner shelf environment immediately south and seaward of the estuary inlet (Figure 2-20). The presence of this mud depocentre is consistent with the discharge of fine suspended sediment from the Pleasant River catchment into the sea due to limited sediment accommodation capacity of this largely intertidal estuary. This will be considered in the discussion.



**Figure 2-20: Marine sediment characteristics in the immediate vicinity of the Pleasant River estuary.** Sources: Bostock et al. (NZ Journal of Geology & Geophysics, 2019) and Oamaru Marine Sediment Map, NZ Oceanographic Institute (1986).

The isotopic biplots showed that the lower estuary marine source was more isotopically similar to the estuary sediment samples than the Pelorus marine source. The estuary sediment source proportions were subsequently modelled using MixSIAR in turn for (1) **Pelorus Marine + Catchment** sources and (2) **Estuary Marine + Catchment** sources. This evaluation demonstrated that the Pelorus marine source was not suitable for the Pleasant River system. In a substantial number of cases, the

performance of the model that included the Pelorus Marine source was poor, as indicated by various indicators of model fit to the data, including the deviance information criterion (DIC, Appendix D) as well as key model outputs (i.e, probability distribution of isotopic source proportions, source correlation matrix plots). Figure 2-21 and Figure 2-22 present model summary output plots for the estuary sediment site E12 (mid-estuary) incorporating the Pelorus and Pleasant River Estuary Marine sources respectively. This comparison illustrates the poor performance of the model using the Pelorus Marine + Catchment source, with unrealistic multi-peaked distributions for the marine and subsoil sources.

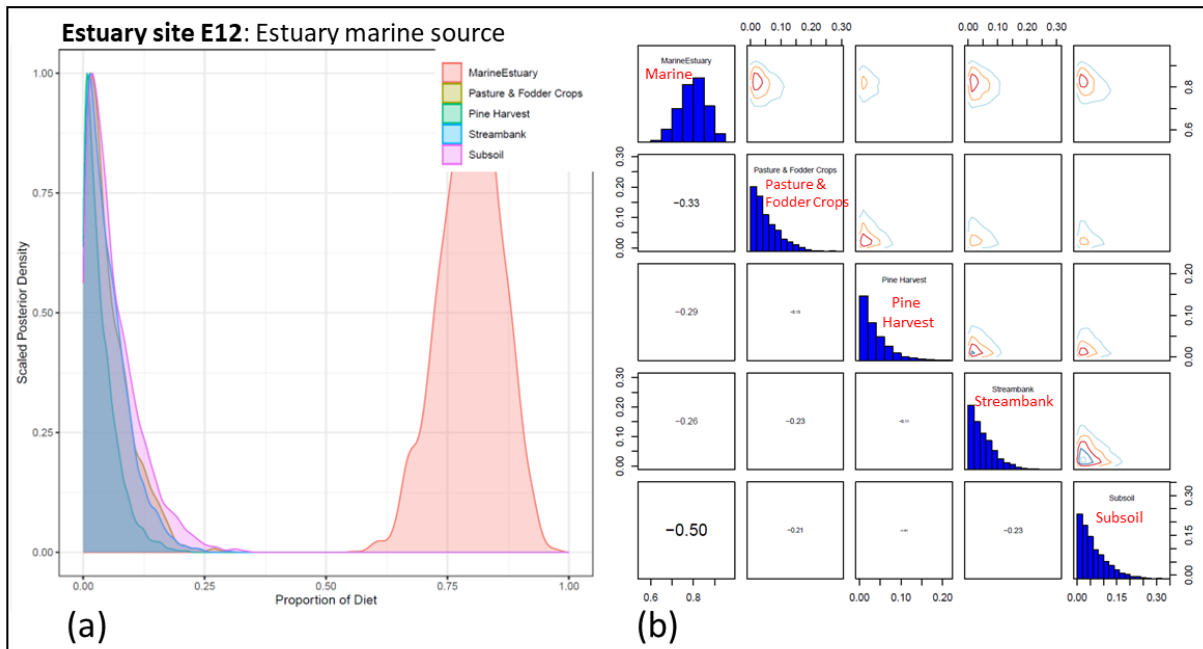


**Figure 2-21: Estuary site E12 output from MixSIAR mixing model incorporating the Pelorus Marine source.** Summary plots: (a) probability distribution of isotopic source proportions not converted to Soil% source proportions; and (b) matrix plots of source correlations and joint posterior probability distributions of source pairs. The probability distributions (isotopic values) for each source are shown on the diagonal. Cells below the diagonal show the correlations between contributions of pairs of sediment sources. Cells above the diagonal show the joint posterior probability distribution for contributions for pairs of sediment sources.

Another aspect of mixing model uncertainty is the joint uncertainty between sources. Matrix plots of source correlations and joint posterior probability distributions of source pairs are provided as an additional diagnostic output for MixSIAR. Figure 2-21(b) indicates strong negative correlations (i.e., -0.7) between the Pelorus Marine and Subsoil sources and also between the Streambank and Subsoil sources. These strong negative correlation means that if the Pelorus Marine source is at the peak of its distribution (in a sediment deposit) then the Subsoil source is likely to be at low end of its range and vice versa. *Matrix plots identify where the isotopic arrangement of sources leads to unavoidable model inadequacy and no amount of additional data collection will reduce this uncertainty.* (Phillips et al. 2014). This is the outcome in most cases for the mixing models incorporating the Pelorus Marine source.

By contrast the mixing models incorporating the **Estuary Marine** source had substantially improved performance across most estuary sampling sites (i.e., reduced uncertainty) as demonstrated for Site E12 (Figure 2-22). The isotopic probability distribution of the sediment sources is well defined, although there is a negative correlation between the Estuary Marine and Subsoil sources, albeit

substantially reduced by comparison with the Pelorus Marine source. Based on these results the Estuary Marine source, based on data from the Pleasant River system was adopted as the marine source for modelling the proportional contributions of each source to the estuarine sediment deposits.



**Figure 2-22: Estuary site E12 output from MiXSIAR mixing model incorporating the Pleasant River Estuary Marine source.** Summary plots: (a) probability distribution of isotopic source proportions not converted to Soil% source proportions; and (b) matrix plots of source correlations and joint posterior probability distributions of source pairs. The probability distributions (isotopic values) for each source are shown on the diagonal. Cells below the diagonal show the correlations between contributions of pairs of sediment sources. Cells above the diagonal show the joint posterior probability distribution for contributions for pairs of sediment sources.

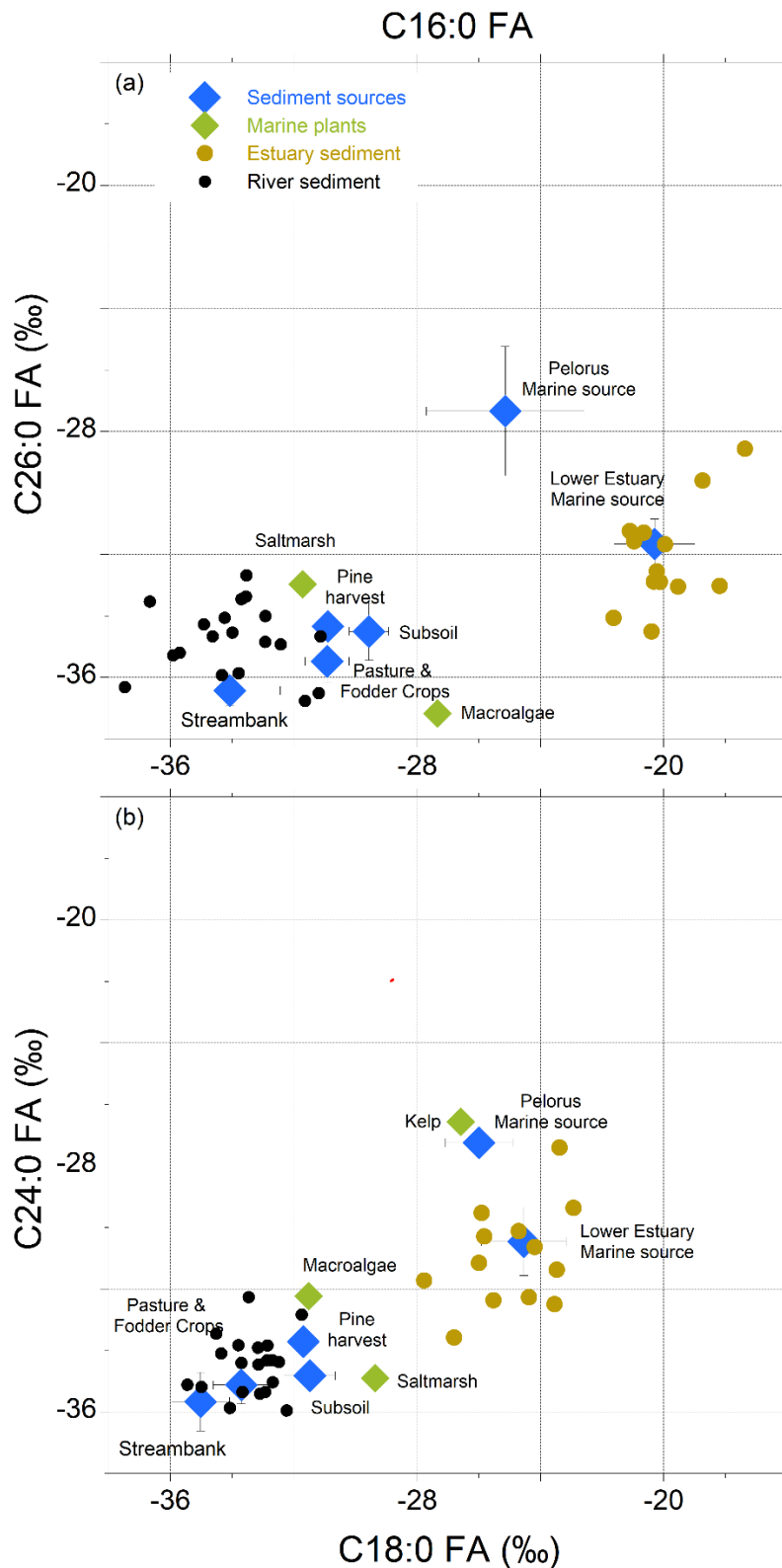
Summary statistics for the  $\delta^{13}\text{C}$  isotopic values for the bulk carbon and Fatty Acid biotracers for each modelled source are presented in Table 2-2. The substantially enriched (i.e., less negative) isotopic values for the Estuary Marine source compared to the catchment sources (particularly Bulk C and short chain FAs C14:0 to C18:0) is characteristic of marine sediment.

**Table 2-2: Summary statistics for Bulk C and FA biotracer %C and  $\delta^{13}\text{C}$  values for catchment and estuary sediment sources used for modelling source proportions in river and estuary sediment deposits.** Isotopic values for single replicate samples of marine plants included in the table for comparison. Data for the Pelorus Marine source (Swales et al., 2021a) are also tabulated.

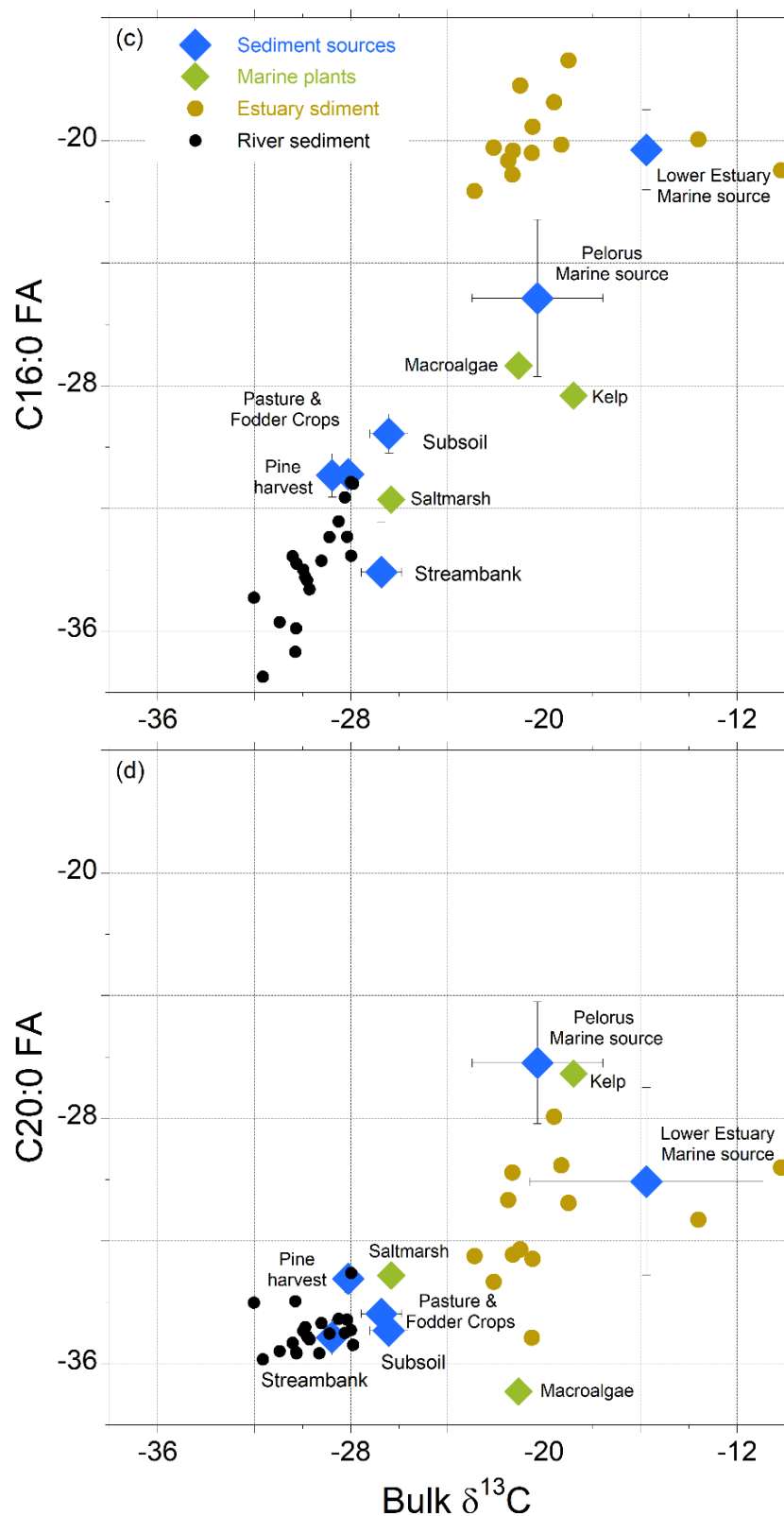
Source	Statistic	%C	Bulk C	C14:0	C16:0	C18:0	C20:0	C22:0	C24:0	C26:0
Pasture & Fodder Crops	Mean	4.7	-28.78	-31.19	-30.92	-33.70	-35.14	-34.82	-35.12	-35.48
	(SD)	(1.6)	(0.45)	(0.89)	(0.71)	(0.92)	(0.57)	(0.63)	(0.62)	(0.67)
Pine Harvest	Mean	4.2	-28.1	-34.03	-30.89	-31.69	-33.23	-32.78	-33.71	-34.3
	(SD)	(1.1)	(0.12)	(0.43)	(0.34)	(0.36)	(0.44)	(0.39)	(0.33)	(0.18)
Subsoil	Mean	0.8	-26.42	-28.79	-29.56	-31.48	-37.92	-34.38	-34.82	-34.51
	(SD)	(0.1)	(0.79)	(1.25)	(0.64)	(0.83)	(0.26)	(0.54)	(0.21)	(0.93)



Source	Statistic	%C	Bulk C	C14:0	C16:0	C18:0	C20:0	C22:0	C24:0	C26:0
<b>Streambank</b>	Mean (SD)	1.1 (0.8)	-26.73 (0.84)	-29.86 (1.53)	-34.07 (1.64)	-32.02 (0.94)	-34.38 (0.21)	-35.37 (0.26)	-35.66 (0.95)	-36.43 (0.48)
<b>EstuaryMarine</b>	Mean (SD)	0.7 (0.5)	-15.86 (5.41)	-20.75 (1.14)	-20.49 (1.30)	-24.52 (1.48)	-29.75 (3.16)	-30.07 (1.24)	-30.23 (0.99)	-31.43 (0.51)
<b>PelorusMarine</b>	Mean (SD)	0.8 (0.1)	-20.27 (0.13)	-23.74 (2.26)	-25.14 (2.56)	-25.99 (1.09)	-26.19 (1.9)	-28.27 (0.80)	-27.24 (0.38)	-27.34 (2.1)
<b>Saltmarsh</b>			-26.33	-29.19	-31.71	-31.52	-33.12	-31.72	-32.23	-32.97
<b>Macroalgae</b>			-21.06	-27.04	-27.34	-29.36	-36.91	-36.29	-34.90	-37.17
<b>Kelp</b>			-18.78	-	-28.32	-26.58	-26.54	-	-26.56	



**Figure 2-23: Isotopic biplots of average FA  $\delta^{13}\text{C}$  values (a) C16:0 versus C26:0 and (b) C18:0 versus C24:0 Fatty Acids for potential catchment sediment sources (blue symbols), river (black) and estuarine sediment (mustard) deposits and marine plant samples (green). Notes: (1) Average  $\delta^{13}\text{C}$  values (per mil, ‰) of potential sources plotted with standard deviations; (2) A missing source for the isotopically enriched estuarine sediment samples is inferred by the isotopic distance of these samples from the catchment sediment sources.**



**Figure 2-24: Isotopic biplots of average FA  $\delta^{13}\text{C}$  values (c) Bulk  $\delta^{13}\text{C}$  versus C16:0 and (d) C20:0 Fatty Acids for potential catchment sediment sources (blue symbols), river (black) and estuarine sediment (mustard) deposits and marine plant samples (green).** Notes: (1) Average  $\delta^{13}\text{C}$  values (per mil, ‰) of potential sources plotted with standard deviations; (2) A missing source for the isotopically enriched estuarine sediment samples is inferred by the isotopic distance of these samples from the catchment sediment sources.

## 2.7 Sediment source modelling

### 2.7.1 River confluences – upstream contributions

The isotopic signatures of the bulk carbon and the FAs extracted from the soil samples were collated with the %C values for each sediment sample, as required for subsequent modelling of source contributions. Samples of river-bed sediment deposits were separated into their confluence triplicates and the proportional contribution (%) of the tributary at each confluence was determined using a two-endmember linear mixing model. Additional details of the two-endmember mixing model are presented in Appendix D.

### 2.7.2 Land use sources

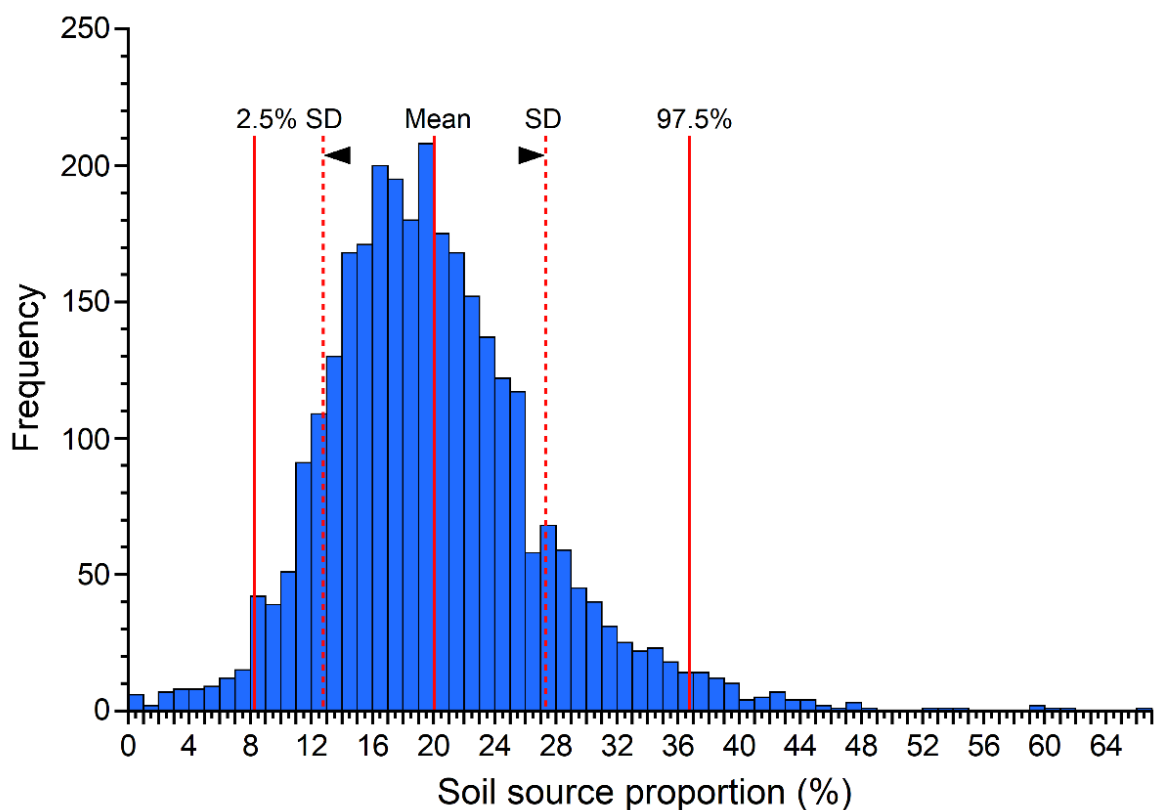
The MixSIAR model (Stock et al. 2018) was used in the present study. MixSIAR incorporates and accounts for uncertainty in the isotopic values of each sediment source as well as their geometry. The geometry is defined by the locations and distances of sources relative to each other and the sediment mixtures in isotopic space. These uncertainties and geometry are reflected in the resulting statistical results of source contributions to a sediment mixture generated by the mixing model. MixSIAR is a Bayesian isotopic mixing model, which incorporates advances in mixing model theory and builds on the earlier MixSIR and SIAR models. These models generate probability distributions for each source using a Monte Carlo-Markov Chain sampling process (Stock and Semmens, 2016, Stock et al. 2018). The MixSIAR output, isotopic source proportions are transformed to % soil proportions based on the carbon content of the sources (Gibbs, 2008). Summary statistics, including the mean, standard deviation and the 95% Credible Interval are calculated from the probability distributions of the soil % source proportions (Figure 2-25). These distributions are also summarised as box plots in the results section of this report. Additional details of the MixSIAR model as implemented in this study are presented in Appendix D.

With the exception of the two-endmember mixing model, mixing models, regardless of tracers used or the mixing system, are based on the same fundamental mixing equation:

$$Y_j = \sum_k p_k \mu_{jk}^S \quad (1)$$

where the tracer value ( $Y_j$ ) for each of  $j$  tracers is equal to the sum of the  $k$  sources tracer means ( $\mu_{jk}^S$ ), multiplied by their proportional contribution to the mixture ( $p_k$ ). This basic equation assumes: (1) all sources contributing to a mixture are known and quantified, (2) tracers are conservative, (3) source, mixture and tracer values are fixed and known, (4)  $p_k = \text{unity}$ , and (5) source tracer values differ (Stock et al. 2018). An analytical solution to this basic equation requires that the system is not under-determined (i.e., number of tracers  $\leq n+1$  sources). Another advantage of MixSIAR is that it employs probability-distribution based solutions for under under-determined systems. These probabilistic models integrate the variability in source and mixture tracer data.





**Figure 2-25: Example of a probability distribution of % soil proportions.** Summary statistics: Mean (20%), Median (19.2%), Standard Deviation (SD 7.2%), 2.5% and 97.5%-iles, defining the 95% Credible Interval (i.e., soil proportion 8 to 37%) for this example.

Mixing model evaluations of source contributions to a sediment mixture can be informed by statistical analyses and independent information about sediment sources, as undertaken in the present study. This information can be used to make decisions about which sources should ultimately be included in a mixing model. Independent information that is relevant in sedimentation studies include estimates of the mass loads from each source to the receiving environment.

## 3 Results

### 3.1 Sources of river-sediment deposits

#### 3.1.1 Two source endmember model

The two-endmember mixing model (2-EMM) results for the individual bulk C and FA sediment tracers in downstream sediment mixtures at each sampled river confluence are presented in Figure 3-1 and Table 3-1. These data provide estimates of the proportional % sediment contribution from the main stem and tributary river sources.

The 2-EMM yielded valid results for all confluences sampled except at PR8 where sediment contributions could not be calculated.

At confluence PR9, the tributary stream was dry. In contrast, PR7 results indicate a significant sediment contribution from Trotters Creek, the U/S Tributary (77%) at this confluence point in the river network. For Watkin Creek and Trotters Creek confluence sites (PR6A and PR5B), located in the upper catchment the %contributions from each U/S source were similar. Higher standard deviations were recorded for these two sites so there is a higher uncertainty in calculated estimates.



**Figure 3-1: Map of Pleasant River Catchment and location of river confluence sampling sites and contributions (red text, %) of upstream main stem and tributary sources to the downstream sediment deposit (mixture). Note: sub-catchment boundaries indicated by dashed lines.**

**Table 3-1: Proportional contribution (%) of upstream sediment sources to the river system at at each confluence sampled in the Pleasant River Catchment.** Calculated by two-endmember mixing model. These results are mean values with standard deviations. The number of valid biotracers is also reported.

Site Description	NIWA Lab Code	Proportional isotopic contribution (%)	Standard Deviation	Number of valid biotracers
PR9 U/S Pleasant River	OA230/38	85	6	5
PR9 U/S Tributary	OA230/39	15	6	
PR9 D/S Pleasant River	OA230/40			
PR8 U/S Pleasant River	OA230/35	-		
PR8 U/S Tributary	OA230/36	-		
PR8 D/S Pleasant River	OA230/37			
PR7 U/S Pleasant River	OA230/32	23	7	4
PR7 U/S Trotters Creek	OA230/33	77	7	
PR7 D/S Pleasant River	OA230/34			
PR6A U/S Trotters Creek	OA230/29	40	13	5
PR6A U/S Tributary	OA230/30	60	13	
PR6A D/S Trotters Creek	OA230/31			
PR5B U/S Watkin Creek	OA230/26	60	16	5
PR5B U/S Tributary	OA230/27	40	16	
PR5B D/S Watkin Creek	OA230/28			

As described in Section 1.4.1, NZ River Maps provides estimates of long-term annual average suspended sediment loads for sub-catchments draining to the Pleasant River Estuary. These data can also be used to specify flows and loads at each river confluence sampled in the present study. These NZRM estimates are summarised in Table 3-2 along with the percentage contribution of annual suspended sediment load for each upstream source and comparison with the 2-EMM estimates for the sediments sampled in May 2022. Table 3-2 shows that the 2-EMM estimates compare favourably with the NZRM long term loads.

These results also indicate that the contribution of sediment was not always proportional to the catchment area. For example, the Trotter Creek sub-catchment contribution for NZRM ( $t\ km^2\ yr^{-1}$ ) and the 2-EMM ( $\% soil\ km^{-2}$ ) were double the contribution of the main stem of the Pleasant River upstream of confluence PR7.



**Table 3-2: Comparison of annual average suspended sediment loads at confluences for upstream sources (% NZ River Maps) with Two Endmember Mixing Model estimates of confluence contributions to downstream mixture (%).** Sources: NZ River Maps <https://shiny.niwa.co.nz/nzrivermaps/> and Table 3-1.

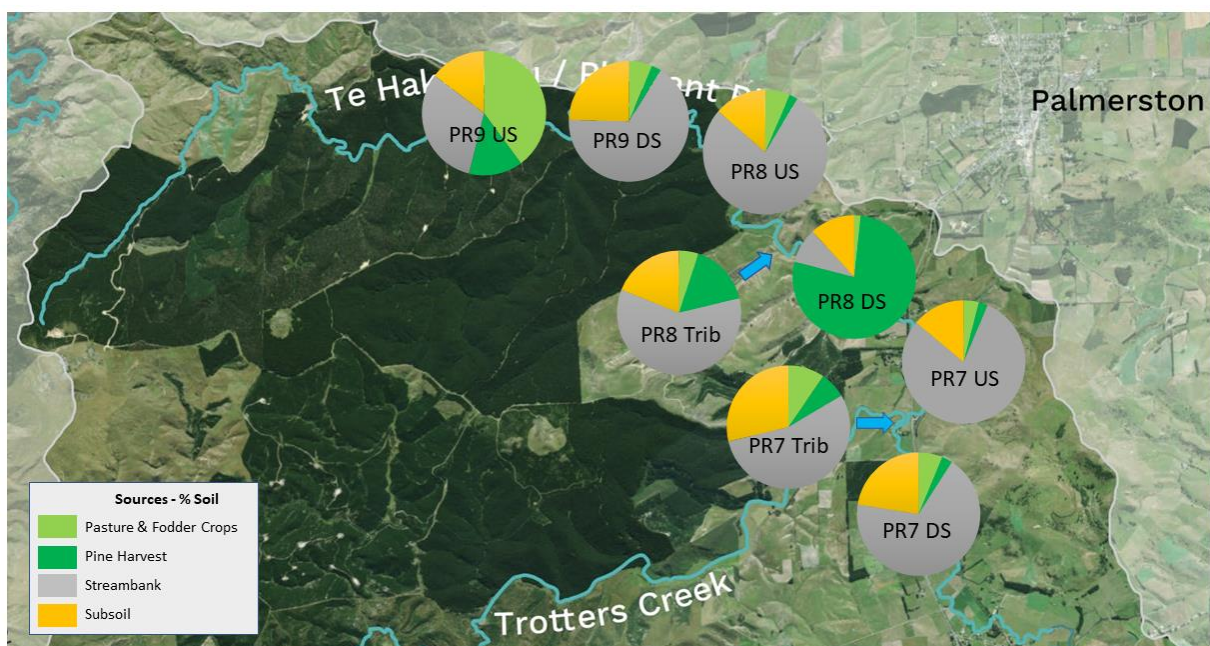
Sub-catchment	Area (km <sup>2</sup> )	Mean flow (m <sup>3</sup> s <sup>-1</sup> )	SS Load (t yr <sup>-1</sup> )	NZRM SS Load contribution (%)	Two End-Member Mixing Model (%)
PR9 U/S Pleasant River	16.7	0.10	1358	78	85
PR9 U/S Tributary	4.8	0.03	337	19	15
PR9 D/S Pleasant River	22.5	0.13	1742		
PR8 U/S Pleasant River	25.1	0.15	1797	77	–
PR8 U/S Tributary	3.4	0.02	475	20	–
PR8 D/S Pleasant River	28.8	0.17	2323		
PR7 U/S Pleasant River	36.7	0.22	2529	25	23
PR7 U/S Trotters Creek	38.6	0.27	7354	74	77
PR7 D/S Pleasant River	75.3	0.52	9939		
PR6A U/S Trotters Creek	10.8	0.08	2650	51	40
PR6A U/S Tributary	11.0	0.08	2525	49	60
PR6A D/S Trotters Creek	21.9	0.16	5202		
PR5B U/S Watkin Creek	6.8	0.05	1245	48	60
PR5B U/S Tributary	3.1	0.02	1342	52	40
PR5B D/S Watkin Creek	10.2	0.08	2588		

### 3.1.2 MixSIAR model

The sources of the river sediment deposits at the sampling sites were also modelled using MiXSIAR. This analysis differs from the 2-EMM in that each sediment sample is analysed individually. Proportional contributions are determined from the geometry of the mixture and sources in isotopic space and source (i.e., land use, streambank erosion) signature variability (uncertainty). These factors are reflected in the resulting statistical results of source contributions to the sediment mixture generated by the mixing model. By contrast, the 2-EMM quantifies the contribution of the two immediately upstream river sources (i.e., main stem and tributary) to the downstream sediment mixture for each valid FA biotracer. These are fundamentally different modelling approaches that provide complementary information.

The MiXSIAR proportional source contributions (mean %Soil) are summarised as pie charts (Figure 3-2 and Figure 3-3). In the upper catchment, sediment deposits are substantially composed of eroded

streambank sediment (i.e., 66-80%) and subsoil (12–29%) at most of the sites. Pasture and Fodder Crop topsoil make up 40% of the sediment deposit at the most upstream site (PR9 US) but at other sites this source is a minor component (i.e., < 10 %) of the deposits. Pine Harvest topsoil contributes most of the sediment deposited at site PR8 DS (mean 77%, 95% CI: 49–95%, Table 3-7). The modelled soil% source proportions accurately reflect the FA isotopic data for this site. This result is, however, anomalous in the context of the upstream sources (i.e., PR8 US, PR8 Trib) and immediate downstream sediment deposits (i.e., PR7 US) that are dominated by the streambank erosion source. This contribution is substantially higher than in the upstream or tributary samples at the PR8 and PR7 confluences where deposition is dominated by streambank sediment. The PR9 Tributary was not modelled as land use is composed entirely of pine forest that was established more than a decade ago.



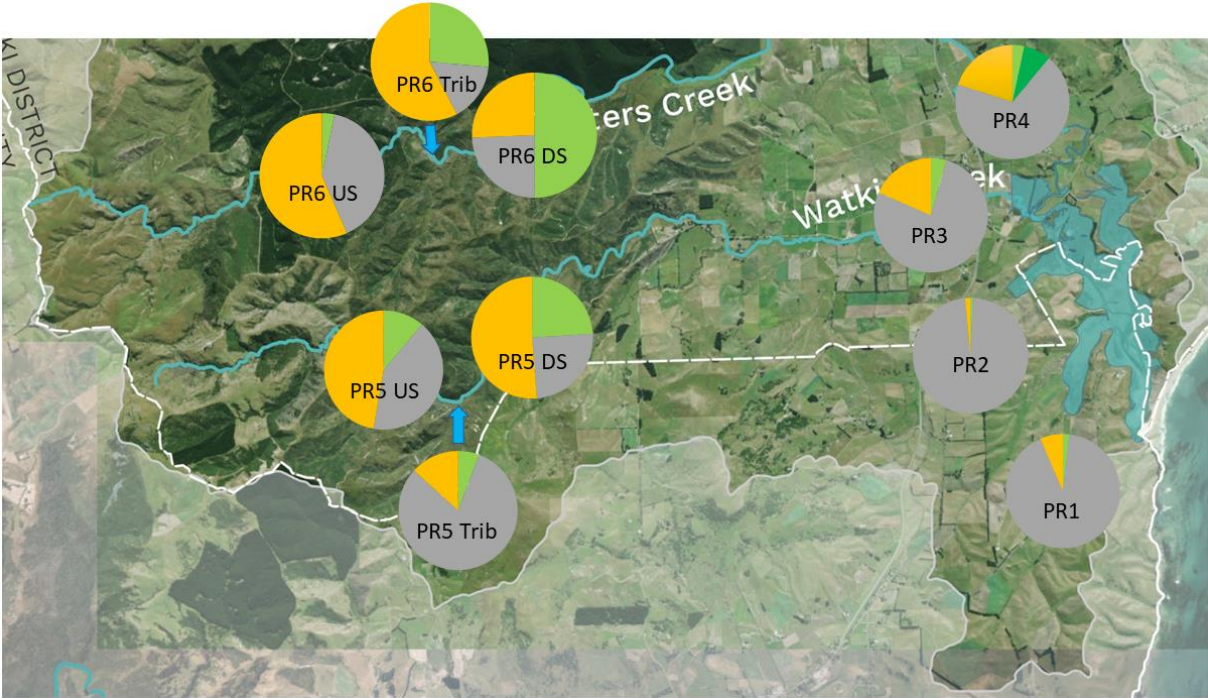
**Figure 3-2: Pleasant River Catchment (northern branch). Average % soil source proportions for river sediment deposits at sampling sites (May 2023).** Calculated by MixSIAR model - average of 3000 model runs.

The southern half of the catchment encompasses sampling sites in the lower reaches of the Pleasant River, the upper reaches of the Trotters and Watkin Creeks and small sub-catchments discharging directly to tidal creeks on the western shore of the estuary. Pine forest establishment (first rotation) continues to occur in the upper Trotters Creek catchment so that no harvesting has occurred to date. Subsoil (26–58%) and streambank erosion (16–40%) dominate sediment deposited at the Trotters Creek PR6 confluence sites. Pasture and Fodder Crop account for 50% of the sediment deposited at the confluence downstream site (PR6 DS) that is a higher proportion than the upstream sources and likely reflect a local effect. Subsoil (25–81%) and streambank erosion (13–31%) also dominate sediment deposited at the Watkin Creek PR5 confluence sites. Pasture and Fodder Crop account for 24% of the sediment deposited at the downstream site (PR6 DS).

At some locations the proportion of a given source in the downstream mixture is less than the two upstream sources. For example, at PR5 the average proportion of streambank sediment in the downstream mixture (~25%) is less than in the two upstream river samples (i.e., ~40 & 80%). This may reflect local contributions from other sources in the confluence reach and/or uncertainty in the average source proportions (% soil). For example, the standard deviation in the average subsoil and

streambank contribution to PR5 DS are ±19% and ±15% respectively. Table 3-3 to Table 3-8 summarise these uncertainties for each river sediment mixture.

At the outlets of the Pleasant River and small sub-catchment discharging to the estuary (i.e., PR1 to PR4) deposited sediment is largely composed of eroded streambank sediment (69–92%) with a secondary contribution from subsoil sources (7–20%). The dominance of streambank erosion in the lower reaches of the catchment are consistent with the geomorphological context (i.e., channel meanders, increase in stream power) and field observations. The pasture and fodder crop topsoil source account for less than 4% at these sites. Pine harvest topsoil accounts for 8% of sediment deposited at the Pleasant River outlet (PR4), which is consistent with harvesting activities in the catchment.



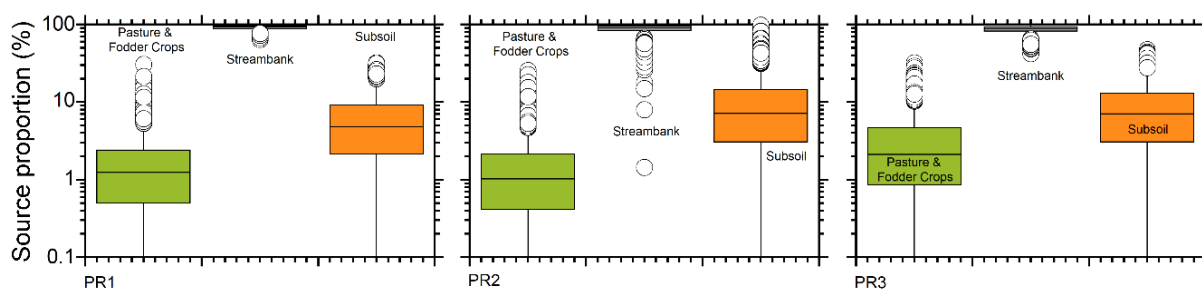
**Figure 3-3: Pleasant River Catchment (southern branch). Average % soil source proportions for river sediment deposits at sampling sites (May 2023).** Calculated by MixSIAR model - average of 3000 model runs.

Summary statistics for the MixSIAR modelling of sediment deposits (%soil source proportions) for each river sampling site are presented in the following sections as tables and box and whisker plots.

### 3.1.3 Catchment outlets to the estuary

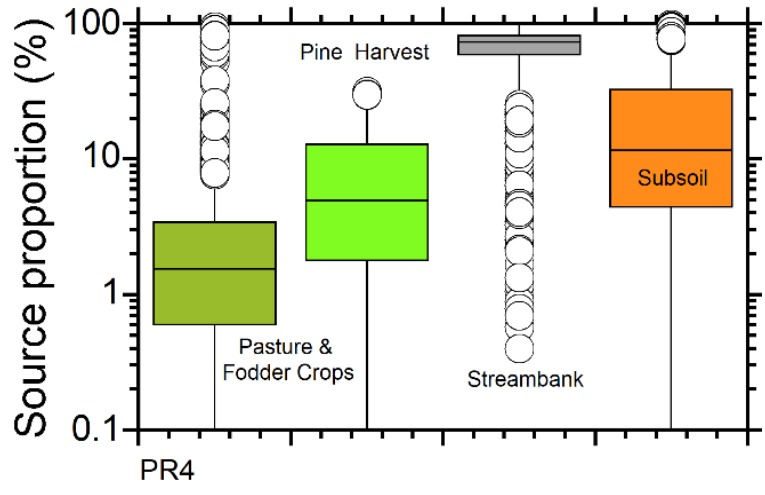
**Table 3-3: MixSIAR summary statistics for source contributions (% soil proportions) to river sediment deposits at catchment outlets.** Uncertainty reported as one standard deviation (SD), 95% credible interval defined by the 2.5 and 97.5 percentiles, and 95% CI range.

Site	Source	Mean	Median	SD	2.5%-ile	97.5%-ile	95% CI range
PR1	Pasture & Fodder Crops	1.8	1.2	2.0	0.05	6.8	6.7
	Streambank	91.7	93.2	6.0	76.2	99.1	22.9
	Subsoil	6.5	4.8	5.8	0.2	22.4	22.3
PR2	Pasture & Fodder Crops	1.7	1.0	2.1	0.04	6.8	6.7
	Streambank	87.8	90.9	10.7	60.3	98.8	38.6
	Subsoil	10.6	7.1	10.8	30.2	38.6	38.4
PR3	Pasture & Fodder Crops	3.8	2.1	4.6	0.08	17.6	17.5
	Streambank	87.2	88.9	8.3	0.2	67.7	30.7
	Subsoil	9.0	7.1	7.5	0.3	27.3	27.5
PR4	Pasture & Fodder Crops	3.4	1.5	8.5	0.06	13.1	23.2
	Pine Harvest	7.7	4.9	7.1	0.2	23.3	13.1
	Streambank	68.8	73.3	18.3	23.9	93.5	69.6
	Subsoil	20.1	11.6	20.2	0.4	67.9	67.5



**Figure 3-4: Sites PR1 - PR3, source proportion distribution (%) summaries for MixSIAR model runs.** Box and whisker plots: median, lower and upper interquartile (IQ), 95% credible interval and outliers (>1.5x IQ distance) of sediment source proportions (%), n = 3000). Three sources: (A) Pasture and Fodder Crops; (B) Streambank; and (C) Subsoil. Note: the lower tail of the distribution is extended by the Y-axis log scale.



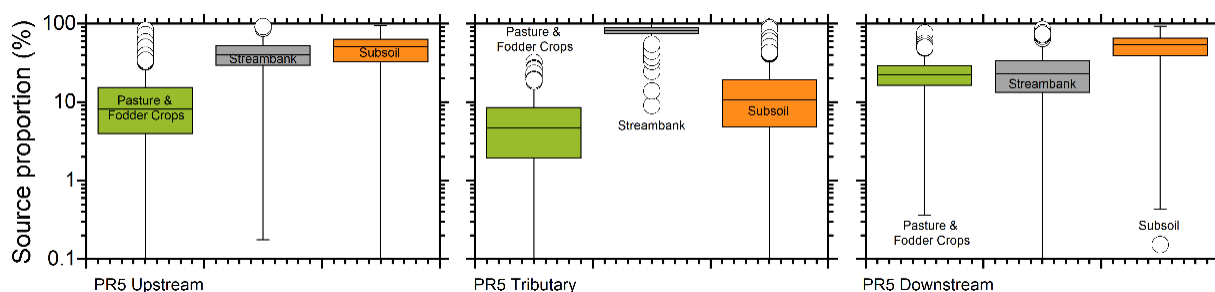


**Figure 3-5: Site PR4, source proportion distribution (%) summaries for MixSIAR model runs.** Box and whisker plots: median, lower and upper interquartile (IQ), 95% credible interval and outliers (>1.5x IQ distance) of sediment source proportions (%), n = 3000). Four sources: (A) Pasture and Fodder Crops; (B) Pine Harvest; (C) Streambank; and (D) Subsoil. Note: the lower tail of the distribution is extended by the Y-axis log scale.

### 3.1.4 Watkin Creek sub-catchment

**Table 3-4: Site PR5 Watkin Creek confluence. MixSIAR summary statistics for proportional contributions (Soil %) of sources to river sediment deposits.** Uncertainty reported as one standard deviation (SD) and the 95% credible interval defined by the 2.5 and 97.5 percentiles. Site descriptions - PR5 main-stem upstream (US), upstream Tributary (Trib) and mixture downstream (DS) of confluence.

Site	Source	Mean	Median	SD	2.5%-ile	97.5%-ile	95% CI range
PR5 US	Pasture & Fodder Crops	11.1	8.1	10.1	0.4	37.8	37.4
	Streambank	41.6	39.8	17.0	12.7	78.2	65.5
	Subsoil	47.3	51.1	20.5	4.8	77.9	73.1
PR5 Trib	Pasture & Fodder Crops	5.7	4.7	4.6	0.2	16.5	16.3
	Streambank	81.0	82.5	10.4	57.0	96.2	39.3
	Subsoil	13.3	10.7	10.9	0.4	39.4	39.0
PR5 DS	Pasture & Fodder Crops	24.0	22.2	10.8	8.0	50.0	42.0
	Streambank	24.7	22.7	15.0	2.1	59.1	57.0
	Subsoil	51.3	54.1	18.8	8.4	80.4	72.0

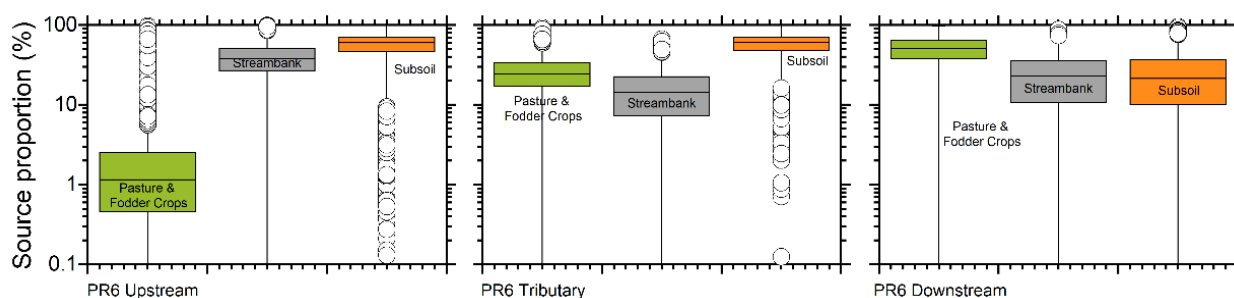


**Figure 3-6: River Confluence PR5 (Watkin Creek), source proportion distribution (%) summaries for MixSIAR model runs.** Box and whisker plots: median, lower and upper interquartile (IQ), 95% credible interval and outliers (>1.5x IQ distance) of sediment source proportions (%), n = 3000). Three sources: (A) Pasture and Fodder Crops; (B) Streambank; and (C) Subsoil. Note: the lower tail of the distribution is extended by the Y-axis log scale.

### 3.1.5 Trotters Creek sub-catchment

**Table 3-5: Site PR6 Trotters Creek confluence. MixSIAR summary statistics for proportional contributions (Soil %) of sources to river sediment deposits.** Uncertainty reported as one standard deviation (SD) and the 95% credible interval defined by the 2.5 and 97.5 percentiles. Site descriptions – PR6 main-stem upstream (US), upstream Tributary (Trib) and mixture downstream (DS) of confluence.

Site	Source	Mean	Median	SD	2.5%-ile	97.5%-ile	95% CI range
PR6 US	Pasture & Fodder Crops	3.2	1.2	10.1	0.04	13.8	13.8
	Streambank	40.3	37.8	21.0	2.7	90.3	87.7
	Subsoil	56.5	60.2	22.2	3.4	94.6	91.2
PR6 Trib	Pasture & Fodder Crops	26.5	24.6	13.8	4.3	60.7	56.4
	Streambank	15.9	14.3	11.0	0.7	41.4	40.7
	Subsoil	57.6	60.5	16.8	16.5	82.6	66.1
PR6 DS	Pasture & Fodder Crops	49.9	51.2	21.1	1.3	85.7	85.7
	Streambank	24.4	22.7	16.0	1.0	58.2	57.2
	Subsoil	25.6	21.5	19.5	0.9	71.7	70.8

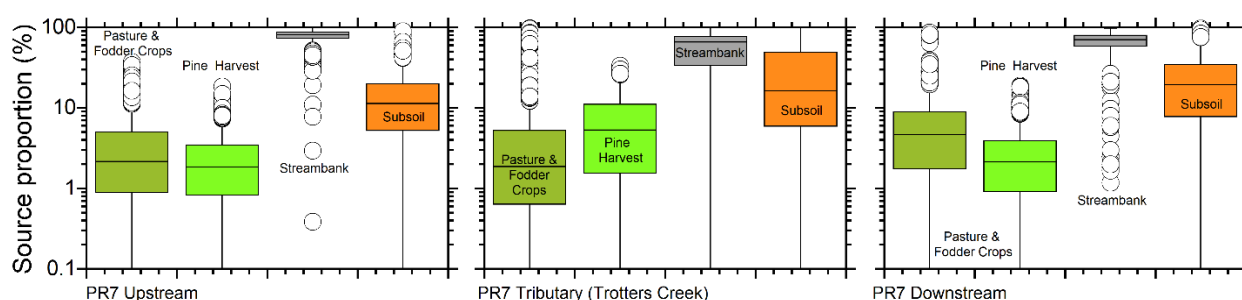


**Figure 3-7: River Confluence PR6, source proportion distribution (%) summaries for MixSIAR model runs.** Box and whisker plots: median, lower, and upper interquartile (IQ), 95% credible interval and outliers ( $>1.5 \times$  IQ distance) of sediment source proportions (%),  $n = 3000$ ). Three sources: (A) Pasture and Fodder Crops; (B) Streambank; and (C) Subsoil. Note: the lower tail of the distribution is extended by the Y-axis log scale.

### 3.1.6 Pleasant River – confluence PR7

**Table 3-6: Confluence PR7 - Pleasant River. MixSIAR summary statistics for proportional contributions (Soil %) of sources to river sediment deposits.** Uncertainty reported as one standard deviation (SD) and the 95% credible interval defined by the 2.5 and 97.5 percentiles. Site descriptions - PR7 main-stem upstream (US), upstream Tributary (Trib) and mixture downstream (DS) of confluence.

Site	Source	Mean	Median	SD	2.5%-ile	97.5%-ile	95% CI range
PR7 US	Pasture & Fodder Crops	4.0	2.2	4.8	0.07	18.3	18.3
	Pine Harvest	2.4	1.9	2.1	0.07	7.4	7.3
	Streambank	79.7	81.5	11.1	55.0	95.5	40.4
	Subsoil	14.0	11.3	11.2	0.5	39.6	39.1
PR7 Trib	Pasture & Fodder Crops	9.6	2.0	20.6	0.06	81.8	81.7
	Pine Harvest	6.9	5.3	6.0	0.1	20.0	19.9
	Streambank	54.8	65.9	27.7	1.1	88.7	87.6
	Subsoil	28.7	16.2	28.8	0.5	94.1	93.6
PR7 DS	Pasture & Fodder Crops	6.3	4.7	6.3	0.2	20.1	19.9
	Pine Harvest	2.8	2.1	2.6	0.1	9.7	9.6
	Streambank	68.4	70.5	70.5	36.1	91.2	55.1
	Subsoil	22.5	19.5	19.5	0.7	59.7	59.0



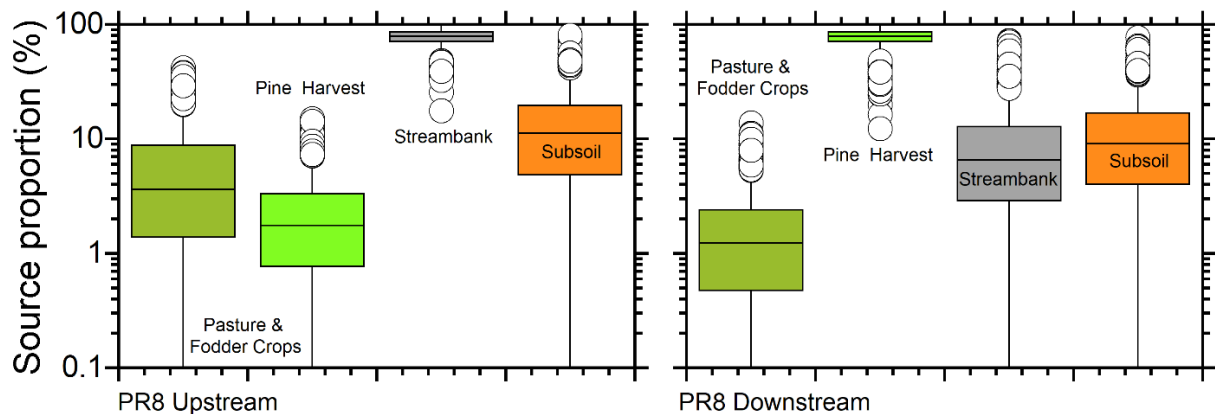
**Figure 3-8: River Confluence PR7, source proportion distribution (%) summaries for MixSIAR model runs.** Box and whisker plots: median, lower, and upper interquartile (IQ), 95% credible interval and outliers (>1.5x IQ distance) of sediment source proportions (%), n = 3000. Four sources: (A) Pasture and Fodder Crops; (B) Pine Harvest; (C) Streambank; and (D) Subsoil. Note: the lower tail of the distribution is extended by the Y-axis log scale.



### 3.1.7 Pleasant River – confluence PR8

**Table 3-7: Confluence PR8 - Pleasant River. MixSIAR summary statistics for proportional contributions (Soil %) of sources to river sediment deposits.** Uncertainty reported as one standard deviation (SD) and the 95% credible interval defined by the 2.5 and 97.5 percentiles. Site descriptions - PR8 main-stem upstream (US), and mixture downstream (DS) of confluence.

Site	Source	Mean	Median	SD	2.5%-ile	97.5%-ile	95% CI range
PR8 US	Pasture & Fodder Crops	6.4	3.7	6.9	0.1	24.5	24.3
	Pine Harvest	2.3	1.8	2.0	0.1	7.0	7.0
	Streambank	77.7	79.0	10.9	52.7	94.3	41.6
	Subsoil	13.6	11.3	11.0	0.4	40.1	39.6
PR8 DS	Pasture & Fodder Crops	1.7	1.2	1.7	0.1	6.2	6.1
	Pine Harvest	77.3	79.0	11.7	49.2	94.7	45.5
	Streambank	9.2	6.5	9.1	0.3	32.6	32.3
	Subsoil	11.8	9.1	10.3	0.5	38.3	37.9

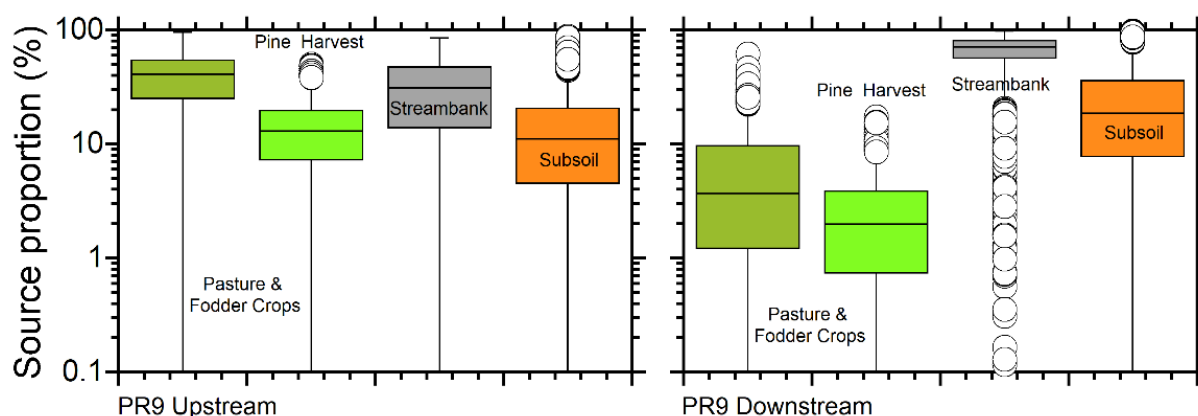


**Figure 3-9: River Confluence PR8, source proportion distribution (%) summaries for MixSIAR model runs.** Box and whisker plots: median, lower, and upper interquartile (IQ), 95% credible interval and outliers (>1.5x IQ distance) of sediment source proportions (%), n = 3000). Four sources: (A) Pasture and Fodder Crops; (B) Pine Harvest; (C) Streambank; and (D) Subsoil. Note: the lower tail of the distribution is extended by the Y-axis log scale.

### 3.1.8 Pleasant River – confluence PR9

**Table 3-8: Confluence PR9 - Pleasant River. MixSIAR summary statistics for proportional contributions (Soil %) of sources to river sediment deposits.** Uncertainty reported as one standard deviation (SD) and the 95% credible interval defined by the 2.5 and 97.5 percentiles. Site descriptions - PR9 main-stem upstream (US), and mixture downstream (DS) of confluence.

Site	Source	Mean	Median	SD	2.5%-ile	97.5%-ile	95% CI range
PR9 US	Pasture & Fodder Crops	39.9	41.2	20.2	1.4	76.8	75.4
	Pine Harvest	14.0	13.0	8.8	0.9	33.7	32.8
	Streambank	31.5	31.1	19.7	1.3	68.2	66.9
	Subsoil	14.6	11.1	13.4	0.4	50.3	50.0
PR9 DS	Pasture & Fodder Crops	6.2	3.7	6.5	0.1	23.0	22.9
	Pine Harvest	2.7	2.0	2.5	0.1	9.1	9.0
	Streambank	66.5	70.9	19.7	10.7	92.2	81.5
	Subsoil	24.6	18.6	21.5	0.8	84.4	83.7



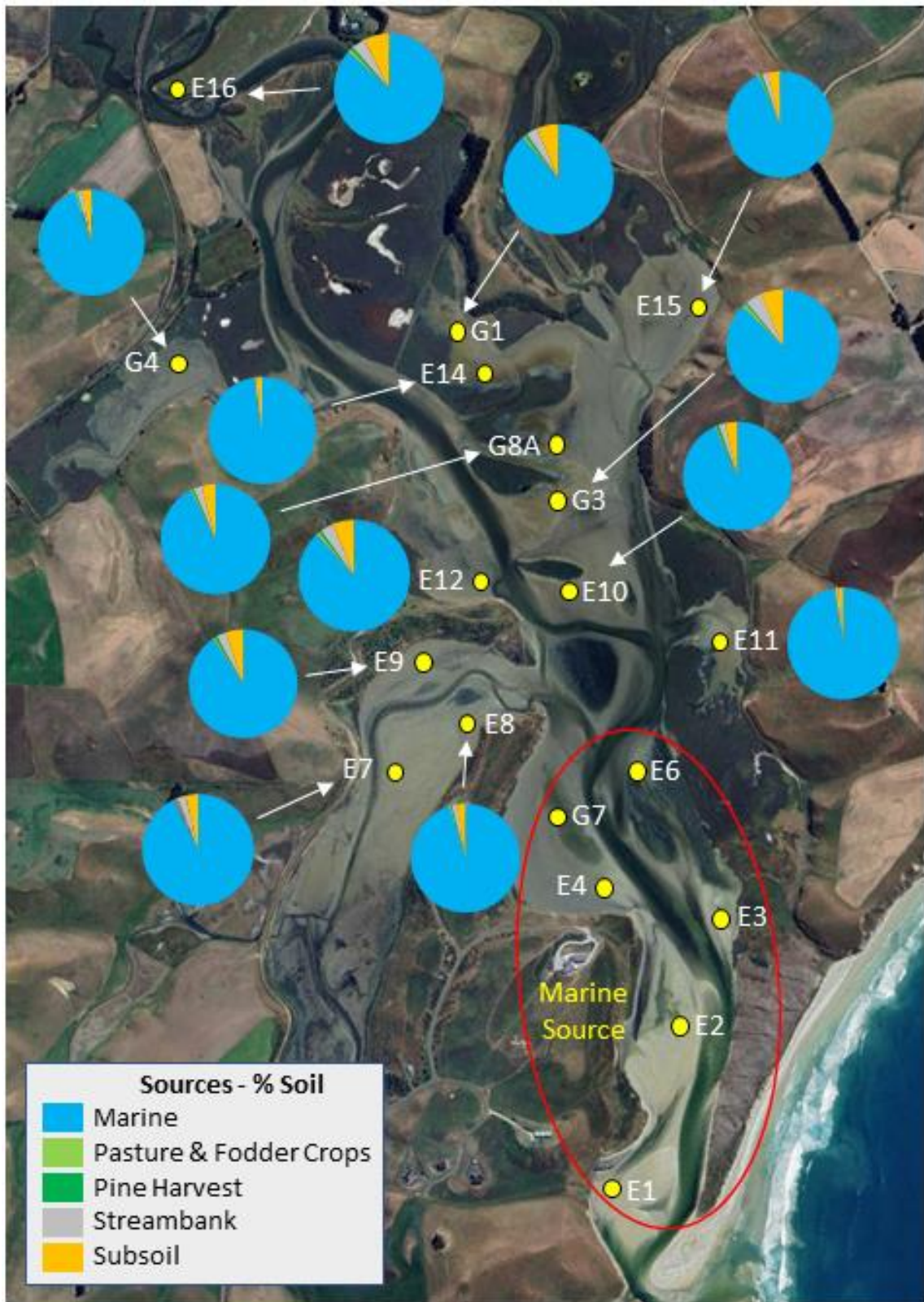
**Figure 3-10: River Confluence PR9 (upper Pleasant River catchment), source proportion distribution (%) summaries for MixSIAR model runs.** Box and whisker plots: median, lower, and upper interquartile (IQ), 95% credible interval and outliers (>1.5x IQ distance) of sediment source proportions (%), n = 3000). Four sources: (A) Pasture and Fodder Crops; (B) Pine Harvest; (C) Streambank; and (D) Subsoil. Note: the lower tail of the distribution is extended by the Y-axis log scale.

## 3.2 Sources of estuary-sediment deposits

Figure 3-11 presents the source proportions (% soil) for recent sediment deposits at the sampled sites. The marine source isotopic signature is based on sediment sampled at sites in the lower estuary, as described in the methods section. These results indicate that majority of the surficial sediment deposited in the estuary is derived from an isotopically-enriched marine source (i.e., 87–97%). These are similar findings to studies of the New River and Jacobs River estuaries in Southland (Gibbs et al., 2014b, 2015) The likely ultimate origin of this marine sediment is considered in the discussion section.

Table 3-9 summarises the contribution of the catchment sources to recent sediment deposition at each estuary sampling site. Catchment sources directly contribute 2.5 – 13.8% (mean: 8.1%) of the recent sediment deposition at the sampled sites. Rescaling the data to consider only the relative contributions of the catchment sources shows that subsoil (mean 53.3%) and streambank (mean 31.7%) erosion contribute most of the catchment sediment to the estuary. Pasture & Fodder Crops and Pine Harvest topsoil contribute similar proportions of sediments, being 7.6% and 7.4% respectively.

The relative contribution of Pasture & Fodder Crops and Pine Harvest topsoil to recent sedimentation in the estuary can be calculated using the land use areas and the catchment mean % soil proportions for both sources (Table 3-9, Figure 2-8). The total area of pine harvest operations over a ~2-year period (September 2019–December 2021) prior to sediment sampling (May 2022) was 1.07 km<sup>2</sup> (Table 2-1). The area of dry stock pasture (including fodder crops) was 74.2 km<sup>2</sup> (i.e., 58% of 128 km<sup>2</sup>, source: ORC). These values yield estimates of specific source contributions for the pasture and fodder and pine harvest sources of 0.1% km<sup>-2</sup> and 6.9% km<sup>-2</sup>. Thus, the yield of topsoil from pine harvest in the estuary sediment was 69-fold larger than for the pasture and fodder crop land use. These land use yield estimates do not include subsoil erosion from both pasture and fodder crops and pine harvest as subsoil sources cannot presently be differentiated. On steepland pasture, subsoil loss occurs from slope failures (Figure 2-8) and farm tracks whereas pine harvest operations expose subsoils to erosion on hillslopes when vegetation is removed as well as on access tracks (Figure 2-4 and Figure 2-7).



**Figure 3-11: Pleasant River Estuary - contributions of sediment sources to recent deposition at sampling sites, May 2023.** Data are average source proportions (% Soil). Samples used to provide the isotopic signature of the Marine Source (E1–E4, E6 and G7).



In a recent CSSI study of sediment sources in the upper Pelorus Sound, a similar evaluation found that pine harvest in the catchment yielded specific source contributions topsoil (% soil km<sup>-2</sup>) that were 51–99-fold higher than for native forest (Swales et al., 2021a).

**Table 3-9: Estuary sedimentation - relative contributions of catchment sources.** MiXSIAR results re-scaled to consider catchment sources based on average %Soil source proportions.

Estuary sampling site	Catchment sources as % of total deposition	Pasture & Fodder Crops	Pine Harvest	Streambank	Subsoil
E7	7.1	8.0	7.0	33.7	51.2
E8	4.7	7.7	8.7	28.8	54.8
E9	10.0	7.8	6.3	32.8	53.1
E10	6.6	7.5	9.7	28.4	54.4
E11	2.5	7.7	9.5	31.3	51.6
E12	12.5	7.9	6.0	32.3	53.7
E14	2.8	7.7	9.3	29.3	53.6
E15	5.9	8.1	10.0	26.9	55.0
E16	13.0	7.1	5.5	31.2	56.3
G1	12.1	7.6	5.1	33.3	53.9
G3	13.8	6.2	3.9	43.1	46.8
G4	4.9	7.4	8.7	28.6	55.2
G6	7.2	7.8	7.0	33.2	52.0
G8A	8.8	7.7	5.8	33.4	53.1
<b>Mean</b>	<b>8.1</b>	<b>7.6</b>	<b>7.4</b>	<b>31.7</b>	<b>53.3</b>
<b>Std Deviation</b>	<b>3.9</b>	<b>0.5</b>	<b>2.0</b>	<b>4.0</b>	<b>2.4</b>
<b>Min</b>	<b>2.5</b>	<b>6.2</b>	<b>3.9</b>	<b>26.9</b>	<b>46.8</b>
<b>Max</b>	<b>13.8</b>	<b>8.1</b>	<b>10.0</b>	<b>43.1</b>	<b>56.3</b>

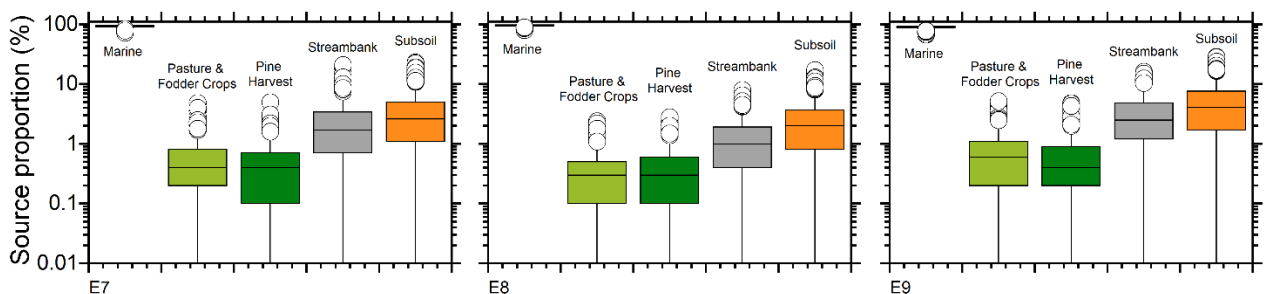
Summary statistics for the MixSIAR modelling of sediment deposits (%soil source proportions) for each site are presented in the following sections as tables and box and whisker plots. These results show the substantial contribution of the marine sediment source to deposition in the Pleasant River estuary in the surficial sediment sampled in May 2022. These samples incorporate surficial sediment from the top-most 1–2 cm of the deposits. Although sediment accumulation rates (SAR) are unknown it is likely that the sediment in these surface scraps include sediment deposited over several years. This is inferred from likely sediment accumulation rates (SAR) of several mm per year

and sediment mixing by physical processes (e.g., wave resuspension) and bioturbation, the relative importance of which will vary with location.

### 3.2.1 Thorburn Road Creek

**Table 3-10: Thorburn Road Creek. MixSIAR summary statistics for proportional contributions (Soil %) of sources to estuarine sediment deposits.** Uncertainty reported as one standard deviation (SD) and the 95% credible interval defined by the 2.5 and 97.5 percentiles. Site descriptions - PR5 main-stem upstream (US), and mixture downstream (DS) of confluence.

Site	Source	Mean	Median	SD	2.5%-ile	97.5%-ile	95% CI range
E7	Marine	92.9	93.6	3.8	83.9	98.3	14.3
	Pasture & Fodder Crops	0.6	0.4	0.5	0.01	2.0	2.0
	Pine Harvest	0.5	0.4	0.5	0.01	1.8	1.8
	Streambank	2.4	1.7	2.2	0.06	8.1	8.0
	Subsoil	3.6	2.6	3.4	0.1	12.8	12.7
E8	Marine	95.3	95.7	2.4	89.6	98.7	9.2
	Pasture & Fodder Crops	0.4	0.3	0.3	0.01	1.3	1.3
	Pine Harvest	0.4	0.3	0.4	0.01	1.4	1.4
	Streambank	1.4	1.0	1.3	0.03	4.8	4.8
	Subsoil	2.6	2.0	2.3	0.07	8.4	8.3
E9	Marine	90.0	90.6	4.5	79.8	97.0	17.2
	Pasture & Fodder Crops	0.8	0.6	0.7	0.02	2.6	2.6
	Pine Harvest	0.6	0.4	0.6	0.02	2.3	2.3
	Streambank	3.3	2.5	2.7	0.13	9.8	9.6
	Subsoil	5.3	4.1	4.6	0.14	17.0	16.8

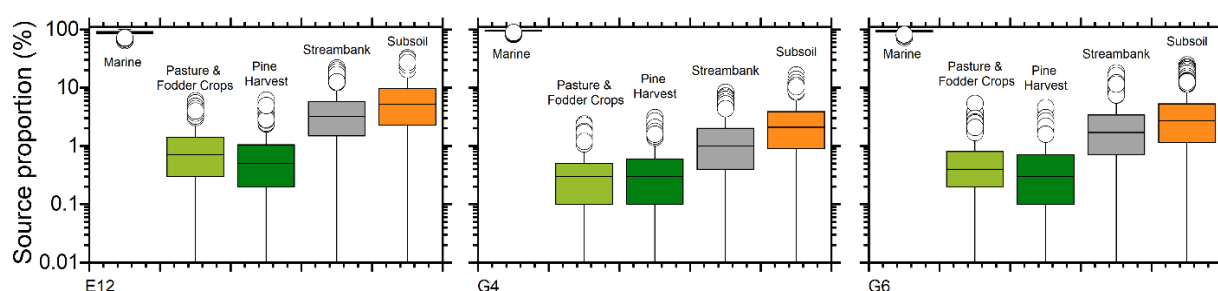


**Figure 3-12: Thorburn Road Creek – estuary sites E7 to E9, source proportion distribution (%) summaries for MixSIAR model runs.** Box and whisker plots: median, lower, and upper interquartile (IQ), 95% credible interval and outliers (>1.5x IQ distance) of sediment source proportions (%; n = 3000). Five sources: (A) Marine; (B) Pasture and Fodder Crops; (C) Pine Harvest; (D) Streambank; and (E) Subsoil. Note: the lower tail of the distribution is extended by the Y-axis log scale.

### 3.2.2 Intertidal flats – west of channel

**Table 3-11: Intertidal flats -west of channel. MixSIAR summary statistics for proportional contributions (Soil %) of sources to estuarine sediment deposits.** Uncertainty reported as one standard deviation (SD) and the 95% credible interval defined by the 2.5 and 97.5 percentiles.

Site	Source	Mean	Median	SD	2.5%-ile	97.5%-ile	95% CI range
<b>E12</b>	Marine	97.2	97.6	1.7	92.9	99.4	6.5
	Pasture & Fodder Crops	0.2	0.2	0.2	0.01	0.8	0.8
	Pine Harvest	0.3	0.2	0.3	0.01	0.9	0.9
	Streambank	0.8	0.6	0.8	0.02	3.0	3.0
	Subsoil	1.5	1.0	1.5	0.04	5.3	5.2
<b>G4</b>	Marine	95.1	95.5	2.5	89.0	98.7	9.7
	Pasture & Fodder Crops	0.4	0.3	0.3	0.01	1.3	1.3
	Pine Harvest	0.4	0.3	0.4	0.01	1.5	1.5
	Streambank	1.4	1.0	1.3	0.04	4.9	4.9
	Subsoil	2.7	2.1	2.4	0.09	8.8	8.8
<b>G6</b>	Marine	92.8	93.7	4.1	82.8	98.4	15.6
	Pasture & Fodder Crops	0.6	0.4	0.5	0.02	2.0	2.0
	Pine Harvest	0.5	0.3	0.5	0.01	1.9	1.9
	Streambank	2.4	1.7	2.2	0.06	8.2	8.2
	Subsoil	3.8	2.7	3.5	0.10	13.1	13.0



**Figure 3-13: Intertidal flats – west of channel – estuary sites E12, G4 and G6, source proportion distribution (%) summaries for MixSIAR model runs.** Box and whisker plots: median, lower, and upper interquartile (IQ), 95% credible interval and outliers (>1.5x IQ distance) of sediment source proportions (%), n = 3000). Five sources: (A) Marine; (B) Pasture and Fodder Crops; (C) Pine Harvest; (D) Streambank; and (E) Subsoil. Note: the lower tail of the distribution is extended by the Y-axis log scale.

### 3.2.3 Intertidal flats – east of channel

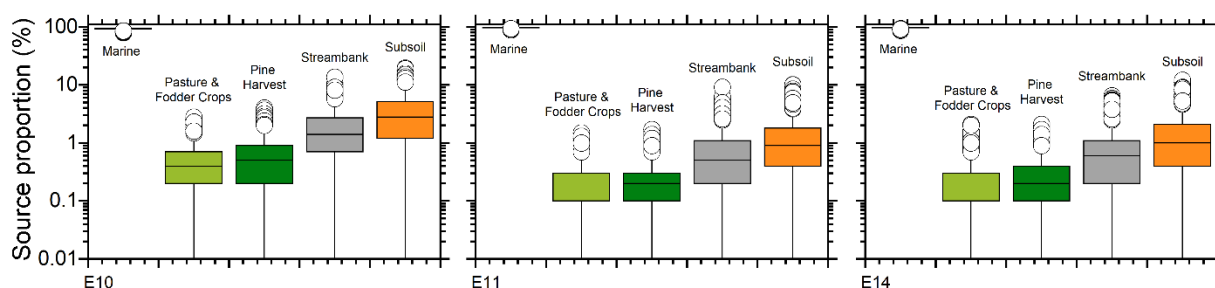
**Table 3-12: Intertidal flats east of channel (NIWA Sites). MixSIAR summary statistics for proportional contributions (Soil %) of sources to estuarine sediment deposits.** Uncertainty reported as one standard deviation (SD) and the 95% credible interval defined by the 2.5 and 97.5 percentiles.

Site	Source	Mean	Median	SD	2.5%-ile	97.5%-ile	95% CI range
<b>E10</b>	Marine	93.4	93.8	3.0	86.5	97.9	11.4
	Pasture & Fodder Crops	0.50	0.4	0.5	0.01	1.6	1.6
	Pine Harvest	0.6	0.5	0.6	0.02	2.0	2.0
	Streambank	1.9	1.4	1.6	0.06	6.1	6.0
	Subsoil	3.4	2.8	3.0	0.13	11.0	10.9
<b>E11</b>	Marine	97.5	97.8	1.5	94.0	99.4	5.4
	Pasture & Fodder Crops	0.2	0.1	0.2	0.00	0.7	0.7
	Pine Harvest	0.2	0.2	0.2	0.01	0.9	0.9
	Streambank	0.8	0.5	0.8	0.02	2.9	2.9
	Subsoil	1.3	0.9	1.3	0.04	4.8	4.8
<b>E14</b>	Marine	97.2	97.6	1.7	92.9	99.4	6.5
	Pasture & Fodder Crops	0.2	0.2	0.2	0.01	0.8	0.8
	Pine Harvest	0.3	0.2	0.3	0.01	0.9	0.9
	Streambank	0.8	0.6	0.8	0.02	3.0	3.0
	Subsoil	1.5	1.0	1.5	0.04	5.3	5.2
<b>E15</b>	Marine	94.14	94.6	2.8	87.55	98.2	10.6
	Pasture & Fodder Crops	0.5	0.4	0.4	0.02	1.6	1.6
	Pine Harvest	0.6	0.5	0.5	0.02	2.0	1.9
	Streambank	1.6	1.2	1.4	0.05	5.2	5.1
	Subsoil	3.2	2.4	2.8	0.12	10.4	10.3
<b>E16</b>	Marine	87.0	87.8	5.9	72.8	95.7	22.9
	Pasture & Fodder Crops	0.9	0.7	0.8	0.03	3.03	3.0
	Pine Harvest	0.7	0.5	0.7	0.02	2.6	2.6
	Streambank	4.1	3.1	3.6	0.12	13.4	13.3
	Subsoil	7.3	5.7	6.3	0.22	23.5	23.3

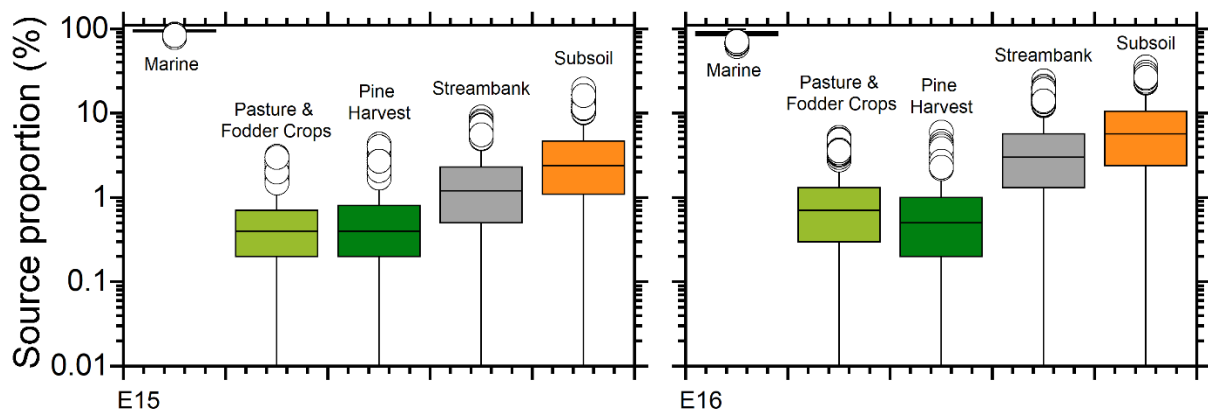


**Table 3-13: Intertidal flats east of channel (Salt Ecology sites). MixSIAR summary statistics for proportional contributions (Soil %) of sources to estuarine sediment.** Uncertainty reported as one standard deviation (SD) and the 95% credible interval defined by the 2.5 and 97.5 percentiles.

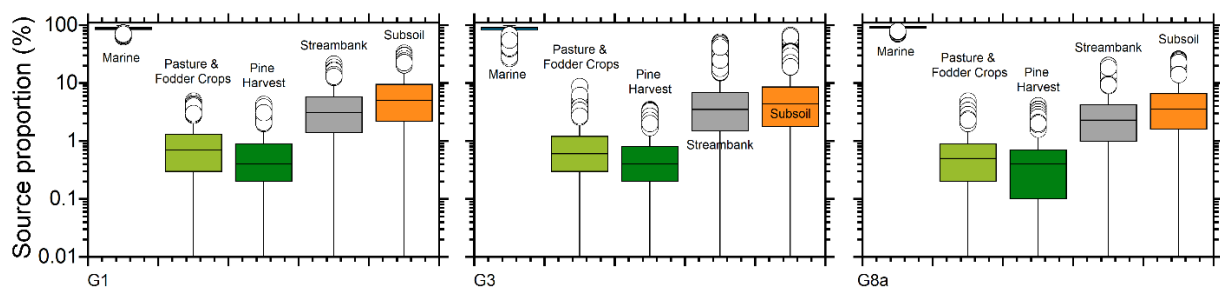
Site	Source	Mean	Median	SD	2.5%-ile	97.5%-ile	95% CI range
<b>G1</b>	Marine	87.9	88.6	5.4	75.6	96.3	20.7
	Pasture & Fodder Crops	0.9	0.7	0.8	0.03	3.1	3.1
	Pine Harvest	0.6	0.5	0.6	0.02	2.1	2.1
	Streambank	4.0	3.1	3.4	0.1	12.7	12.5
	Subsoil	6.5	5.1	5.6	0.2	20.3	20.1
<b>G3</b>	Marine	86.2	89.0	10.1	54.6	96.6	42.0
	Pasture & Fodder Crops	0.9	0.6	0.8	0.02	2.9	2.9
	Pine Harvest	0.5	0.4	0.5	0.02	1.9	1.9
	Streambank	6.0	3.5	8.0	0.2	36.0	35.8
	Subsoil	6.5	4.4	7.1	0.2	24.6	24.5
<b>G8A</b>	Marine	91.2	92.0	4.4	81.0	97.7	16.7
	Pasture & Fodder Crops	0.7	0.5	0.7	0.02	2.4	2.4
	Pine Harvest	0.5	0.4	0.5	0.01	1.9	1.8
	Streambank	2.9	2.3	2.6	0.10	9.5	9.3
	Subsoil	4.7	3.6	4.1	0.13	15.0	14.8



**Figure 3-14: Intertidal flats east of channel – estuary sites E10, E11 and E14, source proportion distribution (%) summaries for MixSIAR model runs.** Box and whisker plots: median, lower, and upper interquartile (IQ), 95% credible interval and outliers (>1.5x IQ distance) of sediment source proportions (%), n = 3000). Five sources: (A) Marine; (B) Pasture and Fodder Crops; (C) Pine Harvest; (D) Streambank; and (E) Subsoil. Note: the lower tail of the distribution is extended by the Y-axis log scale.



**Figure 3-15: Intertidal flats east of channel – estuary sites E15 and E16, source proportion distribution (%) summaries for MixSIAR model runs.** Box and whisker plots: median, lower, and upper interquartile (IQ), 95% credible interval and outliers (>1.5x IQ distance) of sediment source proportions (%), n = 3000). Five sources: (A) Marine; (B) Pasture and Fodder Crops; (C) Pine Harvest; (D) Streambank; and (E) Subsoil. Note: the lower tail of the distribution is extended by the Y-axis log scale.



**Figure 3-16: Intertidal flats east of channel – estuary sites G1, G3 and G8a, source proportion distribution (%) summaries for MixSIAR model runs.** Box and whisker plots: median, lower, and upper interquartile (IQ), 95% credible interval and outliers (>1.5x IQ distance) of sediment source proportions (%), n = 3000). Five sources: (A) Marine; (B) Pasture and Fodder Crops; (C) Pine Harvest; (D) Streambank; and (E) Subsoil. Note: the lower tail of the distribution is extended by the Y-axis log scale.

## 4 Discussion

### 4.1 River sediment sources

Streambank and subsoil erosion were found to be the major sources of sediment depositing in the river system at the time of sampling in May 2022. Both sources contributed as much as 80% of the deposited sediment at the sampling sites. The subsoils cannot be attributed to particular land use, however mapping of areas of soil disturbance due to hillslope failure and vegetation removal would identify erosion hot spots. The source tracing also highlighted the importance of streambank erosion in the upper catchment, upstream from the Trotters Creek confluence. Watkin Creek and lower reaches of the sub-catchments discharging to the estuary (i.e., PR1 to PR4). These results are consistent with previous CSSI sediment tracing studies in New Zealand that show that subsoils and streambank erosion are major sources of sediment accumulating in freshwater and marine receiving environments (e.g., Handley et al., 2017; Olsen and Swales, 2019; Gibbs and Swales, 2019; Swales et al., 2013; 2016a, 2021a). Streambank erosion has elsewhere been identified as an important process in New Zealand catchments, although there has been limited research conducted (Basher, 2013). Streambank erosion rates may increase due to factors including changes in landcover, removal of riparian vegetation, channel straightening and resulting increase in stream power and channel-bank disturbance due to livestock (Hughes, 2016). A general increase in stream power with slope and/or contributing catchment area will also favour streambank erosion in lower catchment floodplains.

Beef and sheep pasture with winter fodder crops (i.e., Kale, Beets) are major land use practices in the catchment. We sampled beef and sheep pasture and fodder crop soils at different stages of the pasture-fodder crop land use practice (i.e., New Kale, Kale Crop 1–2 yr, Fodder Beet). The statistical analysis indicated that the isotopic values of the suite of bulk carbon ( $\delta^{13}\text{C}$ ) fatty acid biotracers for the pasture and fodder crop soil samples could not be discriminated from each other. Incorporating these land uses as individual sources would substantially degrade mixing-model performance. These results indicate that the changes in plant community types, from pasture to crop species, was occurring too frequently for distinctive differences in isotopic signatures to develop. For example, Swales and Gibbs (2020) found that the transition in isotopic values of biotracers for harvested pine to pasture soils occurred over six years. In the present study, cycling between pasture and fodder crops over 1-3 years appeared to have produced a mixed signature rather than measurable differences. These potential sources were thus merged into a single source.

The isotopic bi-plot analysis also indicated that the beef and sheep pasture and fodder crop soils (i.e., New Kale, Kale Crop 1–2 yr, Fodder Beet) were poorly discriminated from each other, so that incorporating these as individual sources would substantially degrade mixing-model performance. Consequently, these four sources were merged into a single source (i.e., Pasture and Fodder Crop).

These surficial sediment samples integrate the effects of sediment transport during recent storms. The most recent notable storm prior to the sampling occurred in January 2021 (pers. comm: Mr Hamish McFarlane, EOCG). It is likely that sediment transported during smaller storm events have contributed to the river deposits that were sampled.

## 4.2 Estuary sedimentation

### 4.2.1 Marine sediment source

The CSSI analysis of the surficial estuarine sediment samples indicated that an isotopically enriched marine source dominates recent sedimentation in the Pleasant River Estuary. A mud-rich sediment deposition zone in the nearshore–inner shelf environment immediately south and seaward of the estuary inlet (Figure 2-20) is the most likely source of this isotopically enriched sediment. Previous CSSI sediment source studies (e.g., Swales et al. 2016a; 2021a) have incorporated a marine source endmember to evaluate the contribution of sources to contemporary and historical estuary sedimentation.

The presence of this mud depocentre immediately offshore from the Pleasant River Estuary suggests that a substantial fraction of the annual catchment suspended sediment load of fine sediment is discharged from the estuary to the sea due to limited sediment accommodation capacity of this largely intertidal system. The influence of sediment accommodation volume is discussed below.

Over time, the isotopic characteristics of this exported terrigenous sediment deposited is altered in the marine environment. Isotopic enrichment can occur by: (1) in situ primary production by plants (e.g., microphytobenthos, seagrass) (Dalsgaard et al. 2003, Alfaro et al. 2006, Yi et al. 2017 ), (2) primary production by plants living in/on bed sediment (as above) that is eroded, transported and redeposited elsewhere in the system, and (3) deposition and incorporation of the organic component of marine seston (i.e., dead phytoplankton) into the terrigenous sediment deposits. Sampling of the nearshore mud depocentre was beyond the scope of the present study so that two alternative marine endmember biotracer data sets were considered: (1) Pelorus-Chetwodes [Swales et al., 2021a]; and (2) flood-tide delta sediment deposits and sandflats (sites E1–E4, E6, E7 and G7) near the estuary mouth.

Data analysis and modelling led us to reject the Pelorus-Chetwodes as a marine endmember source, whereas the isotopic characteristics of the Flood Delta sediment were suitable and produce stable model outputs. Several complimentary lines of evidence and observations supported the inclusion of the flood delta as a representative marine source endmember. Firstly, the isotopic characteristics of the flood-tide delta sediment had bulk  $d^{13}C$  isotopic values (mean  $-15.76$  ‰,  $sd = 4.8$ ) that were substantially isotopically enriched (i.e.,  $\sim 5$  ‰) in comparison to sediment samples from in the middle (mean  $-20.58$ ,  $sd = 1.14$ ) and upper reaches (mean  $-21.22$ ,  $sd = 1.8$ ) of the estuary. The higher variability for flood-tide delta mean bulk  $d^{13}C$  value was accounted for by a single sample. Secondly, analysis of kelp, macroalgae and saltmarsh tissue from the estuary showed that the kelp had a similarly enriched bulk  $\delta^{13}C$  isotopic value to the flood-delta sediment whereas the estuarine plants did not. Lastly, the geomorphology and sedimentology of the flood delta (Figure 1-4) is indicative of sediment import from the marine environment.

### 4.2.2 Sedimentation in the Pleasant River Estuary

In this section, a conceptual model of sedimentation in the Pleasant River Estuary is developed based on the results of the CSSI sediment tracing study, and information from relevant previous studies and the scientific literature.

The Pleasant River Catchment delivers an estimated 12,400 tonnes per year of suspended sediment to the estuary. It is likely that a large fraction of this fine sediment is exported to the marine environment, where it is deposited in the nearshore–inner shelf (Figure 2-20). The trapping capacity



of an estuary is primarily a function of sediment accommodation. Jervey (1988) defined this as *the space available for sediment accumulation*. In estuaries, the potential sediment accommodation volume is generally equivalent to the tidal prism volume, which is the volume of the estuary between the mean low tide and the mean high tide. In sediment infilled estuaries, the tidal prism volume is reduced by the volume of sediment in the intertidal zone. In low-energy environments, such as saltmarshes and mangroves, the sediment accommodation zone extends up to the Highest Astronomical Tide (HAT), the uppermost extent of the tide (e.g., Swales et al., 2016b).

Over geological time scales, the combination of sea-level fluctuations and vertical land motion (VLM) result in cycles of sedimentation and erosion in estuarine and marine depositional environments. In the nearshore and particularly intertidal environments, sediment accommodation volume is also controlled by wave resuspension of sediment (Green and Coco, 2014). In estuaries with sufficient fetch (i.e., ~ 1km +), sediment accommodation is effectively reduced, and can be substantially less than the actual tidal-prism volume of the estuary due to sediment resuspension by waves. This is the case for much of the lower and middle reaches of the Pleasant River Estuary, where intertidal sand flats are found (Figure 1-4 and Figure 1-5).

In New Zealand, many estuaries have largely infilled with sediment due to increased catchment sediment loads associated with soil erosion following large-scale deforestation and establishment of pastoral agriculture over the last ~170 years (e.g., Thrush et al., 2004). More intensive and diverse land use has developed over the last several decades, such as horticulture and production forestry. The historical period has been accompanied by major wetland loss (90% c.f. pre-European). This loss has been more significant in New Zealand than in many other countries and ecosystems in fertile lowlands have been most severely impacted by agriculture (Myers et al., 2013). These wetlands would also have functioned as sinks for eroded catchment soils.

Although we do not have information about sediment accumulation rates (SAR) in the Pleasant River Estuary, it is likely that the system substantially infilled with sediment following large-scale catchment deforestation, with order of magnitude increase in SAR from much less than 1 mm yr<sup>-1</sup> to several mm yr<sup>-1</sup> being typical (e.g., Swales et al., 2002; Hunt, 2019; Huirama et al., 2021). Today, ~76% of the estuary's 0.97 km<sup>2</sup> high tide area is intertidal so that there is limited sediment accommodation volume. Although mud may temporarily deposit on the extensive intertidal sand flats in the mid and lower reaches of the estuary, after storms, much of this mud will be resuspended by waves and exported from the estuary or transported by tidal currents to be deposited in low energy environments. These mud sinks include saltmarsh in the upper intertidal zone and the side arms/tidal creeks (Roberts et al., 2022). In these areas, long-term SAR are likely to be constrained by the creation of new sediment accommodation volume by relative sea level rise (RSLR) (e.g., Swales et al., 2016b). The rate of RSLR incorporates the regional increase in sea level due to ocean warming and continental ice melting and local vertical land motion (VLM). For example, SAR measured in saltmarsh in the Pounaweia Estuary (Catlins, Otago) has approached the rate of RSLR (2.8±0.5 mm yr<sup>-1</sup>) since ~1900 (Gehrels et al., 2008).

In the Pleasant River Estuary, the rate of RSLR is unknown but is likely to be similar to the long-term RSLR the Dunedin tide gauge (1.35±0.15 mm yr<sup>-1</sup>, 1899–2013, Denys et al. 2020). Using this RSLR value, a conservative estimate of the annual increase in the annual sediment accommodation volume in the estuary can be made. Assuming that sedimentation occurs uniformly throughout the estuary then the potential annual sedimentation is given by  $A \times RSLR \times BD$ , where  $A$  is the high tide estuary area (970,000 m<sup>2</sup>) and  $BD$  is the bulk density of a typical wet estuarine sediment (1.2 t m<sup>-3</sup>). This yields a sediment volume of ~1,600 t yr<sup>-1</sup> of potential sediment accumulation created by RSLR that

represents only 12% of the estimated annual catchment sediment load (~12,860 t, Table 1-1). This calculated annual rate of sediment accommodation increase by RSLR represents a maximum value as long-term mud accumulation in the estuary will be largely limited to saltmarsh and tidal-creek sediment sinks.

In this context, the dominant contribution of marine sediment to contemporary sedimentation in the Pleasant River Estuary can be understood. Most of the sediment delivered from the catchment is exported to the sea and some fraction of this exported mud is accumulating in the nearshore-inner shelf mud depocentre (Figure 2-20). This marine sink, composed of eroded catchment soils, is a major source of fine sediment to the estuary due to more frequent sediment delivery to the estuary in comparison to catchment inputs. This is because fine sediment in the marine sink is likely to be resuspended and transported more frequently by waves and currents than catchment flood events that contribute most of the long-term annual sediment load. The catchment is located within a coastal rain-shadow zone (ORC, 2008). The most recent significant flood event prior to sediment sampling occurred in January 2021.

Although we do not have information about nearshore wave conditions near the Pleasant River Estuary, previous work suggests that waves will frequently resuspend fine sediment in the nearshore. Prevailing wind directions along the North Otago coast are from the east and north-east and are relatively consistent through the year. At Dunedin (Musselburgh) monthly wind speeds average 12.1 to 15.7 km hr<sup>-1</sup> and strong winds (> 30 km hr<sup>-1</sup> occur 14 times per year (Macra, 2015). Wave climate on the North Otago coast is primarily dominated by swell (typical height 2–3 m, period 6–12 s, Pickrill, 1979). At Karitane - Blueskin Bay (~10 km south of Pleasant River Estuary), the intensity and effectiveness of the southerly swell is considerably reduced by wave refraction around the Otago Peninsula. Local winds play a more important role in wave propagation. The gradual shelf slope means that these shorter-period waves undergo limited refraction and consequently most of the energy associated with north-easterly waves is expended in the nearshore zone in comparison to the longer-period southerly swell (Fenwick and Stenton-Dozy, 2016). These observations suggest that fine sediment is resuspended and transported into the Pleasant River Estuary on a weekly–monthly basis.

### 4.3 Sediment management in the Pleasant River system

This study has identified the major contemporary sources of sediment in the Pleasant River system. A number of observations regarding sediment management in this system can be made:

- The results of the 2-EMM analysis yield sub-catchment proportional contributions in general agreement with the NZRM long-term load estimates (Table 3-2). For example, the Trotters Creek sub-catchment accounted for 77% of the downstream sediment mixture (PR7) in the main stem of the Pleasant River. NZ River Maps indicates that 74% of the total catchment annual average load is derived from soil erosion in the Trotters Creek sub-catchment (9,900 t yr<sup>-1</sup>, Table 1-1) although accounting for only 30% of the total catchment area. A substantial fraction of land use in this sub-catchment is dry stock pasture, however establishment of pine forest is occurring. Land use intensification and/or disturbance of vegetation cover on steeplands will likely exacerbate soil erosion in this sub-catchment.

- Given the underlying susceptibility of the Trotters Creek catchment to soil erosion it would be prudent to plan future land use that is consistent with long-term restoration plans for the Pleasant River system.
- Streambank and subsoil erosion are the primary sources of sediment depositing in the river system (Figure 3-2 and Figure 3-3), accounting for greater than 80% of sediment deposited at most river sampling sites (mean %soil values). At catchment outlets (i.e., PR1–PR4), streambank erosion accounted for as much as 98% of deposited sediment. Streambank and hillslope slip mapping would inform soil conservation activities in line with restoration outcomes sought by the community.
- Topsoil from harvested pine and the pasture-fodder crop sources contributed similar proportions of sediment deposited at estuary sampling sites (i.e., ~7.5% of catchment input). This study suggests that pine harvest areas have proportional yields (% soil km<sup>-2</sup>) that are about 69-fold higher than yields from pasture and fodder crop land use. Production forestry practices result in ongoing vegetation removal and thereby exposure of steepland soils to erosion throughout the catchment. Production forestry is a major and growing land use in the Pleasant River catchment and large areas of first rotation pine forest have yet to be harvested. Careful management of future pine forest harvesting will be required to mitigate excessive soil erosion. The results of the study suggest that the Trotters sub-catchment will be particularly susceptible to soil erosion.
- Marine sediment accumulating in the estuary is likely to be soils originally eroded from the land with this legacy sediment subsequently returned to the estuary by coastal processes. The close proximity of the nearshore mud deposition zone, seaward of the estuary mouth (Figure 2-20), suggests that much of this legacy sediment originated from the Pleasant River. The dominance of the marine source in the estuarine sediment (i.e., 87–97%) indicates that coastal processes regularly transport this isotopically enriched sediment back into the estuary. Most of this fine sediment is accumulating in the sheltered side arms/creeks and saltmarsh habitat. These mud sinks will be “topped up” from time to time by catchment floods. Managing the major catchment sources of sediment would reduce the supply of marine sediment over the long-term, assuming that most of the sediment originates from the Pleasant River.
- Sediment management in the Pleasant River catchment will also be required to mitigate the chronic effects of episodic fine-sediment inputs associated with catchment flood events. These effects potentially include reduced optical water quality (i.e., visual clarity, light penetration), smothering of benthic communities and changes sediment quality (e.g., sediment oxygen status). For example, the loss of subtidal seagrass habitat in New Zealand estuaries and shallow coastal environments (Tan et al. 2020) has been exacerbated by poor optical water quality (e.g., Mangan et al., 2020) and increased substrate mud content associated with fine-sediment inputs (Zabarte-Maeztu et al., 2021). Seagrass is presently absent in the estuary (Roberts et al., 2022) despite large areas of intertidal flat being available.

## 5 Acknowledgements

We extend our thanks to Sam Thomas (ORC Coastal Scientist), Hamish McFarlane and Stephanie Scott of the East Otago Catchment Group and landowners in the Pleasant River Catchment for providing background information, identifying sites, and enabling site access for sampling. In particular, we thank Mr Hamish McFarlane, farmer and member of the East Otago Catchment Group, for sharing his knowledge of pasture-cropping practices in the catchment (Section 2.2.1). We also extend our thanks to Matt Dale (Waterscape Connections Ltd) and Ngai Tahu Forests for arranging access and transport for sampling river sediments at sites PR6 and PR5. Thanks also to Venture Forestry Ltd for kindly allowing access to sample soils at harvested pine forest sites on Patterson Rd. Drs Keryn Roberts and Leigh Stevens (Salt Ecology) kindly shared estuary habitat maps with us for planning the estuary sediment sampling. We thank our NIWA Dunedin colleagues Elliot Bowie, Martin Bylsma and Eva Leunissen for their able support in the field. CSIA analyses of samples were performed by Dr Chris Yarnes and his team at the University of California (Davis), Stable isotope Facility. We thank Dr Max Gibbs (NIWA Emeritus Scientist) for reviewing this technical report.



## 6 References

- Alfaro A.C., Thomas F., Sergent L., Duxbury M. (2006) Identification of trophic interactions within and estuarine food web (northern New Zealand) using fatty acid biomarkers and stable isotopes. *Estuarine, Coastal and Shelf Science*, 70: 271–286.
- Anderson M.J, Willis T.J. (2003). Canonical analysis of principal coordinates: a useful method of constrained ordination for ecology. *Ecology*, 84(2): 511–525.
- Basher L.R. (2013) Erosion processes and their control in New Zealand. In: Dymond J.R. (ed.) *Ecosystem services in New Zealand – conditions and trends*. Manaaki Whenua Press, Lincoln, New Zealand: 363–378.
- Blake W.H., Ficken K.J., Taylor P., Russell M.A., Walling D.E. (2012) Tracing crop-specific sediment sources in agricultural catchments. *Geomorphology*, 139: 3222–329.
- Booker D.J., Whitehead A.L. (2017) NZ River Maps: An interactive tool for mapping predicted freshwater variables across New Zealand. [accessed 28 March 2018] <https://shiny.niwa.co.nz/nzrivermaps/>.
- Bostock H., Jenkins C., Mackay K., Carter L., Nodder S., Orpin A., Pallentin A., Wysoczansk R. (2019) Distribution of surficial sediments in the ocean around New Zealand/Aotearoa. Part A: continental slope and deep ocean. *New Zealand Journal of Geology and Geophysics*, 62(1): 1-23, DOI: 10.1080/00288306.2018.1523198
- Dalsgaard J., St. John M., Kattner G., Müller-Navarra D., Hagen W. (2003) Fatty acid trophic markers in the pelagic marine environment. *Advances in Marine Biology*, 46: 225–340.
- Denys P.H., Beavan R.J., Hannah J., Pearson C.F., Palmer N., Denham M., Hreinsdottir S. (2020) Sea level rise in New Zealand: the effects of vertical land motion on century-long tide gauge records in a tectonically active region. *Journal of Geophysical Research: Solid Earth*, 125: e20198JB018055.
- Eyles G., Fahey B. (2006) The Pakuratahi Land Use Study: A 12-year paired catchment study of the environmental effects of *Pinus radiata* forestry. *Landcare Report to Hawke's Bay Regional Council*: 128.
- Fenwick G., Fenton-Dozy J. (2016) Blueskin Bay inshore dredged sediment deposition: assessment of ecological effects. *NIWA Client Report CHC2015-102*: 48, prepared for Port Otago Ltd.
- Foote N.R. (2016) *Environmental and biological characteristics of East Otago estuaries along a gradient of marine connectivity*. MSc thesis, University of Otago: 140.
- Gehrels W.R., Hayward B.W., Newnham R.M. Southall K.E. (2008) A 20<sup>th</sup> century acceleration of sea level rise in New Zealand. *Geophysical Research Letters*, 35: L02717.
- Gibbs M.M. (2008) Identifying source soils in contemporary estuarine sediments: a new compound specific isotope method. *Estuaries and Coasts*, 31: 344–359.

- Gibbs M.M. (2014a) Protocols on the use of Compound-Specific Stable Isotopes to identify and apportion soil sources from land use. Revised 2013. *Contract Report*: 126, to Joint FAO/IAEA Division of Nuclear Techniques in Food and Agriculture.
- Gibbs M., Olsen G., Stewart M. (2014b) Jacobs River Estuary sediment sources assessment. *NIWA Client Report* HAM2014-003: 32, prepared for DairyNZ. Project code DNZ13201
- Gibbs M., Olsen G., Stewart M. (2015) New River Estuary sediment sources tracking pilot study. *NIWA Client Report* HAM2014-002: 39, prepared for Southland Regional Council. Project code ENS13203.
- Gibbs M.M., Swales A. (2019) Historical sediment source apportionment in the Waimea Estuary. *NIWA Client Report* 2002012HN: 44, prepared for Tasman District Council: 44.
- Gibbs M.M., Leduc D., Nodder S.D., Kingston A., Swales A., Rowden A.A., Mountjoy J., Olsen G., Ovenden R., Brown J., Bury S., Graham B. (2020) Novel application of a compound-specific stable isotope (CSSI) tracking technique demonstrates connectivity between terrestrial and deep-sea ecosystems via submarine canyons. *Frontiers in Marine Science*, 7(608): doi: 10.3389/fmars.2020.00608
- Glaser B. (2005) Compound-specific stable-isotope ( $\delta$  C-13) analysis in soil science. *Journal of Plant Nutrition and Soil Science*. 1685: 633–648.
- Green M.O., Coco, G. (2014) Review of wave-driven sediment resuspension and transport in estuaries. *Reviews of Geophysics*, 52: 2013RG000437, <https://rmascience.co.nz/wp-content/uploads/2020/01/Green-and-Coco-RoG-2013.pdf>
- Hancock G.J., Revill A.T. (2013) Erosion source discrimination in a rural Australian catchment using compound-specific isotope analysis (CSIA). *Hydrological Processes*, 27(6): 923–932.
- Handley S, Gibbs M, Swales A, Olsen G, Ovenden R, Bradley A. (2017) A 1,000-year seabed history Pelorus Sound/Te Hoiere, Marlborough. *NIWA Client Report* 2016119NE: 117. Prepared for Marlborough District Council, Ministry of Primary Industries, and the Marine Farming Association. Project Code MDC15401.
- Hughes A.O. (2016) Riparian management and stream bank erosion in New Zealand. *New Zealand Journal of Marine and Freshwater Research*, 50(2): 277–290.
- Huirama M., Swales A., Olsen G., Ovenden R. (2021) *Sediment accumulation Rates in Waimapu, Waikarea and Tuapiro Estuaries, Tauranga Harbour*. *NIWA Client Report* 2021255HN: 75 for Bay of Plenty Regional Council. <https://atlas.boprc.govt.nz/api/v1/edms/document/A3937376/content>
- Hume T.M., Snelder T., Weatherhead M., Liefing R. (2007) A controlling factor approach to estuary classification. *Ocean and Coastal Management*, 50(11–12): 905–929.
- Hunt S. (2019) Summary of historic estuarine sedimentation measurements in the Waikato region and formulation of a historic baseline sedimentation rate. *Waikato Regional Council Technical Report* 2019/08: 30. ISSN2230-4363 (online)

- IAEA (2019) *Guidelines for sediment tracing using the compound specific stable isotope technique*. International Atomic Energy Agency (IAEA) TECDOC-1881, ISBN 978-92-0-158519-6. Prepared by the Joint FAO/IAEA Division of Nuclear Techniques in Food and Agriculture, Vienna, Austria: 68.
- Jervey M.T. (1988) Quantitative geological modelling of siliciclastic rock sequences and their seismic expressions. In: Wilgus C.K., Hastings B.S et al. (eds). *Sea Level Changes: An Integrated Approach*. Society of Economic Palaeontologists and Mineralogists Special Publication 42: 47–69.
- Jones H.F.E., Pilditch C.A., Hamilton D.P., Bryan K.R. (2017) Impacts of a bivalve mass mortality event on an estuarine food web and bivalve grazing pressure. *N. Z. Journal of Marine and Freshwater Research*, 51(3): 370–392.
- Kohn M.J. (2010) Carbon isotope compositions of terrestrial C3 plants as indicators of (paleo)ecology and (paleo)climate. *PNAS*, 107(46): 19691–19695  
[www.pnas.org/cgi/doi/10.1073/pnas.1004933107](http://www.pnas.org/cgi/doi/10.1073/pnas.1004933107)
- MacDiarmid A., McKenzie A., Sturman J., Beaumont J., Mikaloff-Fletcher S., Dunne J. (2012) *Assessment of anthropogenic threats to New Zealand marine habitats*. Wellington, New Zealand: Ministry of Agriculture and Forestry.
- Macra G.R. (2015) *The Climate and Weather of Otago*, 2<sup>nd</sup> Edition. NIWA Science and Technology Series Number 67 ISSN 1173-0382: 44.
- Mangan S., Lohrer A.M, Thrush S.F., Pilditch C.A. (2020) Water column turbidity not sediment nutrient enrichment moderates micro phytobenthic primary production. *Journal of Marine Science and Engineering*, 8: 732, doi:10.3390/jmse8100732.
- Ministry for the Environment (2020). *Essential Freshwater policies and regulations: implementation guidance*. <https://environment.govt.nz/acts-and-regulations/freshwater-implementation-guidance/>
- Myers S.C., Clarkson B.R., Reeves P.N., Clarkson B.D. (2013) Wetland management in New Zealand: Are current approaches and policies sustaining wetland ecosystems in agricultural landscapes? *Ecological Engineering*, 56: 107–120.
- O’Loughlin, C.L. Watson, A.J. (1979) Root-wood strength deterioration in Radiata pine after clear-felling. *New Zealand Journal of Forestry Science*, 9(3): 284-293.
- Oamaru Marine Sediment Map (1986). NZ Oceanographic Institute, Wellington.
- Olsen G., Swales A. (2019) Whangamarino wetland sediment source tracing CSSI study. *NIWA Client Report 2020031HN*: 30, prepared for Waikato Regional Council.
- Otago Daily Times (2021) *Catchment restoration work to receive \$4m*, 21 December 2021.
- Otago Regional Council (2008). *The Water Resources of the Waikouaiti River*: 31. ISBN 1-877265-73-X.  
<https://www.orc.govt.nz/managing-our-environment/water/wetlands-and-estuaries/waitaki-district/pleasant-river-estuary-wetland-complex>

<https://www.orc.govt.nz/our-council-our-region/our-council/partnership-with-kai-tahu/jobs-for-nature/toitu-te-hakapupu-the-pleasant-catchment-river-restoration-project>

- Owens, P.N., Blake, W.H., Gaspar, L., Garteuille, D., Koiter, A.J., Lobbb, D.A., Petticrew, E.L., Reiffarth, D.G., Smith, H.G., Woodward, J.C. (2016) Fingerprinting and tracing the sources of soils and sediments: Earth and ocean science, geoarchaeological, forensic, and human health applications. *Earth Science Reviews*, 162: 1–23.
- Pickrill R.A., Mitchell J.S. (1979) Ocean wave characteristics around New Zealand. *New Zealand Journal of Marine and Freshwater Research*, 13(4): 501–520.
- Pivato M., Carniello, L., Moro, I., D’Odorico, P. (2018) On the feedback between water turbidity and microphytobenthos growth in shallow tidal environments. *Earth Surface Processes and Landforms*, 44: 1192–1206.
- Phillips, C., Marden, M., Basher, L. (2012) Plantation-forest harvesting and landscape response – what we know and what we need to know. *New Zealand Journal of Forestry*, 56(4): 4–12.
- Phillips, D.L., Inger, R., Bearhop, S., Jackson, A.L., Moore, J.W., Parnell, A.C., Semmens, B.X., Ward, E.J. (2014) Best practices for use of stable isotope mixing models in food-web studies. *Canadian Journal of Zoology*, 92: 823–835.
- Roberts K., Stevens L., Forrest B. (2022). *Broadscale intertidal habitat mapping of Pleasant River (Te Hakapupu) Estuary*. Salt Ecology Report 086: 66, prepared for Otago Regional Council.
- Schiel D.R., Howard-Williams C. (2015) Controlling inputs from the land to sea: limit-setting, cumulative impacts and ki uta ki tai. *Marine and Freshwater Research*, 67(1): 57–64.
- Smith, H.G., Karam, D.S., Lennard, A.T. (2018) Evaluating tracer selection for catchment sediment fingerprinting. *Journal of Soils and Sediments*, 18: 3005–3019.
- Smith, H.G., Spiekermann, R., Dymond, J., Basher, L. (2019) Predicting spatial patterns in riverbank erosion for catchment sediment budgets. *New Zealand Journal of Marine and Freshwater Research*, 53: 338–362. <https://doi.org/10.1080/00288330.2018.1561475>
- Stock B.C., Semmens B.X. (2016) Unifying error structures in commonly used biotracer mixing models. *Ecology*, 97(10): 2562–2569.
- Stock B.C., Jackson, A., Ward, E.J., Parnell, A.C., Phillips, D.L., Semmens, B.X. (2018). Analyzing mixing systems using a new generation of Bayesian tracer mixing models. *PeerJ* 6: e5096: DOI 10.7717/peerj.5096.
- Swales, A., Williamson, R.B., Van Dam, L.F., Stroud, M.J. (2002) Reconstruction of urban stormwater contamination of an estuary using catchment history and sediment profile dating. *Estuaries*, 25(1): 43–56.
- Swales A, Gibbs M, Pritchard M, Budd R, Olsen G, Ovenden R, Costley K, Hermanspahn N, Griffiths R. (2013). Whangarei Harbour sedimentation. Sediment accumulation rates

- and present-day sediment sources. *NIWA Client Report HAM2013–143*: 104, prepared for Northland Regional Council.
- Swales A., Gibbs M.M., Stephens T., Olsen G., Budd R., Ovenden R., Costley K. (2016a) Sources of eroded soils and their contribution to long-term sedimentation in the Firth of Thames. *NIWA Client Report HAM2016-001*: 68, prepared for Waikato Regional Council and Dairy NZ.
- Swales A., Denys P., Pickett V.I., Lovelock C.E. (2016b) Evaluating deep subsidence in a rapidly accreting mangrove forest using GPS monitoring of surface-elevation benchmarks and sedimentary records. *Marine Geology*, 380: 205–218.
- Swales A., Gibbs M. (2020) Transition in the isotopic signatures of fatty-acid soil biomarkers under changing land use: insights from a multi-decadal chronosequence. *Science of the Total Environment*, 722: 137850 (on-line)  
<https://doi.org/10.1016/j.scitotenv.2020.137850>
- Swales, A., Gibbs, M., Handley, S., Olsen, G., Ovenden, R., Wadhwa, S., Brown, J. (2021a) Sources of eroded soils and their contribution to long-term sedimentation in the inner Pelorus Sound/Te Hoiere. *NIWA Client Report 2020247HN*: 168
- Swales, A., Gibbs, M., Handley, S., Hudson, N. (2021b) *Sources of eroded soils and contribution to sedimentation in Pelorus Sound/Te Hoiere*. Public summary of NIWA technical report for Marlborough District Council.  
[https://www.marlborough.govt.nz/repository/libraries/id:2ifzri1o01cxbymxkwz/hierarchy/documents/environment/coastal/sedimentation-reports-list/Tracing\\_the\\_sediment\\_in\\_Pelorus\\_Sound.pdf](https://www.marlborough.govt.nz/repository/libraries/id:2ifzri1o01cxbymxkwz/hierarchy/documents/environment/coastal/sedimentation-reports-list/Tracing_the_sediment_in_Pelorus_Sound.pdf)
- Tan Y-M., Dalby O., Kendrick G.A., Statton J. Sinclair E.A., Fraser M.W., Macreadie P.I., Gillies C.L., Coleman R.A., Waycott M., van Dijk K., Verges A., Ross J.D., Campbell M.L., Matheson F.E., Jackson E.L., Irving A.D., Govers L.L.; Connolly R.M., McLeod I.M., Rasheed M.A., Kirkman H., Flindt M.R., Lange T., Miller A.D., Sherman C.D.H. (2020) Seagrass restoration is possible: insights and lessons from Australia and New Zealand. *Frontiers in Marine Science*, <https://doi.org/10.3389/fmars.2020.00617>
- Thrush, S.F., Hewitt, J.E., Cummings, V.J., Ellis, J.I., Hatton, C., Lohrer, A., Norkko, A. (2004) Muddy waters: elevating sediment input to coastal and estuarine habitats. *Frontiers in Ecology and the Environment*, 2: 299–306.
- Upadhyay H.R., Bode S., Griepentrog M., et al. (2017) Methodological perspectives on the application of compound-specific stable isotope fingerprinting for sediment source apportionment. *Journal of Soils and Sediments*, DOI 10.1007/s11368-017-1706-4
- Wildhaber, Y.S., Liechti, R., Alewell, C. (2012) Organic matter dynamics and stable isotopes for tracing sources of suspended sediment. *Biogeosciences Discuss*, 9: 453–483.
- Wilmshurst, J.M., Anderson, A.J., Higham, T.F., Worthy, T.H. (2008) Dating the late prehistoric dispersal of Polynesians to New Zealand using the commensal Pacific rat. *Proceedings of the National Academy of Sciences*, 105: 7676–7680.



Yi, Z., Xu, M., Di, X., Brynjolfsson, S., Fu, W. (2017) Exploring valuable lipids in Diatoms. *Frontiers in Marine Science*, 4:17. doi: 10.3389/fmars.2017.00017.

Zabarte-Maeztu I., Matheson F. E., Manley-Harris M., Davies-Colley R. J., Hawes, I. (2021b) Interaction of substrate muddiness and low irradiance on seagrass: A mesocosm study of *Zostera muelleri*. *Aquatic Botany*, 175: 103435.  
<https://www.sciencedirect.com/science/article/abs/pii/S030437702100084X?via%3Dihub>



## Appendix A Summary of CSSI Method

In this section we describe how stable isotopes are used to identify the sources of catchment sediments deposited in lakes, estuaries and coastal waters and explain how isotopic data are interpreted.

Stable isotopes are non-radioactive and are a natural phenomenon in many elements. In the NIWA Compound Specific Stable Isotope (CSSI) method, carbon (C) stable isotopes are used to determine the provenance of sediments (Gibbs, 2008). About 98.9% of all carbon atoms have an atomic weight (mass) of 12. The remaining ~1.1% of C atoms have an extra neutron in the atomic structure, giving it an atomic weight (mass) of 13. These are the two stable isotopes of carbon. Naturally occurring carbon also contains an extremely small fraction (about two trillionths) of radioactive carbon-14 (<sup>14</sup>C). Radiocarbon dating can be used to determine long-term sedimentation rates.

To distinguish between the two stable isotopes of carbon, they are referred to as light (<sup>12</sup>C) and heavy (<sup>13</sup>C) isotopes. Both of these stable isotopes of carbon have the same chemical properties and react in the same way. However, because <sup>13</sup>C has the extra neutron in its atom, it is slightly larger than the <sup>12</sup>C atom. This causes molecules with the <sup>13</sup>C atoms in their structure to react slightly slower than those with <sup>12</sup>C atoms, and to pass through cell walls in plants or animals at a slower rate than molecules with <sup>12</sup>C atoms. Consequently, more of the <sup>12</sup>C isotope passes through the cell wall than the <sup>13</sup>C isotope, which results in more <sup>12</sup>C on one side of the cell wall than the other. This effect is called isotopic fractionation and the difference can be measured using a mass spectrometer. Because the fractionation due to passage through one cell-wall step is constant, the amount of fractionation can be used to determine chemical and biological pathways and processes in an ecosystem. Each cell wall transfer or “step” is positive and results in enrichment of the <sup>13</sup>C content.

The amount of fractionation is very small (about one thousandth of a percent of the total molecules for each step) and the numbers become very cumbersome to use. A convention has been developed where the difference in mass is reported as a ratio of heavy-to-light isotope. This ratio is called “delta notation” and uses the symbol “δ” before the heavy isotope symbol to indicate the ratio i.e., δ<sup>13</sup>C. The units are expressed as “per mil” which uses the symbol “‰”. The delta value of a sample is calculated using the equation:

$$\delta^{13}\text{C} = \left[ \left( \frac{R_{\text{sample}}}{R_{\text{standard}}} \right) - 1 \right] 1000$$

where *R* is the molar ratio of the heavy to light isotope <sup>13</sup>C/<sup>12</sup>C. The international reference standard for carbon was a limestone, Pee Dee Belemnite (PDB), which has a <sup>13</sup>C/<sup>12</sup>C ratio of 0.0112372 and a δ<sup>13</sup>C value of 0 ‰. As all of this primary standard has been consumed, secondary standards calibrated to the PDB standard are used. Relative to this standard most organic materials have a negative δ<sup>13</sup>C value.

Atmospheric CO<sub>2</sub>, which is taken up by plants in the process of photosynthesis, presently has a δ<sup>13</sup>C value of about -8.5. In turn, the δ<sup>13</sup>C signatures of organic compounds produced by plants partly depends on their photosynthetic pathway, primarily either C<sub>3</sub> or C<sub>4</sub>. During photosynthesis, carbon passes through a series of reactions or trophic steps along the C<sub>3</sub> or C<sub>4</sub> pathways. At each trophic step, isotopic fractionation occurs and organic matter in the plant (i.e., the destination pool) is depleted by 1 ‰. The C<sub>3</sub> pathway is longer than the C<sub>4</sub> pathway so that organic compounds produced by C<sub>3</sub> plants have a more depleted δ<sup>13</sup>C signature. There is also variation in the actual amount of fractionation between plant species having the same photosynthetic pathway. This results in a range

of  $\delta^{13}\text{C}$  values, although typical bulk values for  $\text{C}_3$  and  $\text{C}_4$  plants vary around  $-26\text{‰}$  and  $-12\text{‰}$  respectively. The rate of fractionation also varies between the various types of organic compounds produced by plants. Thus, by these processes a range of organic compounds each with unique  $\delta^{13}\text{C}$  signatures are produced by plants that can potentially be used as natural tracers or biomarkers.

The instruments used to measure stable isotopes are called “isotope ratio mass spectrometers” (IRMS) and they report delta values directly. However, because they have to measure the amount of  $^{12}\text{C}$  in the sample, and the bulk of the sample C will be  $^{12}\text{C}$ , the instrument also gives the percent C ( $\%C$ ) in the sample.

When analysing the stable isotopes in a sample, the  $\delta^{13}\text{C}$  value obtained is referred to as the bulk  $\delta^{13}\text{C}$  value. This value indicates the type of organic material in the sample and the level of biological processing that has occurred. (Biological processing requires passage through a cell wall, such as in digestion and excretion processes and bacterial decomposition). The bulk  $\delta^{13}\text{C}$  value can be used as one of the sediment-source tracers in an isotopic mixing model. For example, fresh soil from forests has a high organic content with  $\%C$  in the range 5% to 20% and a low bulk  $\delta^{13}\text{C}$  value in the range  $-28\text{‰}$  to  $-40\text{‰}$ . As biological processing occurs, bacterial decomposition converts some of the organic carbon to carbon dioxide ( $\text{CO}_2$ ) gas which is lost to the atmosphere. This reduces the  $\%C$  value and, because microbial decomposition has many steps, the bulk  $\delta^{13}\text{C}$  value increases by  $\sim 1\text{‰}$  for each step. Pastureland soils and marine sediments typically have bulk  $\delta^{13}\text{C}$  values in the range  $-24\text{‰}$  to  $-26\text{‰}$  and  $-20\text{‰}$  to  $-22\text{‰}$ , respectively. Wastewater and dairy farm effluent have bulk  $\delta^{13}\text{C}$  values more enriched than  $-20\text{‰}$ . Consequently, a dairy farm where animal waste has been spread on the ground as fertilizer, will have bulk  $\delta^{13}\text{C}$  values higher (more enriched) than pasture used for sheep and beef grazing.

There are occasions when the inorganic component of the soil imparts a highly modified  $\delta^{13}\text{C}$  isotopic signature to the soil such that the  $\delta^{13}\text{C}$  value cannot be used for modelling of soil sources. This phenomenon occurs for example in Karst (limestone) soils, such as in the upper Whangarei Harbour associated with the Portland sediment.

In addition to the bulk  $\delta^{13}\text{C}$  value, organic carbon compounds in the sediment can be extracted and the  $\delta^{13}\text{C}$  values of the carbon in each different compound can be measured. These values are referred to as compound-specific stable isotope (CSSI) values. A forensic technique recently developed to determine the provenance of sediment uses both bulk  $\delta^{13}\text{C}$  values and CSSI values from each sediment sample in a deposit for comparison with signatures from a range of potential soil sources for different land cover types. This method is called the CSSI technique (Gibbs, 2008).

The CSSI technique is based on the concepts that:

1. land cover is primarily defined by the plant community growing on the land, and
2. all plants produce the same range of organic compounds but with slightly different CSSI values because of differences in the way each plant species grows and also because each land cover type has a characteristic composition of plant types that contribute to the CSSI signature.

The compounds commonly used for CSSI analysis of sediment sources are natural plant fatty acids (FAs) which bind to the soil particles as labels called biomarkers. While the amount of a biomarker may decline over time, the stable isotope values of the FA biomarkers do not change.

These stable isotope values for the suite of FA biomarkers in a soil provide positive identification of the source of the soil by land cover type.

The sediment at any location in an estuary or harbour can be derived from many sources including river inflows, coastal sediments and harbour sediment deposits that have been mobilised by tidal currents and wind-waves. The contribution of each sediment source to the sediment mixture at the sampling location will be different. To separate and apportion the contribution of each source to the sample, a mixing model is used. The CSSI technique uses the mixing model IsoSource (Phillips and Gregg, 2003). The IsoSource mixing model is described in more detail in a following section.

While the information on stable isotopes above has focused on carbon, these descriptions also apply to nitrogen (N), which also has two stable isotopes,  $^{14}\text{N}$  and  $^{15}\text{N}$ . The bulk N content (%N) and bulk isotopic values of N,  $\delta^{15}\text{N}$ , also provide information on land cover in the catchment but, because the microbial processes of nitrification and denitrification can cause additional fractionation after the sediment has been deposited, bulk  $\delta^{15}\text{N}$  cannot be used to identify sediment sources. The fractionation step for N is around +3.5‰ with bulk  $\delta^{15}\text{N}$  values for forest soils in the range +2‰ to +5‰. Microbial decomposition processes result in bulk  $\delta^{15}\text{N}$  values in the range 6‰ to 12‰ while wastewater and dairy effluent can produce bulk  $\delta^{15}\text{N}$  values up to 20‰. However, the use of synthetic fertilizers such as urea, which has  $\delta^{15}\text{N}$  values of -5‰, can result in bulk  $\delta^{15}\text{N}$  values <0‰.

### Sample analyses

An aliquot of each dry sediment sample was acidified with 1 N hydrochloric acid to remove inorganic carbonate before analysing for bulk organic C stable isotopes. About 50 mg of each acidified sample was combusted in a helium gas stream in a Fisons N1500 Elemental Analyser coupled via a ConFlo-II interface to a Thermo-Finnegan Continuous Flow Isotope Ratio Mass Spectrometer (CF-IRMS).

For  $\delta^{13}\text{C}$ , CF-IRMS measurements typically have a precision of  $\pm 0.1$  ‰ or better and the instrument also provides the proportion of organic C and N (%) in each sample.

Aliquots (20 to 40 g) of the non-acidified dry sediment were extracted with hot dichloromethane (100 °C) under high pressure (1500 psi) in a Dionex Accelerated Solvent Extractor (ASE 2000) to extract the fatty acids bound to the sediment particles. The FAs were methylated using 5% boron trifluoride catalyst in methanol to produce fatty acid methyl esters (FAMES). These FAMES were analysed by gas chromatography (GC)-combustion-IRMS to produce compound-specific stable isotope  $\delta^{13}\text{C}$  values i.e., CSSI values. Method details and data interpretation protocols were described previously by Gibbs (2008).

Fatty acids are highly polar, so they cannot be analysed directly as they will bind to the gas chromatograph (GC) column during analysis. Consequently, they must be derivatised into their methyl esters, which are non-polar, using a catalyst such as boron trifluoride ( $\text{BF}_3$ ) in methanol (MeOH). Each FA methyl ester (FAME) consists of the FA carbons plus one carbon from the MeOH used for the derivatisation step. The analytical values from the GC-combustion-isotope ratio mass spectrometer (GC-C-IRMS) were corrected for the added carbon in a methyl-group from the methanol used in the derivatisation to obtain the CSSI value for each FA using the equation:

$$\delta^{13}\text{C}_{\text{FA}} = (\delta^{13}\text{C}_{\text{FAME}} - (1-X) * \delta^{13}\text{C}_{\text{Methanol}}) / X$$

where FA is the fatty acid and X is the fractional contribution of the FA to the FAME. X can be calculated from the number of carbons in the FA molecule divided by the number of carbon atoms in the FAME derived from the FA. For example, the FA stearic acid (C18:0) has 18 carbon atoms whereas the FAME produced, methyl stearate, has 19 carbon atoms, including one added carbon from the methanol, and thus has an X value of 18/19 or 0.9474.  $\delta^{13}\text{C}_{\text{FA}}$  is the FA CSSI value corrected



for the methyl- group,  $\delta^{13}\text{C}_{\text{FAME}}$  is the uncorrected isotopic value for the FAME and  $\delta^{13}\text{C}_{\text{Methanol}}$  is the isotopic value for the methanol used in the derivatisation step.

The CG-C-IRMS analysis uses FA standards, both internal and external, of known CSSI  $\delta^{13}\text{C}$  value for the calibration of the soil FAMES and uses the retention times of the standards to confirm the identity of each FA being measured. This methyl-group correction was applied to all FAMES.

Several corrections are applied to the raw data to enable direct comparison of data between batches and for samples of varying ages (in the case of the sediment cores):

- Methyl-group (MeOH, FAME only) corrections to the  $\delta^{13}\text{C}$  signature of each batch.
- Soil and sediment samples are often analysed in batches. This requires inter-batch corrections for individual FAs to be applied relative to a master batch. These corrections account for slight differences arising from sample processing (extraction and derivatisation) and IRMS instrument set up and/or setting values for internal lab calibration standards between batches. The master batch maybe the first batch or the largest batch in a series. These inter-batch corrections are made using a NIWA FAME standards that are analysed with each batch.
- These inter-batch and methyl-corrected  $\delta^{13}\text{C}$  FA data were finally adjusted for the Suess Effect to the year 2015 AD (i.e., sediment cores only). The Suess Effect describes the progressive depletion of the atmospheric  $\text{CO}_2$   $\delta^{13}\text{C}$  signature, which is largely due to the combustion of fossil fuels since the early 1700s. This process also results in a depletion of soil  $\delta^{13}\text{C}$  signatures as plants utilise  $\text{CO}_2$  in photosynthesis and subsequently label potential soil sources (Verburg, 2007, Gibbs et al. 2014b). The annual rate of  $\delta^{13}\text{C}$   $\text{CO}_2$  depletion in New Zealand is -0.025‰ (per mil) per year (source: NIWA).

This Suess Effect correction is critical to enable direct comparison of sediment deposits with sources of varying ages, which has resulted in a  $\sim 2.15\%$  depletion in  $\delta^{13}\text{C}$  values since 1700.

## Data processing and presentation

The %C and suite of CSSI values for the extracted FAMES were assembled into a matrix table and modelled using IsoSource to estimate the number ( $n$ ) of isotopically feasible proportions of the main sediment sources at each sampling location. In successive model iterations, potential sources were added or removed to find an isotopic balance where the confidence level was high (lowest  $n$  value) and uncertainty was low. The isotopically feasible proportions of each soil source are then converted to soil proportions using the %C of each soil on a proportional basis. That is, the higher the %C in the soil, the less of that soil source is required to obtain the isotopic balance. In general, soil proportions less than 5% were considered possible but potentially not present. Soil proportions  $>5\%$  were considered to be present within the range of the mean  $\pm$  SD.

## CSSI Method

The CSSI method applies the concept of using the  $\delta^{13}\text{C}$  signatures of organic compounds produced by plants to distinguish between soils that develop under different land-cover types. With the exception of monocultures (e.g., wheat field), the  $\delta^{13}\text{C}$  signatures of each land-cover type reflects the combined signatures of the major plant species that are present.

For example, the isotopic signature of a lowland native forest in the upper North Island will be dominated by kauri, rimu, totara and tānekaha. A monoculture, such as pine forest, by comparison

will impart an isotopic signature that largely reflects the pine species, as well as, potentially, any understory plants.

The application of the CSSI method for sediment-source determination involves the collection of soil samples from potential subcatchment and/or land cover sources as well as sampling of sediment deposits in the receiving environment. These sediment deposits are composed of mixtures of terrigenous soils, with the contribution of each source potentially varying both temporally and spatially. The sampling of catchment soils provides a library of isotopic signatures of potential soil sources that are used to model the most likely sources of soils in sediment deposited at any given location and/or time.

Straight-chain FAs with carbon-chain lengths of 12 to 26 atoms (C12:0 to C26:0) have been found to be particularly suitable for sediment-source determination as they are bound to fine sediment particles and long-lived (i.e., decades to millennia). Fatty acids including myristic (C14:0): palmitic (C16:0), stearic (C18:0), arachidic (C20:0) and behenic (C22:0) have commonly been used to evaluate present and historical sources of terrigenous sediments. Although breakdown of these FA to other compounds eventually occurs, the signature of a remaining FA in the mixture does not change.

The stable isotope compositions of N and C and the CSSI of carbon in the suite of fatty acid (FA) biomarkers are extracted from catchment soils and sediments. It is the FA signatures of the soils and sediments that are used in this study to determine sediment sources. Gibbs (2008) describes the CSSI method in detail.

### Conversions of isotopic proportions to soil proportions

The IsoSource model provides estimates of the isotopic-proportional contributions of each land-cover (i.e., soil) type in each sediment sample. Thus, these results are in terms of carbon isotopic proportions and not source soil proportions. Furthermore, the stable isotope tracers account for a small fraction, typically less than 2%, of total organic carbon (OC) in the soil and OC accounts for typically <10% of the soil by weight. These factors mean that the contribution of each source soil to a sediment mixture will scale with the soil carbon content. Consequently, a linear correction based on the soil OC is required to estimate the proportion of each soil source in a sediment sample from a receiving environment (Gibbs 2008).

To convert the isotopic proportions to soil proportions ( $S_n\%$ ) the simple linear correction equation below was used:

$$S_n\% = \frac{I_n/C_n\%}{\sum_n^1 (I_n/C_n\%)} * 100$$

Where  $I_n$  is the mean feasible isotopic proportion of source soil  $n$  in the mixture estimated using an isotopic mixing model and  $C_n\%$  is the percentage organic carbon in the source soil.

Because this calculation only uses the OC% in the source soils for linear scaling, the proportional contribution of each source soil is not influenced by any loss of carbon (e.g., total carbon, FAs etc.) in the sediment mixture due to biodegradation. The level of uncertainty in the mean soil proportion is the same as that defined by the standard deviation about the mean isotopic proportion.

A simple example of this linear correction is illustrated here by considering a solution composed of a mixture of three different sodium (Na) salts which provide equal proportions of Na to the mixture (3

x 1/3 each): sodium chloride (NaCl, molecular weight 58.45), sodium nitrate (NaNO<sub>3</sub>, mw 85.0), and sodium sulphate (Na<sub>2</sub>SO<sub>4</sub>, mw 142.0). Consider each of these salts to represent a different source soil, each of which are present in a sediment mixture. The %Na represents the % carbon in each source soil. The %Na in each salt is calculated by dividing the atomic weight of sodium (23) by the molecular weight of each salt compound, but also recognising how many atoms of sodium are present in the molecule.

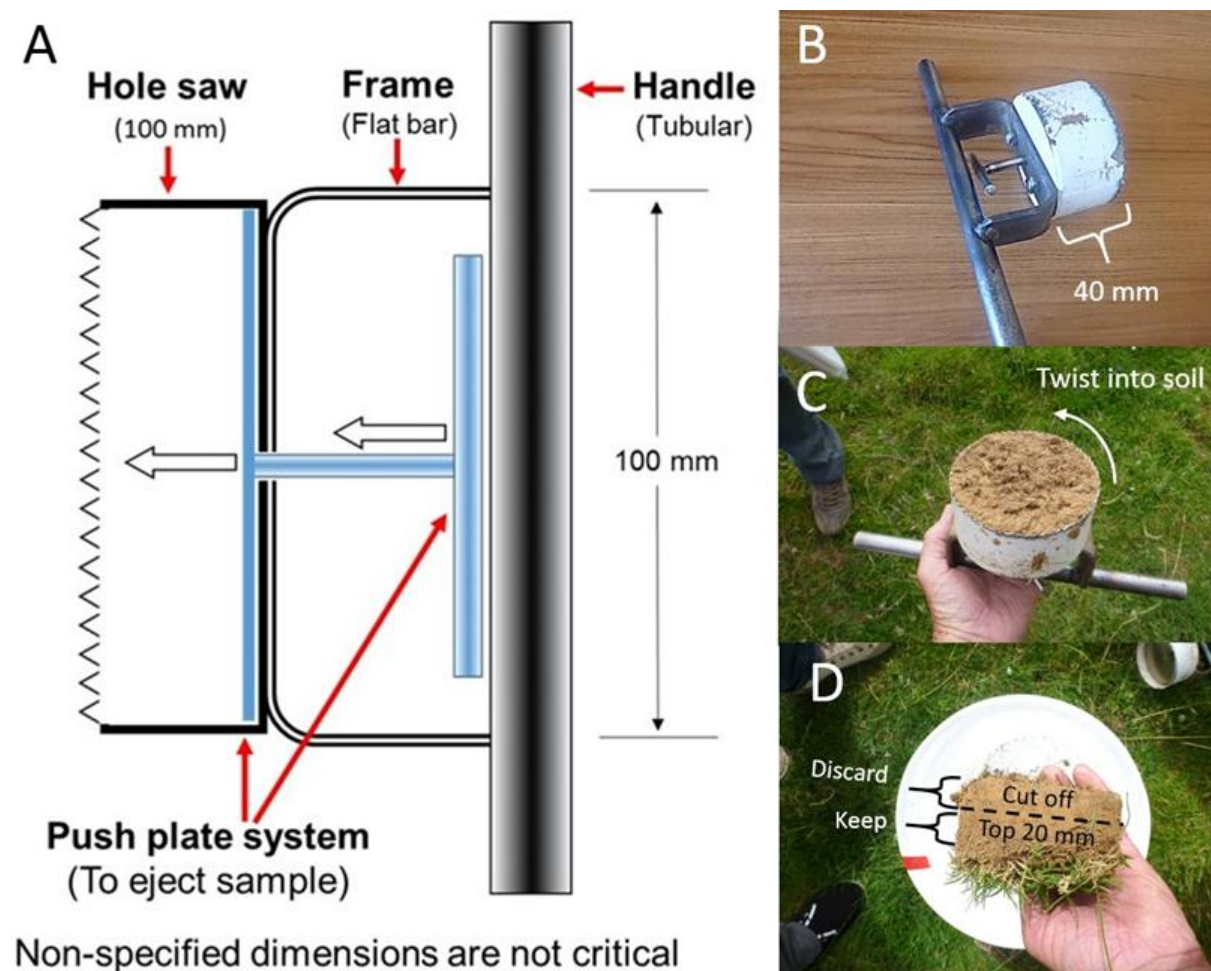
Table C-1 below presents the calculations required to apply the linear correction equation using the sodium salts example in order to determine how much of each salt is in the mixture. The ratio M%/S% for each salt and sum of this ratio (3.11) represent the numerator and denominator respectively in the conversion equation. Thus, for example the proportion of NaCl salt in the mixture is given by (0.85/3.11)\*100 = 27.3%.

**Table C-1: Example of the linear correction method to convert the isotopic proportions to soil proportions.** Using sodium (Na) salt compounds as analogies to various soil sources present in a mixture.

Salt type	%Na in salt (S%)	%Na in mixture (M%)	M%/S%	% salt in mixture
NaCl	39.4	33.3	0.85	20.5
NaNO <sub>3</sub>	27.1	33.3	1.23	29.8
Na <sub>2</sub> SO <sub>4</sub>	32.4	33.3	1.03	33.1
SUM			3.11	

## Appendix B Soil sampling method

Topsoil and subsoil samples were collected at sampling sites using a purpose-built hand corer to ensure equivalent soil volumes were collected to prevent any bias in the composite sample. The hand corer was cleaned of any residual soil prior to use at each new site by taking a sample at the new site and discarding it before commencing the actual sampling. Soil plugs were obtained by twisting the corer into the soil. On retrieval, that soil was then extruded. The saw teeth effectively cut through the root sward in the ground. The core barrel is about 40 mm long and provides enough friction for the soil plug to come out of the ground inside the corer (Figure D-1). Each soil plug was partially extruded leaving the 0–20 mm depth section inside the corer and allowing the exposed 20–40 mm depth section to be cut off and discarded. The soil in the upper 0–20 mm depth layer was crumbled from the plant root mass and combined into a bulk composite sample in a 20-L plastic bucket. Coarse plant material (twigs, leaves, roots), stones, seeds, worms and insects were removed by hand picking. The composite soil sample was mixed thoroughly by hand before a 200–400 g aliquot of the mixture was sealed in zip-lock type sealable plastic bag for laboratory analysis.



**Figure B-1: Hand corer for soil sampling.** A) Schematic cross section showing the push plate system used to extrude the soil from the corer after collection, B) side view of the hand corer showing the push plate handle ready for coring, C) a view of the inverted corer after collecting a pasture core, and D) the soil plug extruded from the corer ready for trimming to 20 mm thickness before combining in the composite sample. Note: this

soil plug would normally be retained in the corer until the soil sample in the 20-40 mm core section had been removed.



## Appendix C Soil source library for Pleasant River system

**Table C-1: Soil/sediment source library isotopic data from sampled sites – Pleasant River system.** Mean data are the isotopic values of the fatty acids extracted from the land use soils. Std deviations are for the mean data by land use. Note: sources listed in alphabetical order as output by MixSIAR model.

Land use	%C	$\delta^{13}\text{C}$	C14:0	C16:0	C18:0	C20:0	C22:0	C24:0	C26:0
Mean values	%	‰	‰	‰	‰	‰	‰	‰	‰
<b>Modelled sources</b>									
Marine (Estuary) Sediment (n = 6)	0.74	-15.86	-20.75	-20.349	-24.52	-29.75	-30.07	-30.23	-31.43
Pasture & Fodder Crops (n = 20)	4.72	-28.78	-31.19	-30.92	-33.70	-35.14	-34.82	-35.12	-35.48
Pine Harvest (n = 5)	4.18	-28.11	-34.02	-30.89	-31.69	-33.23	-32.78	-33.71	-34.33
Stream Bank (n = 4)	1.12	-26.73	-29.86	-34.07	-35.02	-34.38	-35.37	-35.66	-36.43
Subsoil (n = 4)	0.80	-26.42	-28.79	-29.56	-31.48	-34.92	-34.38	-34.82	-34.51
<b>Sources not modelled</b>									
Beef & Sheep Pasture (n = 6)	5.84	-29.17	-31.62	-30.91	-33.94	-35.66	-35.35	-35.39	-35.69
Fodder crops (Kale, Beet) (n = 14)	4.34	-28.66	-31.03	-30.93	-33.61	-34.95	-34.63	-35.02	-35.40
Saltmarsh estuary Rep 1	35.72	-26.33	-29.19	-31.71	-31.52	-33.12	-31.72	-32.23	-32.97
Macroalgae – Rep 1	7.42	-21.06	-27.04	-27.34	-29.36	-36.91	-36.29	-34.90	-37.17
Kelp estuary – Rep 1	36.18	-18.78		-28.32	-26.58	-26.54		-26.56	
<b>Std Deviation</b>									
Marine (Estuary) Sediment	0.50	5.41	1.14	1.30	1.48	3.16	1.24	0.99	0.51
Pasture & Fodder Crops	1.64	0.45	0.89	0.71	0.92	0.57	0.63	0.62	0.67
Pine Harvest	1.05	0.12	0.43	0.34	0.36	0.44	0.39	0.33	0.18
Stream Bank	0.80	0.84	1.53	1.64	0.94	0.21	0.26	0.95	0.48
Subsoil	0.14	0.79	1.25	0.64	0.83	0.26	0.54	0.21	0.93
<b>Sources not modelled</b>									
Beef & Sheep Pasture	1.82	0.58	0.82	0.76	1.08	0.42	0.41	0.62	0.58
Fodder crops (Kale, Beet)	1.45	0.33	0.89	0.71	0.88	0.50	0.59	0.61	0.70

## Appendix D Mixing model descriptions and performance

### Two-endmember model

The two-endmember mixing model assumes that the FA isotopic values of a well-mixed sediment mixture downstream of a river confluence is the sum of the proportional contribution of the FA isotopic values of inputs from each upstream source, **A** and **B**, where A can be the tributary and B can be the main stem of the river.

$$\delta^{13}\text{C}_{\text{mixture}} = f\text{A}\delta^{13}\text{C}_{\text{A}} + f\text{B}\delta^{13}\text{C}_{\text{B}} \quad (1)$$

Where fA and fB are the fractions or proportions of each source. This equation can also be rewritten

$$1 = f\text{A} + f\text{B} \quad (2)$$

To solve for fA, the equation is rewritten as:

$$f\text{A} = (\delta^{13}\text{C}_{\text{mixture}} - \delta^{13}\text{C}_{\text{B}}) / (\delta^{13}\text{C}_{\text{A}} - \delta^{13}\text{C}_{\text{B}}) \quad (3)$$

and for fB, the equation is rewritten as:

$$f\text{B} = (\delta^{13}\text{C}_{\text{mixture}} - \delta^{13}\text{C}_{\text{A}}) / (\delta^{13}\text{C}_{\text{B}} - \delta^{13}\text{C}_{\text{A}}) \quad (4)$$

The caveat for the two-endmember mixing model is that the isotopic value of each FA tracers in the mixture must be between the values of the sources A and B. Theoretically, this should be the case where only tributaries upstream contribute to the mixture downstream, and where both upstream sources are dissimilar. In the case where the downstream mixture has similar  $\delta^{13}\text{C}$  tracer values to one of the upstream sources then modelling of the A and B source contributions will not be valid. This situation indicates incomplete mixing of the two source sediments and the mixture (i.e., flood sediment deposit) should be resampled further downstream.

### MixSIAR model

The Bayesian mixing model, MixSIAR (Stock et al. 2018), employed in the study is used to construct the probability distributions of sources to a sediment mixture. A key advantage of MixSIAR is that it can account for uncertainty in the isotopic signatures of each source and resulting estimates of source contributions to a sediment mixture.

Probability model-fitting to the observed data is based on a Markov Chain Monte Carlo (MCMC) method whereby the isotopic proportions of potential sources are estimated by repeated random sampling and discarding those which are not “*probabilistically consistent with the data*” (Phillips et al. 2014). Subsequent estimates are required to be similar to previous ones, thereby creating a Markov Chain (Phillips et al. 2014). Model output consists of a sample of the posterior proportions derived from the MCMC simulation and represent true probability distributions of source proportions that can be summarised by various descriptive statistics, including the 95% credible interval. MixSIAR includes diagnostic tests to determine convergence of the MCMC on the posterior distributions for all variables in the model.

The MCMC settings for the modelling were: three chains, chain lengths of 300,000, “burn in” of 200,000 and “thin” value of 100. This generated model output containing 3000 samples of posterior source proportions (sum = 1). Typical model run times (run length: long) for four sources and the

eight tracers (i.e., bulk  $\delta^{13}\text{C}$  and seven Fatty Acids) were ~2 minutes/run using a laptop computer with an Intel i7 processor. A continuous effects model, with a process only (i.e.,  $n = 1$ ) error structure, was employed to estimate the posterior distributions of sources for each individual sediment mixture sampled from the river and estuary. This process-only error structure implements the MixSIR model (Moore and Semmens, 2008) within the MixSIAR suite, so that uncertainty includes the source variance only and no distinction is made from sources of variance associated with the trophic discrimination factors (TDF) (Stock and Semmens, 2015: 2016). Specification of TDF to account for differences in the isotopic values of consumers' tissues and diet is a major source of uncertainty in estimating source contributions in food-web applications (Phillips et al. 2014, Stock and Semmens 2016). In the context of the present study, the fact that TDF are not required for sediment tracing studies, as well as the application of historical land use information to constrain potential sources, are key advantages. Bayesian estimates of source proportions can be informed by reliable priors based on data and thereby constrain the model and reduce uncertainty. For example, in food web studies, the gut contents of fish (i.e., prey species and relative abundance) can be used to construct priors in MixSIAR. In the present study, reliable/semi-quantitative information on the relative contributions of various sediment sources at the river sites were unknown so that an "uninformative prior" was applied. An uninformative prior is one where all combinations of isotopic proportions (sum = 1) are equally likely (Stock and Semmens, 2015).

#### MixSIAR model convergence diagnostics

Diagnostic tests of convergence of the Markov chain to a stationary distribution for all variables and measures of model fit provided with MixSIAR output are used to evaluate model performance for each sediment mixture analysed. These diagnostics are described here:

**Gelman-Rubin test:** the Gelman-Rubin test requires more than one Markov Chain Monte Carlo (MCMC) to be calculated (default number of chains = 3), with a value of 1 at convergence. A value of less than 1.1 is generally acceptable (Stock and Semmens, 2015). In the present study, most model variables had Gelman-Rubin values of less than 1.05.

**Geweke test:** the Geweke test is a two-sided z-test that compares the means of the first and second halves of each MCMC chain (i.e., expect 5% of model variables to be outside +/- 1.96). At model convergence these means should be the same, with large z-scores indicating rejection (Stock and Semmens, 2015).

**DIC:** the deviance information criterion (DIC, Spiegelhalter et al. 2002) provides another measure of model fit to the data and is commonly applied to Bayesian models where the posterior distributions have been estimated using MCMC methods. Model fit improves inversely with the DIC value. For example, a DIC value of < 20 indicates a very-good model fit whereas a DIC > 40 indicates a relative poor model fit. The DIC assumes that the posterior distribution is approximately multivariate normal.

Table D-1 and D-2 present diagnostic model convergence information for the Pleasant River and Estuary sediment deposits (mixtures) sampled from the river and estuary in May 2022.

**Table D-1: Summary of MixSIAR model convergence – River sediment deposits.** Results for diagnostic tests of convergence of the Markov chain to a stationary distribution for all variables and measures of model fit.

Site	Gelman-Rubin			Geweke			DIC
	>1.01	>1.05	>1.10	Chain 1	Chain 2	Chain 3	
PR1	0	0	0	0	0	0	47.58
PR1A	0	0	0	0	0	0	57.98
PR2	0	0	0	0	0	4	52.09
PR3	0	0	0	0	0	0	43.78
PR4	4	2	2	0	0	0	52.15
PR5 Upstream	0	0	0	0	0	0	24.42
PR5 Tributary	0	0	0	0	0	0	39.04
PR5 Downstream	0	0	0	0	0	0	16.09
PR6 Upstream	0	0	0	0	2	4	51.73
PR6 Tributary	0	0	0	0	0	0	17.12
PR6 Downstream	0	0	0	0	0	0	30.42
PR7 Upstream	0	0	0	0	0	0	43.38
PR7 Tributary	0	0	0	2	0	4	55.03
PR7 Downstream	0	0	0	2	2	2	38.38
PR8 Upstream	0	0	0	0	0	2	38.00
PR8 Tributary	0	0	0	6	0	0	43.06
PR8 Downstream	0	0	0	2	0	2	39.00
PR9 Upstream	0	0	0	4	0	2	27.62
PR9 Tributary	0	0	0	0	0	0	48.88
PR9 Downstream	0	0	0	2	0	2	44.46

**Figure D-2: Summary of MixSIAR model convergence – Estuary sediment deposits.** Results for diagnostic tests of convergence of the Markov chain to a stationary distribution for all variables and measures of model fit.

Site	Gelman-Rubin			Geweke			DIC
	>1.01	>1.05	>1.10	Chain 1	Chain 2	Chain 3	
E7-Estuary	0	0	0	0	0	0	25.02
E8-Estuary	0	0	0	0	2	2	12.96
E9-Estuary	0	0	0	0	0	0	17.23
E10-Estuary	0	0	0	2	4	2	38.75
E11-Estuary	0	0	0	0	0	0	41.11
E12-Estuary	0	0	0	4	2	2	22.98
E14-Estuary	0	0	0	0	0	2	37.54
E15-Estuary	0	0	0	0	0	0	12.81
E16-Estuary	0	0	0	0	0	0	25.34
G1-Estuary	0	0	0	0	0	0	20.55
G3-Estuary	0	0	0	0	0	2	40.41
G4-Estuary	0	0	0	0	2	0	14.32
G6-Estuary	0	0	0	4	0	0	29.00
G8A-Estuary	0	0	0	0	0	0	27.18



## Appendix E Sampling information

**Table E-1: Pleasant River Sampling Location Data.**

NIWA Code	Date	ID	Type	Site Name	Rep No.	Coordinates WGS84, Decimal degrees		Coordinates NZTM 2000, Decimal degrees	
						Latitude	Longitude	Easting	Northing
OA230/1	18/05/2022	SaltEcology	ESTUARY	G1	1	-45.550053	170.720069	1422036	4953414
OA230/2	18/05/2022	SaltEcology	ESTUARY	G3	1	-45.553785	170.723913	1422348	4953008
OA230/3	18/05/2022	SaltEcology	ESTUARY	G4	1	-45.551291	170.712734	1421467	4953260
OA230/4	18/05/2022	SaltEcology	ESTUARY	G6	1	-45.555618	170.723104	1422290	4952802
OA230/5	18/05/2022	SaltEcology	ESTUARY	G7	1	-45.560025	170.722585	1422264	4952311
OA230/6	18/05/2022	SaltEcology	ESTUARY	G8A	1	-45.552517	170.722777	1422255	4953146
OA230/7	18/05/2022	NIWA	ESTUARY	E1	1	-45.567087	170.724552	1422439	4951531
OA230/8	18/05/2022	NIWA	ESTUARY	E2	1	-45.563890	170.727048	1422624	4951892
OA230/9	18/05/2022	NIWA	ESTUARY	E3	1	-45.561502	170.728100	1422699	4952160
OA230/10	18/05/2022	NIWA	ESTUARY	E4	1	-45.561640	170.724439	1422413	4952136
OA230/11	18/05/2022	NIWA	ESTUARY	E6	1	-45.559320	170.726241	1422547	4952398
OA230/12	18/05/2022	NIWA	ESTUARY	E7	1	-45.559677	170.718412	1421937	4952341
OA230/13	18/05/2022	NIWA	ESTUARY	E8	1	-45.557777	170.720985	1422132	4952558
OA230/14	18/05/2022	NIWA	ESTUARY	E9	1	-45.557038	170.719573	1422019	4952637
OA230/15	18/05/2022	NIWA	ESTUARY	E10	1	-45.556813	170.724386	1422394	4952672
OA230/16	18/05/2022	NIWA	ESTUARY	E11	1	-45.556728	170.727837	1422663	4952689
OA230/17	18/05/2022	NIWA	ESTUARY	E12	1	-45.555528	170.721245	1422145	4952808
OA230/18	18/05/2022	NIWA	ESTUARY	E14	1	-45.551343	170.720714	1422090	4953272
OA230/19	18/05/2022	NIWA	ESTUARY	E15	1	-45.549839	170.726218	1422515	4953451
OA230/20	18/05/2022	NIWA	ESTUARY	E16	1	-45.546025	170.711999	1421393	4953843

NIWA Code	Date	ID	Type	Site Name	Rep No.	Coordinates WGS84, Decimal degrees		Coordinates NZTM 2000, Decimal degrees	
						Latitude	Longitude	Easting	Northing
OA230/21	18/05/2022	NIWA	River Source	PR1	1	-45.565584	170.709379	1421251	4951664
OA230/22	18/05/2022	NIWA	River Source	PR1A	1	-45.567382	170.715240	1421714	4951478
OA230/23	17/05/2022	NIWA	River Source	PR2	1	-45.554706	170.701486	1420600	4952855
OA230/24	17/05/2022	NIWA	River Source	PR3	1	-45.543507	170.703694	1420737	4954104
OA230/25	17/05/2022	NIWA	River Source	PR4	1	-45.535472	170.708232	1421066	4955007
OA230/26	17/05/2022	NIWA	Confluence	PR5B-U/S Watkin Creek	1	-45.563610	170.624750	1414640	4951692
OA230/27	17/05/2022	NIWA	Confluence	PR5B-U/S Tributary	1	-45.563767	170.625078	1414666	4951675
OA230/28	17/05/2022	NIWA	Confluence	PR5B-D/S Watkin Creek	1	-45.563352	170.625049	1414663	4951721
OA230/29	17/05/2022	NIWA	Confluence	PR6A-U/S Trotters Creek	1	-45.535088	170.616873	1413931	4954842
OA230/30	17/05/2022	NIWA	Confluence	PR6A-U/S Tributary	1	-45.534533	170.616859	1413928	4954904
OA230/31	17/05/2022	NIWA	Confluence	PR6A-D/S Trotters Creek	1	-45.534669	170.617508	1413979	4954890
OA230/32	16/05/2022	NIWA	Confluence	PR7-U/S Pleasant River	1	-45.515246	170.695708	1420023	4957226
OA230/33	16/05/2022	NIWA	Confluence	PR7-U/S Tributary	1	-45.514745	170.695940	1420040	4957282
OA230/34	16/05/2022	NIWA	Confluence	PR7-D/S Pleasant River	1	-45.515919	170.694520	1419933	4957149
OA230/35	16/05/2022	NIWA	Confluence	PR8-U/S Pleasant River	1	-45.493350	170.671955	1418097	4959605
OA230/36	16/05/2022	NIWA	Confluence	PR8-U/S Tributary	1	-45.494865	170.672060	1418111	4959437
OA230/37	16/05/2022	NIWA	Confluence	PR8-D/S Pleasant River	1	-45.494230	170.673345	1418209	4959511
OA230/38	16/05/2022	NIWA	Confluence	PR9-U/S Pleasant River	1	-45.482955	170.653544	1416625	4960718
OA230/39	16/05/2022	NIWA	Confluence	PR9-U/S Tributary	4	-45.483238	170.653521	1416624	4960687
OA230/40	16/05/2022	NIWA	Confluence	PR9-D/S Pleasant River	5	-45.482763	170.656257	1416837	4960746
OA230/42	16/05/2022	NIWA	Landuse	Pine Harvest	1	-45.520926	170.666653	1417772	4956530
OA230/43	16/05/2022	NIWA	Landuse	Pine Harvest	2	45.520990	170.668427	1417896	4956510
OA230/44	16/05/2022	NIWA	Landuse	Pine Harvest	3	-45.521139	170.668231	1414325	4961397
OA230/45	17/05/2022	NIWA	Landuse	Pine Harvest	4	-45.476241	170.624391	1414364	4961380

NIWA Code	Date	ID	Type	Site Name	Rep No.	Coordinates WGS84, Decimal degrees		Coordinates NZTM 2000, Decimal degrees	
						Latitude	Longitude	Easting	Northing
OA230/46	17/05/2022	NIWA	Landuse	Pine Harvest	5	-45.476410	170.624890	1412928	4961198
OA230/47	16/05/2022	NIWA	Landuse	Sheep & Beef Pasture	1	-45.477658	170.606457	1418179	4959565
OA230/48	16/05/2022	NIWA	Landuse	Sheep & Beef Pasture	2	-45.492790	170.672990	1418176	4959670
OA230/50	16/05/2022	NIWA	Landuse	Sheep & Beef Pasture	3	-45.509592	170.703187	1421112	4955371
OA230/52	16/05/2022	NIWA	Landuse	Sheep & Beef Pasture	4	-45.532214	170.708953	1420427	4952524
OA230/54	17/05/2022	NIWA	Landuse	Sheep & Beef Pasture	5	-45.557640	170.699149	1419457	4956984
OA230/58	16/05/2022	NIWA	Landuse	Kale Crop New	1	-45.517283	170.688380	1412352	4960993
OA230/60	16/05/2022	NIWA	Landuse	Kale Crop New	2	-45.479348	170.599021	1411421	4962218
OA230/62	17/05/2022	NIWA	Landuse	Kale Crop New	3	-45.468080	170.587591	1420934	4955711
OA230/65	16/05/2022	NIWA	Landuse	Kale Crop New	4	-45.529111	170.706808	1420520	4952538
OA230/67	17/05/2022	NIWA	Landuse	Kale Crop New	5	-45.557539	170.700350	1420379	4956667
OA230/69	17/05/2022	NIWA	Landuse	Kale Crop-pasture 1-2yrs	1	-45.520370	170.700060	1420519	4956527
OA230/70	17/05/2022	NIWA	Landuse	Kale Crop-pasture 1-2yrs	2	-45.521660	170.701800	1416697	4951232
OA230/73	18/05/2022	NIWA	Landuse	Kale Crop-pasture 1-2yrs	3	-45.568287	170.650911	1416653	4951227
OA230/74	18/05/2022	NIWA	Landuse	Kale Crop-pasture 1-2yrs	4	-45.568324	170.650351	1416620	4951245
OA230/75	18/05/2022	NIWA	Landuse	Kale Crop-pasture 1-2yrs	5	-45.568153	170.649930	1419799	4954851
OA230/76	17/05/2022	NIWA	Landuse	Fodder Beet	1	-45.536550	170.691960	1419799	4954851
OA230/77	17/05/2022	NIWA	Landuse	Fodder Beet	2	-45.536505	170.692245	1419821	4954857
OA230/78	17/05/2022	NIWA	Landuse	Fodder Beet	3	-45.536447	170.692511	1419841	4954864
OA230/79	17/05/2022	NIWA	Landuse	Fodder Beet	4	-45.550062	170.693648	1419973	4953354
OA230/80	17/05/2022	NIWA	Landuse	Fodder Beet	5	-45.550257	170.693594	1419970	4953332
OA230/81	16/05/2022	NIWA	Landuse	Slip/Subsoil	1	-45.475670	170.616510	1413707	4961442
OA230/82	16/05/2022	NIWA	Landuse	Slip/Subsoil	2	-45.510961	170.709326	1421073	4957733
OA230/83	17/05/2022	NIWA	Landuse	Slip/Subsoil	3	-45.521888	170.701540	1420500	4956501

NIWA Code	Date	ID	Type	Site Name	Rep No.	Coordinates WGS84, Decimal degrees		Coordinates NZTM 2000, Decimal degrees	
						Latitude	Longitude	Easting	Northing
OA230/84	16/05/2022	NIWA	Landuse	Slip/Subsoil	4	-45.519206	170.660152	1417259	4956706
OA230/85	17/05/2022	NIWA	Landuse	Streambank erosion	1	-45.547413	170.679838	1418887	4953617
OA230/86	17/05/2022	NIWA	Landuse	Streambank erosion	2	-45.547728	170.679884	1418892	4953582
OA230/87	17/05/2022	NIWA	Landuse	Streambank erosion	3	-45.519412	170.696860	1420126	4956766
OA230/88	17/05/2022	NIWA	Landuse	Streambank erosion	4	-45.535961	170.708126	1421059	4954953
OA230/89	18/05/2022	NIWA	Marine Source	Salt Marsh-Estuary	1	-45.549289	170.717531	1421835	4953493
OA230/94	18/05/2022	NIWA	Marine Source	Macroalgae-Estuary	1	-45.566312	170.716385	1421800	4951599
OA230/99	18/05/2022	NIWA	Marine Source	Kelp-Estuary	1	-45.568135	170.726300	1422579	4951419